THEORETICAL AND COMPUTATIONAL INVESTIGATIONS OF MINIMAL ENERGY PROBLEMS

By

Matthew T. Calef

Dissertation

Submitted to the Faculty of the

Graduate School of Vanderbilt University

in partial fulfillment of the requirements

for the degree of

DOCTOR OF PHILOSOPHY

in

Mathematics

August, 2009

Nashville, Tennessee

Approved:

Douglas Hardin

Edward Saff

Mark Ellingham

Akram Aldroubi

Marcus Mendenhall

© Copyright by Matthew T. Calef 2009
All Rights Reserved

ACKNOWLEDGEMENTS

There are many who have made my years at Vanderbilt positive ones. Two are deserving of special recognition. The first is my advisor, Douglas Hardin, who provided invaluable insight into the topics I've spent the last three years studying. In addition he was generous with his time and patient in helping me to understand. I am fortunate to have had such an advisor. The second is my wife Heather Andrews. From her wisdom and experience, she offered encouragement and a perspective on the process of graduate school that helped me through its inevitable challenges.

I would like to thank the Mathematics Department for giving me the opportunity to study at Vanderbilt and for educating me. I have learned more from my professors here than I imagined possible. In particular I would like to thank Emmanuele DiBenedetto. His grounded approach to presenting analysis provides the tools for becoming an analyst. His understanding of connections with application has helped me to see the concrete value in this area of study.

I am grateful to my other committee members for their input. Mark Ellingham's explanation of an algorithm for determining graph-isomorphisms played a large role in my numerical work. I am grateful to Marcus Mendenhall for our many Friday discussions on numerical techniques and other subjects. Edward Saff's vision for the field of minimal energy problems has influenced my thinking regarding questions to pursue. Finally, at the end of this process, I am seeing the wisdom of the advice Akram Aldroubi gave me during my qualifying exam.

The community of graduate students and post-docs has made the Vanderbilt

Mathematics Department a great place to do mathematics. In particular I would like to thank, in no particular order, Maxym Yattselev, Brett Wick, Adam Weaver, Tara Davis, Justin Fitzpatrick, Abey Lopez, Thomas Sinclair, Adam Dailey-McIlrath, Jeremy LeCrone, Piotr Nowak, Jan Spakula and Bogdan Nica for their camaraderie and shared enjoyment of mathematics.

Lastly I would like to thank those who generously offered their time to proofread this document: Heather Andrews, Douglas Hackworth, Douglas Hardin and Justin Fitzpatrick. Whatever errors remain are my responsibility and this dissertation is better because of their efforts.

TABLE OF CONTENTS

Appendicies

LIST OF TABLES

LIST OF FIGURES

CHAPTER 1

INTRODUCTION

Many static systems in nature reside in a local energy minimum subject to some constraint. A bowstring choses a shape that minimizes the potential energy stored in the bow subject to the constraint that the bowstring passes through the tips of the bow and the archer's fingers. A marble on an uneven floor can come to rest only at a point that is a local minimum of gravitational potential energy. A catenary minimizes gravitational potential energy and also describes the shape of a slack chain hanging from two points. The only stable locations for two electrons constrained to a sphere are those which minimize the electrostatic energy. Because this phenomenon is so common, it has been studied extensively.

In our examination of constrained energy minimization we shall focus on a class of energies derived from the electrostatic energy. If the electrons in the previous example are located at points x_1 and x_2 in the Euclidean space $\mathbb{R}^3$, then the electrostatic energy is, up to a constant,

$$\frac{1}{|x_1 - x_2|}.$$

This is the quantity that would result from fixing the first electron at x_1 and moving the second electron from infinity to x_2 while integrating the force due to the first electron over the distance travelled by the second. More generally, one may consider the energy required to assemble a collection of N electrons located at points $x_1, \ldots, x_N$. In this case the energy takes into account every pair of electrons and is, up to the same constant,

$$\sum_{i=1}^{N-1} \sum_{j=i+1}^{N} \frac{1}{|x_i - x_j|}. \tag{1.1}$$

In 1904 Thomson considered the following classical problem [48]: How does one

arrange N electrons on the sphere $\mathbb{S}^2$ so as to minimize the electrostatic energy? The physical model behind this problem is related to self-assemblage, viral morphology, best-packing, formation of colloids and coding theory; progress on this problem has broad application. However, the difficulty of this problem increases sharply with N the number of electrons. In the last century advances in mathematics and technology have provided complete and convincing descriptions of such minimal configurations in only a handful of cases. The broadest results for this problem are qualitative in nature, and describe properties of the configurations as a whole.

One of these properties is that the locations of the minimizing configuration of electrons provide good sampling points for $\mathbb{S}^2$. More precisely: Let $f : \mathbb{S}^2 \to \mathbb{R}$ be continuous, and let $\omega_N^1 := \{x_1, \dots x_N\} \subset \mathbb{S}^2$ denote the locations of the electrons in the N-point energy minimizing configuration, then

$$\lim_{N\to\infty} \frac{1}{N} \sum_{x\in\omega_N^1} f(x) = \int f d\sigma,$$

where σ is the surface area measure on $\mathbb{S}^2$ normalized to have total mass 1. This convergence, which is described in terms of continuous functions, is called *weak-star* convergence and is described in Chapter 2. We shall denote this convergence with a starred arrow. While weak-star convergence applies to measures and more generally to elements in a dual space, we shall write $\omega_N^1 \overset{*}{\to} \sigma$ to indicate

$$\frac{1}{N} \sum_{x\in\omega_N^1} \delta_x \overset{*}{\to} \sigma, \tag{1.2}$$

where δ_x is the Dirac measure centered at the point x.

We shall consider two generalizations of Thomson's problem. Instead of $\mathbb{S}^2$, we consider electrons on a compact set A of Hausdorff dimension d residing in $\mathbb{R}^p$. Further, for a value of $s > 0$ we replace the kernel $|\cdot|^{-1}$ with the Riesz s-kernel $|\cdot|^{-s}$.

To further introduce this subject we present some notation and review background results. Let $\omega_N = \{x_1, \dots x_N\}$ be a collection of $N > 1$ distinct points in $\mathbb{R}^p$, then

$$E_s(\omega_N) := \sum_{i=1}^{N} \sum_{j \neq i} \frac{1}{|x_i - x_j|^s}$$

and

$$\mathcal{E}_s(A, N) = \min\{E_s(\omega_N) \, : \, \omega_N \subset A\}$$

The compactness of A and the lower semicontinuity of the Riesz kernel ensures that there is a (not necessarily unique) N point configuration denoted ω_N^s that achieves the minimum $\mathcal{E}_s(A, N)$. Let μ be a measure on A. The s-energy of μ is

$$I_s(\mu) := \iint \frac{1}{|x - y|^s} d\mu(y) d\mu(x).$$

The quantity $I_s(\mu)$ may be thought of as the generalized electrostatic energy of a continuous charge distribution represented by the measure μ. Relatedly the quantity

$$U_s^{\mu}(x) := \int \frac{1}{|x - y|^s} d\mu(y)$$

is the s-potential of the measure μ.

The continuous version of the discrete optimization problem is to find a probability measure supported on a compact set A that minimizes the quantity I_s over the set of probability measures supported on A. If $0 < s < d$ where d is the Hausdorff dimension of the set A, then there is a unique minimizing probability measure $\mu^{s,A}$ (cf. [21, 30].) that is called the *(s-)equilibrium measure*. The uniqueness of $\mu^{s,A}$ follows from the positivity of the Riesz kernel (cf. [22, 30]). For example, in the case that A is the interval $[-1, 1]$ and $s \in (0, 1)$, it is well-known (cf. [25]) that $d\mu^{s,[-1,1]}(x) = c_s(1 - x^2)^{\frac{s-1}{2}} dx$ where c_s is chosen so that $\mu^{s,[-1,1]}$ is a probability measure.

The generalization from the Coulomb kernel to the Riesz s-kernel is a natural one and

several values of s are worth noting. In the space $\mathbb{R}^p$ the kernel for $s = p-2$ is the harmonic or Newtonian kernel and plays the same role the coulomb kernel does in $\mathbb{R}^3$. The case "$s = 0$" indicates the logarithmic kernel $-\log|x-y|$. A motivation for this is as follows: the derivative of the logarithmic kernel with respect to $|x-y|$ is the limit of the derivatives of $\frac{1}{s}|x-y|^{-s}$ with respect to $|x-y|$ as s deceases to 0. Alternatively, the generalized electric field derived from the logarithmic potential is the limit as $s \downarrow 0$ of the fields derived from the Riesz potentials scaled by $1/s$.

The case when s equals d is also a critical value because, in contrast to the case $s < d$, $I_d(\mu) = \infty$ for every probability measure μ that is supported on A (cf. [34] also Lemma 2.4.2.) As a heuristic consider the case $A = [-1,1] \subset \mathbb{R}$ hence $d = 1$. It is apparent that the function $|x|^{-s}$ is Lebesgue integrable only for values of $s < 1$. Put in physical terms, the self-energy of any continuous charge distribution on a d-dimensional conductor is infinite for the case $s = d$.

Because the discrete electrostatic energy ignores the self-energy, discrete constrained problems such as a generalized Thomson problem are well-posed for all positive values of s. By raising the discrete s-energy to the power $1/s$ and taking the limit as s increases to infinity, only the largest term in the sum (1.1) remains. In this limit the optimization problem is equivalent to the best packing problem.

Our theoretical interest is to understand the behavior of the equilibrium measures on a d-dimensional compact set A as $s \uparrow d$. For $A = [-1,1]$, we see directly from the above expression that $\mu^{s,A}$ converges in the weak-star sense as $s \uparrow 1$ to normalized Lebesgue measure restricted to A. It is natural to ask how general is this phenomena. We are further motivated by results concerning the following related discrete minimal energy problem.

When $s < d$ the above continuous and discrete problems are related by the following two results (cf. [30]). First, $E_s(\omega_N^s)/N^2 \to I_s(\mu^{s,A})$ as $N \to \infty$. Second, the sequence of

configurations $\{\omega_N^s\}_{N=1}^\infty$ has asymptotic distribution $\mu^{s,A}$, that is,

$$\omega_N^s \xrightarrow{*} \mu^{s,A}. \tag{1.3}$$

Note that the normalized surface area measure σ in (1.2) is the $s = 1$ equilibrium measure for $\mathbb{S}^2$.

In the case $s \geq d$ the lack of an equilibrium measure necessitates new techniques for the discrete problem. An effective approach to the discrete equilibrium for this range of s was presented in [24] and [3] for d-rectifiable sets. A set A is said to be *d-rectifiable* (cf. [18, §3.2.14]) if it is the Lipschitz image of a bounded set in $\mathbb{R}^d$. In this case the results of interest are

$$\omega_N^s \xrightarrow{*} \mathcal{H}_A^d/\mathcal{H}^d(A) \qquad \text{as } N \to \infty. \tag{1.4}$$

(Here and in the rest of the paper $\mathcal{H}^d$ denotes the Hausdorff measure and μ_E denotes the restriction of a measure μ to a μ-measurable set E. e.g. $\mathcal{H}_A^d = \mathcal{H}^d(\cdot \cap A)$.) For technical reasons, the results in [24] and [3] for the case $s = d$ further require that A be a subset of a d-dimensional C^1 manifold, although it is conjectured that this hypothesis is unnecessary. Recall that a function $\varphi : A \to \mathbb{R}^p$ is Lipschitz if there is a constant L so that

$$|\varphi(x) - \varphi(y)| \leq L|x - y|$$

for all $x, y \in A$ and is bi-Lipschitz if

$$\frac{1}{L}|x - y| \leq |\varphi(x) - \varphi(y)| \leq L|x - y|$$

or all $x, y \in A$.

The limits (1.3) and (1.4) suggest that $\mu^{s,A} \xrightarrow{*} \mathcal{H}_A^d/\mathcal{H}^d(A)$ as $s \uparrow d$ whenever A is d-rectifiable. If A is strongly $(\mathcal{H}^d, d)$-rectifiable or is a strictly self-similar d-fractal (see Sections 3.1.2 and 3.1.4 for these definitions), we show that this is indeed the case. A

primary tool in our work is the following normalized d-energy of a measure

$$\tilde{I}_d(\mu) := \lim_{s\uparrow d}(d-s)I_s(\mu).$$

and the normalized d-potential

$$\tilde{U}^{\mu}_d(x) := \lim_{s\uparrow d}(d-s)U^{\mu}_s(x)$$

We will also rely on several notions of density. We let $B(x,r) \subset \mathbb{R}^p$ denote the closed ball in $\mathbb{R}^p$ of radius r centered at x. Given a measure μ, the traditional d-dimensional point-density at x is

$$\Theta_d(\mu, x) := \lim_{r\downarrow 0} \frac{\mu(B(x,r))}{r^d}.$$

However, there are many sets, such as fractals (cf. [34]), for which, at $\mathcal{H}^d_A$-almost all $x \in A$, this limit doesn't exist. However, Bedford and Fisher in [1] consider the following averaging integral:

$$D^2_d(\mu, x) := \lim_{\varepsilon\downarrow 0} \frac{1}{|\log\varepsilon|}\int_{\varepsilon}^{1} \frac{1}{r}\frac{\mu(B(x,r))}{r^d}dr,$$

which they call an *order-two density* of μ at x. It is known (cf. [16,38,51]) that for a class of sets including strictly self-similar d-fractals and strongly $(\mathcal{H}^d, d)$-rectifiable sets $D^2_d(\mathcal{H}^d_A, x)$ is positive, finite and constant $\mathcal{H}^d_A$-a.e. We shall denote this $\mathcal{H}^d_A$-a.e. constant as $D^2_d(A)$.

We denote by $\mathcal{M}^+(A)$ and $\mathcal{M}^+_1(A)$ the set of Radon measures on A and the set of Borel probability measures on A respectively. If μ and ν are two Radon measures, then we use the notation $\mu \ll \nu$ to indicate that $\nu(E) = 0$ implies that $\mu(E) = 0$. Finally, the dimension of a strongly $(\mathcal{H}^d, d)$-rectifiable set is a positive integer, while the dimension of a strictly self-similar d-fractal may take on positive non-integer values. For a strictly self-similar d-fractal it is known (cf. [35]) that $\mathcal{H}^d(A) \in (0,\infty)$.

With this we state our main results.

Theorem 3.3.1. *Let A be a strictly self-similar d-fractal or a strongly $(\mathcal{H}^d, d)$-rectifiable set of positive $\mathcal{H}^d$ measure and let $\lambda^d := \mathcal{H}^d_A/\mathcal{H}^d(A)$, then*

(1) The limit $\tilde{I}_d(\mu)$ exists for all $\mu \in \mathcal{M}^+(A)$ and

$$\tilde{I}_d(\mu) = \begin{cases} dD_d^2(A) \int \left(\frac{d\mu}{d\mathcal{H}^d_A}\right)^2 d\mathcal{H}^d_A & \text{if } \mu \ll \mathcal{H}^d_A, \\ \infty & \text{otherwise.} \end{cases}$$

(2) If $\tilde{I}_d(\mu) < \infty$, then the limit $\tilde{U}^\mu_d$ equals $\frac{d\mu}{d\mathcal{H}^d_A}$ μ-a.e. and

$$\tilde{I}_d(\mu) = \int \tilde{U}^\mu_d d\mu.$$

(3) $\tilde{I}_d(\lambda^d) < \tilde{I}_d(\nu)$ for all $\nu \in \mathcal{M}^+_1(A) \backslash \left\{\lambda^d\right\}$.

Theorem 4.1.1. *Let $A \subset \mathbb{R}^p$ be a compact strongly $(\mathcal{H}^d, d)$-rectifiable set such that $\mathcal{H}^d(A) > 0$. Let $\lambda^d := \mathcal{H}^d_A/\mathcal{H}^d(A)$. Then $\mu^{s,A} \xrightarrow{*} \lambda^d$ as $s \uparrow d$.*

Theorem 4.1.2. *Let $A \subset \mathbb{R}^p$ be a compact strictly-self similar d-fractal. Let $\lambda^d := \mathcal{H}^d_A/\mathcal{H}^d(A)$. Then $\mu^{s,A} \xrightarrow{*} \lambda^d$ as $s \uparrow d$.*

There are two motivations for the normalizing factor $(d - s)$. The first motivation arises from a Fourier analytic expression of energy. If a finite measure μ is supported in $\mathbb{R}^d$, then for $s < d$ we may write the s-energy of μ in terms of its Fourier transform as follows (cf. [30, 50]):

$$I_s(\mu) := c(s,d) \int_{\mathbb{R}^d} |\xi|^{s-d} |\hat{\mu}(\xi)|^2 d\xi. \tag{1.5}$$

The constant $c(s,d)$ has the property that

$$\lim_{s \uparrow d} (d - s) c(s,d) = K_d,$$

where K_d depends only on the dimension of the ambient space $\mathbb{R}^d$ (cf. [30].) One may take the limit inside the integral and the normalized d-energy becomes, up to a constant,

the L^2-norm of the Fourier transform of μ. For certain μ this is equal to the L^2-norm of the Radon-Nikodým derivative of the measure μ with respect to $\mathcal{L}^d$, the d-dimensional Lebesgue measure. The second motivation arises from a result of Zähle [52] which was generalized by her student Hinz [26]. If μ is a finite measure and if $D_d^2(\mu, x)$ exists and is finite, then $\tilde{U}_d^\mu(x)$ exists and $D_d^2(\mu, x) = d\tilde{U}_d^\mu(x)$. These two results provide the foundation for a proof of Theorem 3.3.1.[1]

The proof of Theorem 4.1.1 relies on an estimate based on (1.5) that compares the s-energy of a measure μ for two different values of s. The constant K_d depends on the dimension of the embedding space and not on the dimension of the set A. However, the Riesz energies depend only on the relative distances within A and so the estimate holds for any isometric embedding of A into a higher dimensional space. The approach used in the proof is to relax the isometric embedding to a bi-Lipschitz embedding, and to show that A can be assembled from a collection of bi-Lipschitz embeddings in a manner which preserves the necessary estimate.

The proof of Theorem 4.1.2 relies on a localization property of the fractals in question to replace the original optimization problem with a coarser problem that gives a compatible answer. As $s \uparrow d$ this coarse problem approximates the original problem arbitrarily well.

In addition to these theoretical results we present some numerical experiments for the discrete energy on $\mathbb{S}^2$ for $s = 0$, 1, 2 and 3. While these numerical experiments do not lead to provable results, they provide data that can be used to examine conjectures. In particular we look at higher order terms in the asymptotic expansion of $\mathcal{E}_s(\mathbb{S}^2, N)$ and the conjecture that the number of stable minima on the sphere grows exponentially with N.

We also present two algorithms, which to this author's knowledge, are new. The first reduces and estimates the effect of roundoff error in sums of many numbers e.g. the sum

[1] In his work on reconstructing measures from their moments Putinar [41] considers an alternate normalization for the d-energy.

associated to $E_s(\omega_N)$. The second employs computational geometry and graph-theory to speed the process of counting distinct configurations.

The rest of this document is organized as follows: Chapter 2 contains a summary of the theoretical basis for potential theory as it applies to Riesz energies. The central result is the existence and uniqueness of the equilibrium measure $\mu^{s,A}$; Chapter 3 examines classes of sets relevant to the material at hand, notions of density and provides a proof of Theorem 3.3.1; Chapter 4 presents proofs of Theorems 4.1.1 and 4.1.2; Chapter 5 describes the numerical experiments and presents an initial analysis of the data; Chapter 6 proposes some future work.

CHAPTER 2

BACKGROUND

This chapter presents an overview of the theoretical foundations and results for potential theory and discrete minimal energy problems in $\mathbb{R}^p$. The key ingredients are measure theory in $\mathbb{R}^p$, which provides the right setting for certain minimization problems, weak-star topologies, which provide compactness, and Fourier analysis, which provides an invaluable alternative view for many of the problems arising in potential theory. Because this chapter aims to provide an overview, proofs for common theorems (e.g. the Radon-Nikodým theorem) are omitted. Proofs are included if they provide an important idea or technique, and are not overly technical.

2.1 Measures on $\mathbb{R}^p$

2.1.1 Basic Definitions and Results

Let $\mathcal{A}$ be a collection of subsets of $\mathbb{R}^p$. Intuitively a measure $\mu : \mathcal{A} \to \mathbb{R}_+ \cup \{\infty\}$ is a function that assigns sizes to elements of $\mathcal{A}$ in a consistent manner i.e. $\mu(E)$ indicates the size of E for $E \in \mathcal{A}$. For example one may construct a measure μ_f from a continuous function $f : \mathbb{R}^p \to \mathbb{R}_+$ as follows

$$\mu_f(E) := \int_E f(x)\, dx.$$

(Here and in the rest of this paper dx denotes the traditional volume element from $\mathbb{R}^p$.)

An example of a measure that is not represented by a function is the Dirac-delta measure

δ_{x_0} centered at a point $x_0 \in \mathbb{R}^p$ and defined as follows:

$$\delta_{x_0}(E) := \begin{cases} 1 & x_0 \in E, \\ 0 & x_0 \notin E. \end{cases}$$

For our purposes a measure will also be used to represent a charge distribution. If μ is our charge distribution, then $\mu(E)$ indicates the amount of charge within the set E. With this interpretation the Dirac-delta measure δ_{x_0} is a point charge centered a x_0.

We shall review the portions of measure theory that 1) make precise what is meant by assigning size in a consistent manner and 2) are employed in the rest of this paper. This section is drawn from and covered more thoroughly in [9, 34, 44].

Let $\mathcal{A}$ be a collection of subsets of $\mathbb{R}^p$. $\mathcal{A}$ is a *σ-algebra* if

(1) $\varnothing \in \mathcal{A}$,

(2) $\mathbb{R}^p \backslash E \in \mathcal{A}$ whenever $E \in \mathcal{A}$ and

(3) $\bigcup_{n=1}^{\infty} E_n \in \mathcal{A}$ for any countable collection of sets $\{E_n\}_{n=1}^{\infty} \subset \mathcal{A}$.

It is a straightforward consequence of DeMorgan's Law that if $\mathcal{A}$ is a σ-algebra, then the countable intersection of sets in $\mathcal{A}$ is also in $\mathcal{A}$, i.e. requirement three holds for intersections.

A function $\mu : \mathcal{A} \to \mathbb{R}_+$ is a measure if all of the following hold.

(1) $\mathcal{A}$ is a σ-algebra. If $E \in \mathcal{A}$, we say that E is μ-measurable. This requirement ensures that countable set operations of μ-measurable sets result in a μ-measurable set.

(2) $\mu(E) \in [0, \infty]$ for all $E \in \mathcal{A}$.

(3) μ is *countably additive*. By this we mean that given any countable collection $\{E_n\}_{n=1}^{\infty} \subset \mathcal{A}$ where $E_i \cap E_j = \varnothing$ for $i \neq j$ we have

$$\mu\left(\bigcup_{n=1}^{\infty} E_n\right) = \sum_{n=1}^{\infty} \mu(E_n).$$

(4) There is some $E' \in \mathcal{A}$ so that $\mu(E') < \infty$.

It follows immediately from these definitions that μ is *monotone* i.e. if $E_1, E_2 \in \mathcal{A}$ are such that $E_1 \subset E_2$, then $\mu(E_1) \leq \mu(E_2)$. Further μ is *countably subadditive*, that is, given any countable collection $\{E_n\}_{n=1}^{\infty} \subset \mathcal{A}$,

$$\mu\left(\bigcup_{n=1}^{\infty} E_n\right) \leq \sum_{n=1}^{\infty} \mu(E_n).$$

A set is said to be *Borel* if it is the result of countably many set operations (unions, intersections, complements) on open sets, e.g. closed sets are Borel, the countable intersection of open sets is Borel and the countable union of closed sets is Borel. A measure is said to be Borel if its domain $\mathcal{A}$ contains the Borel sets. Since $\mathcal{A}$ is a σ-algebra, showing that $\mathcal{A}$ contains either the open sets or the closed sets is sufficient to show that the measure is Borel.

Given a measure μ and its domain $\mathcal{A}$, we shall extend $\mathcal{A}$ as necessary to include any subset $N \subset \mathbb{R}^p$ whenever $N \subset E \in \mathcal{A}$ and $\mu(E) = 0$. That is, subsets of measurable sets of measure zero are measurable. This is referred to as *completing the measure space* (cf. [9, ch. 2]) and can be accomplished so that μ remains a measure.

Of particular interest is the Hausdorff measure defined as follows: Begin with the collection of sets

$$\mathcal{Q}_\delta := \{Q \subset \mathbb{R}^p : \operatorname{diam} Q < \delta\},$$

where $\delta > 0$. Note that any set $E \subset \mathbb{R}^p$ may be covered by a countable collection of sets in $\mathcal{Q}_\delta$. For this reason $\mathcal{Q}_\delta$ is referred to as a *sequential cover*. Define an intermediate function $\mathcal{H}_\delta^d$ whose domain consists of all subsets of $\mathbb{R}^p$ as

$$\mathcal{H}_\delta^d(E) := \inf\left\{\sum_{i=1}^{\infty} (\operatorname{diam} Q_i)^d \ : \ \{Q_i\}_{i=1}^{\infty} \subset \mathcal{Q}_\delta \text{ and } E \subset \bigcup_{i=1}^{\infty} Q_i\right\},$$

where the infimum is taken over every sequence of sets $\{Q_i\}_{i=1}^{\infty} \subset \mathcal{Q}_\delta$ whose union covers

E. The Hausdorff outer-measure is then defined for any $E \subset \mathbb{R}^p$ as

$$\mathcal{H}^d(E) := \lim_{\delta \downarrow 0} \mathcal{H}^d_\delta(E). \tag{2.1}$$

Since $\mathcal{H}^d_\delta(E)$ is non-decreasing as δ decreases to zero, the limit in (2.1) always exists. Following the standard Carathéodory Construction, the domain of $\mathcal{H}^d$ is restricted to sets E that satisfy

$$\mathcal{H}^d(A) = \mathcal{H}^d(A \cap E) + \mathcal{H}^d(A \backslash E)$$

for every set $A \subset \mathbb{R}^p$. This ensures the domain of $\mathcal{H}^d$ is a σ-algebra that contains the closed sets (cf. [9, ch. 2]) and hence $\mathcal{H}^d$ is a Borel measure. Note that the definition of $\mathcal{H}^d$ does not depend on p the dimension of the space upon which it is defined.

This construction provides a family of measures parameterized by d. When d is 1, 2 or 3 one might think of $\mathcal{H}^d$ as a generalized length, area or volume respectively, although d need not be in $\mathbb{N}$. This gives rise to a notion of dimension referred to as the *Hausdorff dimension* (cf. [9, 34]) defined as follows:

$$\dim A := \sup\{d \,:\, \mathcal{H}^d(A) > 0\} = \inf\{d \,:\, \mathcal{H}^d(A) < \infty\}.$$

One may verify that if $d < \dim A$, $\mathcal{H}^d(A) = \infty$ and if $d > \dim A$, $\mathcal{H}^d(A) = 0$. In the case $d = \dim A$, $\mathcal{H}^d(A)$ does not have to be positive and finite.

In the case when $d = p$ we have

$$0 < \mathcal{H}^d(B(x, r)) = \mathcal{H}^d(B(y, r)) < \infty \tag{2.2}$$

for all $x, y \in \mathbb{R}^d$ and $r > 0$. (Here and in the rest of the paper $B(x, r)$ denotes the closed ball centered at x of radius r.) It is known (cf. [34, ch. 3]) that if two measures μ and ν each satisfy the condition in (2.2), then there is a $c \in (0, \infty)$ such that $\mu = c\nu$. From this

it follows that for $\mathcal{H}^d$ defined on $\mathbb{R}^d$, $\mathcal{H}^d = c\mathcal{L}^d$ where $\mathcal{L}^d$ is the d-dimensional Lebesgue measure. The constant of proportionality c is computed in e.g. [14].

A Borel measure μ is said to be *Radon* if $\mu(K) < \infty$ for every compact set $K \subset \mathbb{R}^p$. A measure μ is finite if $\mu(\mathbb{R}^p) < \infty$. With this we have the following:

Proposition 2.1.1 (cf. [9]). *Let E be a Borel set and μ a finite Borel measure, then*

(1) $\mu(E) = \sup\{\mu(K) : K \subset E \text{ where } K \text{ is compact}\}$.

(2) $\mu(E) = \inf\{\mu(O) : E \subset O \text{ where } O \text{ is open}\}$.

Put another way, the μ-measure of a Borel set E can be approximated arbitrarily well by either compact sets within E or open sets enclosing E.

Any finite Borel measure is Radon. In particular if A is of finite $\mathcal{H}^d$ measure, then the restriction of $\mathcal{H}^d$ to A (which we shall denote as $\mathcal{H}^d_A := \mathcal{H}^d(\cdot \cap A)$) is Radon. The measure $\mathcal{H}^d$ on $\mathbb{R}^p$ is Radon when $d \geq p$, and in fact is zero for $d > p$. When $d < p$, $\mathcal{H}^d$ is not Radon.

A natural extension of a measure is a *signed measure*, which assigns positive and negative values to subsets. To avoid the ambiguity of considering the difference of two infinite quantities, a signed measure may assign the value $+\infty$ or $-\infty$, but not both. Given a σ-algebra of subsets, an example of a signed measure is any function $\nu : \mathcal{A} \to \mathbb{R}$ of the form $\nu = \mu^+ - \mu^-$ where $\mu^+, \mu^- : \mathcal{A} \to \mathbb{R}$ are measures and one of them is finite. It is a consequence of the Jordan decomposition theorem that any signed measure has exactly this representation. To present the Jordan decomposition theorem we shall need the following:

Two measures $\mu, \nu : \mathcal{A} \to \mathbb{R}$ are said to be *mutually singular* (this relationship is denoted $\mu \perp \nu$) if $\mathbb{R}^p$ can be partitioned into two disjoint sets $A, B \in \mathcal{A}$ so that $\mathbb{R}^p = A \cup B$ and $\mu(E \cap B) = 0$ and $\nu(E \cap A) = 0$ for every set $E \in \mathcal{A}$. Intuitively μ resides within A and ν resides within B. With this we have the following:

Theorem 2.1.2 (Jordan Decomposition Theorem (cf. [9])). *Let ν be a signed measure on $\mathbb{R}^p$, then there are two measures μ^+ and μ^- one of which is finite such that $\mu^+ \perp \mu^-$ and $\nu = \mu^+ - \mu^-$*

As an example consider the signed measure $\nu = \mathcal{H}^1_{[0,2]} - \mathcal{H}^1_{[1,3]}$ on $\mathbb{R}^1$. The Jordan decomposition of ν is $\nu = \mathcal{H}^1_{[0,1]} - \mathcal{H}^1_{[2,3]}$.

Given a signed measure ν with Jordan decomposition $\mu^+ - \mu^-$ one denotes by $|\nu|$ the quantity $\mu^+ + \mu^-$. The expression $|\nu|$ is referred to as the *total variation*[1] of ν and is a measure itself. Two signed measures μ and ν are said to be mutually singular if $|\mu| \perp |\nu|$.

The *support of a measure* μ – denoted $\operatorname{supp}\mu$ – is the complement of the union of open sets of $|\mu|$-measure 0. Taking the perspective of charge distributions, $\operatorname{supp}\mu$ is the smallest closed set that contains all the charge represented by $|\mu|$.

We say that a pointwise condition holds *μ-almost everywhere* or μ-a.e. if the set of points where the condition doesn't hold is of μ-measure 0. Analogously we may refer to *μ-almost all* or μ-a.a. x to mean every $x \in \mathbb{R}^p$ with the possible exception of a set of μ-measure 0.

While we are interested in measures because they can be used to represent charge distributions, the development of measure theory was originally motivated by the study of integrable functions. A significant theoretical milestone in this direction is the Lebesgue integral, which is described more thoroughly and completely in other texts (cf. [9, 44, 49].) A heuristic interpretation of the Lebesgue integral is that

$$\int_{\mathbb{R}^p} f(x)\, d\mu(x)$$

integrates the function f according to a weighting encoded by the measure μ. For this quantity to be well defined the function f must be *μ-measurable*. By this we mean that the sets $\{x \in \mathbb{R}^p \ : \ f(x) > \alpha\}$ must be μ-measurable for every $\alpha \in \mathbb{R}$. At times we shall

[1] An alternative definition of total variation can be found in [44, ch. 6]

omit the integration variable if it is clear from context. Similarly if we omit the domain of integration, it should be assumed to be the support of the measure μ, e.g. the above may also be written as

$$\int f d\mu.$$

An integral written with respect to the volume element dx is equivalent to integration against the Lebesgue measure.

Finally, we shall introduce some useful collections of measures. Let $A \subset \mathbb{R}^p$ be a compact set and define

$$\mathcal{M}(A) := \{\mu \ : \ \mu \text{ is a signed measure, supp } |\mu| \subset A \text{ and } |\mu|(A) < \infty\},$$

$$\mathcal{M}^+(A) := \{\mu \in \mathcal{M}(A) \ : \ \mu \text{ is an (unsigned) measure}\} \text{ and}$$

$$\mathcal{M}_1^+(A) := \{\mu \in \mathcal{M}^+(A) \ : \ \mu(A) = 1\}.$$

Note that $\mathcal{M}(A)$ is a vector space.

2.1.2 **Comparing Radon Measures**

Given two signed measures μ and ν, we say that μ is *absolutely continuous with respect to* ν if $|\nu|(E) = 0$ implies that $|\mu|(E) = 0$ for any Borel set E. This relationship is denoted $\mu \ll \nu$.

The next two theorems will be used repeatedly in the following chapters. These theorems are presented at varying levels of generality in different texts, we present versions that are most applicable to the material that follows.

Theorem 2.1.3 (Lebesgue Decomposition Theorem). *Let μ and ν be Radon measures on $\mathbb{R}^p$. There exists a unique pair of Radon measures $\mu^{\ll}$ and $\mu^{\perp}$ so that $\mu = \mu^{\ll} + \mu^{\perp}$, $\mu^{\ll} \ll \nu$ and $\mu^{\perp} \perp \nu$.*

As an example let $A \subset \mathbb{R}^d$ be compact. The Lebesgue decomposition of $\mathcal{H}^d$ with respect to $\mathcal{H}^d_A$ is $\mathcal{H}^d = \mathcal{H}^d_A + \mathcal{H}^d_{\mathbb{R}^d \setminus A}$, where $\mathcal{H}^d_{\mathbb{R}^d \setminus A} \perp \mathcal{H}^d_A$ and trivially $\mathcal{H}^d_A \ll \mathcal{H}^d_A$. As another

example let δ_{x_0} be the Dirac-delta measure at $x_0 \in \mathbb{R}^d$, then the Lebesgue decomposition of δ_{x_0} with respect to $\mathcal{H}^d$ is simply $0 + \delta_{x_0}$ because δ_{x_0} is purely singular and contains no portion absolutely continuous with respect to $\mathcal{H}^d$.

Theorem 2.1.4 (Radon-Nikodým Theorem). *Let μ and ν be Radon measures on $\mathbb{R}^p$. Let $\mu = \mu^{\ll} + \mu^{\perp}$ be the Lebesgue decomposition of μ with respect to ν. Then there is a ν-measurable function denoted $\frac{d\mu^{\ll}}{d\nu}$ so that*

$$\mu^{\ll}(E) = \int_E \frac{d\mu^{\ll}}{d\nu} d\nu,$$

for any Borel set E. Furthermore this function is given by the limit

$$\frac{d\mu^{\ll}}{d\nu}(x) = \lim_{r \downarrow 0} \frac{\mu^{\ll}(B(x,r))}{\nu(B(x,r))}$$

and is finite ν-a.e. Additionally

$$\lim_{r \downarrow 0} \frac{\mu^{\perp}(B(x,r))}{\nu(B(x,r))} = \infty$$

$\mu^{\perp}$-a.e.

The value of this theorem is that if $\mu \ll \nu$ then there is a function called the Radon-Nikodým derivative that allows μ to be represented as an integral of this function where the integration is performed with respect to ν. One may think of the Radon-Nikodým derivative as a measure-theoretic Jacobian.

2.1.3 Image Measures and Lipschitz Maps

The *image measure* $\varphi_{\#}\mu$ associated with a compactly supported Radon measure μ on $\mathbb{R}^p$ and a continuous function $\varphi : \text{supp}\{\mu\} \to \mathbb{R}^{p'}$ is defined by

$$\varphi_{\#}\mu(E) := \mu(\varphi^{-1}(E))$$

for any Borel set $E \subset \mathbb{R}^{p'}$. The function $\varphi_{\#}\mu$ is a compactly supported Radon measure on $\mathbb{R}^{p'}$ and integration with respect to $\varphi_{\#}\mu$ is given by

$$\int f \, d\varphi_{\#}\mu = \int f(\varphi) \, d\mu,$$

for any non-negative $\varphi_{\#}\mu$-measurable function f (cf. [34, ch. 1]). Intuitively we map a measure from the domain of f to the range of f.

Given a set $A \subset \mathbb{R}^p$, a function $\varphi : A \to \mathbb{R}^{p'}$ is said to be *Lipschitz* if there is a non-negative and finite constant L so that

$$|\varphi(x) - \varphi(y)| \leq L|x - y|$$

for all $x, y \in A$. There is no restriction on p' other than it be a natural number. A function $\varphi : A \to \mathbb{R}^{p'}$ is said to be *bi-Lipschitz* if there is a positive and finite constant L so that

$$\frac{1}{L}|x - y| \leq |\varphi(x) - \varphi(y)| \leq L|x - y|.$$

The next two lemmas show that the ratio of the $\mathcal{H}^d$ measure of a set to the $\mathcal{H}^d$ measure of the bi-Lipschitz image of the set is bounded above and below by the Lipschitz constant. In particular, bi-Lipschitz functions preserve Hausdorff dimension. This will be important as we shall consider image measures derived from Lipschitz functions. We include a proof as one is not readily available in the introductory texts.

Lemma 2.1.5. *Let $A \subset \mathbb{R}^p$ and $\varphi : A \to \mathbb{R}^{p'}$ be Lipschitz with constant L and let $d > 0$. Then $\mathcal{H}^d(\varphi(A)) \leq L^d \mathcal{H}^d(A)$.*

Proof. If $\mathcal{H}^d(A) = \infty$, then the claim trivially holds. If $L = 0$, then $\varphi(A)$ is a point, $\mathcal{H}^d(\varphi(A)) = 0$ and the claim again holds. Assume $\mathcal{H}^d(A) < \infty$ and $L > 0$. Let $\varepsilon > 0$ and $\delta > 0$. Set $\delta_1 = \delta/L$. Let $\{Q_n\}_{n=1}^{\infty}$ be a collection of subsets of $\mathbb{R}^p$ so that

$$Q_n \subset A \text{ and } \operatorname{diam} Q_n < \delta_1 \text{ for all } n \in \mathbb{N},$$

$A \subset \bigcup_{n=1}^{\infty} Q_n$ and

$\sum_{n=1}^{\infty}(\text{diam } Q_n)^d < \mathcal{H}^d_{\delta_1}(A) + \varepsilon$.

Then $\varphi(Q_n) < \delta$ for $n \in \mathbb{N}$ and $\varphi(A) \subset \bigcup_{n=1}^{\infty} \varphi(Q_n)$. We conclude

$$\begin{aligned} \mathcal{H}^d_{\delta}(\varphi(A)) &< \sum_{n=1}^{\infty}(\text{diam } \varphi(Q_n))^d \\ &< L^d \sum_{n=1}^{\infty}(\text{diam } Q_n)^d \\ &< L^d(\mathcal{H}^d_{\delta_1}(A) + \varepsilon) < L^d(\mathcal{H}^d(A) + \varepsilon) \end{aligned}$$

Since δ and ε were chosen independently, we may take a limit as $\delta \downarrow 0$ and then the a limit as $\varepsilon \downarrow 0$ to obtain the result. □

Corollary 2.1.6. *Let $A \subset \mathbb{R}^p$ and $\varphi : A \to \mathbb{R}^{p'}$ be bi-Lipschitz with constant L and let $d > 0$. Then $L^{-d}\mathcal{H}^d(A) \leq \mathcal{H}^d(\varphi(A)) \leq L^d\mathcal{H}^d(A)$.*

Proof. By definition L cannot equal 0. Lemma 2.1.5 ensures $\mathcal{H}^d(\varphi(A)) \leq L^d\mathcal{H}^d(A)$. Bi-Lipschitz functions have Lipschitz inverses and so we let $\psi := \varphi^{-1}$ and $B = \varphi(A)$. Applying Lemma 2.1.5 again gives

$$\mathcal{H}^d(\psi(B)) \leq L^d\mathcal{H}^d(B) \text{ and hence } L^{-d}\mathcal{H}^d(A) \leq \mathcal{H}^d(\varphi(A)).$$

□

2.2 Weak-Star Compactness of Bounded Subsets of $\mathcal{M}(A)$

In this section we introduce the dual space associated to a vector space. We discuss a compactness property of the closed unit ball in the dual space and then show that the collection of signed measures with supports in a bounded set A whose total variation is bounded above has this compactness property. Finally, we shall discuss the significance of this result in terms of optimization problems on measures.

2.2.1 **Dual Spaces of Vector Spaces**

If V is a vector space with norm $\|\cdot\|$, then $L : V \to \mathbb{R}$ is said to be a *bounded linear functional on* V if

(1)
$$L(\alpha x + \beta y) = \alpha L(x) + \beta L(y)$$
for all $\alpha, \beta \in \mathbb{R}$ and all $x, y \in V$ and

(2) there is a positive finite constant M_L depending on L so that $|L(x)| \leq M_L\|x\|$ for all $x \in V$.

We shall denote by V^* the set of all bounded linear functionals on V and refer to it as the *dual space of* V. One may quickly check that V^* is itself a vector space. Linearity of V^* is meant in the following sense

$$(\alpha L_1 + \beta L_2)(x) = \alpha L_1(x) + \beta L_2(x),$$

where $L_1, L_2 \in V^*$. The norm of a bounded linear functional L is given by

$$\|L\| := \sup\{|L(x)| \, : \, x \in V, \, \|x\| = 1\}.$$

As an example consider the case $V = \mathbb{R}^p$, then any element $L \in V^*$ may be represented as an inner product with an element of $\mathbb{R}^p$. That is, there is a unique $a \in \mathbb{R}^p$ so that

$$L(x) = \langle x, a \rangle \tag{2.3}$$

for all $x \in \mathbb{R}^p$. The norm of L is then $|a|$. It is straightforward to see that any element $a \in \mathbb{R}^p$ gives rise to a bounded linear functional on $\mathbb{R}^p$ via equation (2.3) (The Cauchy-Schwarz inequality establishes boundedness.) In this case $\mathbb{R}^{p*}$ is isomorphic to $\mathbb{R}^p$ and the bijection

$\mathbb{R}^{p*} \ni L_a \leftrightarrow a \in \mathbb{R}^p$ is given by equation (2.3). Linearity of the bijection follows from the bi-linearity of the inner product.

This next example is a generalization of the previous example and is central to the theory in the rest of this document. Let $A \subset \mathbb{R}^p$ be a compact set. Let $C(A)$ denote the functions that are continuous on A. The sum of two continuous functions is continuous and a continuous function times a scalar is continuous and so $C(A)$ with the *sup-norm* $\|f\|_{C(A)} := \sup_{\{x \in A\}} |f(x)|$ is a vector space. (Continuous functions are bounded on compact sets hence the norm is finite for all $f \in C(A)$.)

$\mathcal{M}(A)$ is a vector space and linearity in $\mathcal{M}(A)$ is meant in the following sense

$$(\alpha\mu_1 + \beta\mu_2)(E) = \alpha\mu_1(E) + \beta\mu_2(E),$$

where E is any Borel set. The norm in $\mathcal{M}(A)$ is $\|\mu\|_{\mathcal{M}(A)} := |\mu|(A)$. We then have the following important theorem:

Theorem 2.2.1 (Riesz Representation Theorem (cf. [44])). *Let $A \in \mathbb{R}^p$ be a compact set. The dual space of $C(A)$ is isometrically isomorphic to $\mathcal{M}(A)$ and the bijection $C(A)^* \ni L_\mu \leftrightarrow \mu \in \mathcal{M}(A)$ is given by*

$$L_\mu(f) = \int f \, d\mu \tag{2.4}$$

for $f \in C(A)$.

Linearity of the bijection follows from the linearity of the Lebesgue integral with respect to both the integrand and the measure. Boundedness of the functional L_μ follows from the finiteness of $\mu(A)$ and the fact that functions that are continuous on a compact set are bounded above and below.

In comparing the two previous examples one might think of equation (2.4) as a generalized inner product that pairs continuous functions with measures and is linear in both arguments.

2.2.2 **Helly's Selection Theorem**

Given a vector space V, the dual space V^* may be given the so-called *weak-star topology*. The precise definition of the weak-star topology can be found in [9, ch. 6], although we are more concerned with convergence of sequences in this topology, which is characterized as follows: A sequence $\{L_n\}_{n=1}^{\infty} \subset V^*$ converges in the weak-star topology to $L \in V^*$ if and only if

$$\lim_{n\to\infty} L_n(x) = L(x)$$

for every $x \in V$. In this sense we view the convergence of a sequence in the weak-star topology through the lens of elements in V.

In terms of the Riesz Representation Theorem $\{\mu_n\}_{n=1}^{\infty} \subset \mathcal{M}(A)$ converges to $\mu \in \mathcal{M}(A)$ in the weak-star topology if, and only if,

$$\lim_{n\to\infty} \int f \, d\mu_n = \int f \, d\mu \tag{2.5}$$

for every $f \in C(A)$. It should be noted that for a specific $f \in C(A)$ equation (2.5) is a statement about convergence of real numbers. Further, the rate of convergence in (2.5) depends on f.

Another topology on $\mathcal{M}(A)$ is the norm topology, which is induced by the total variation metric: $d(\mu_1, \mu_2) = |\mu_1 - \mu_2|(A)$. Convergence of a sequence $\{\mu_n\}_{n=1}^{\infty}$ to μ in the norm topology means that $\lim_{n\to\infty} |\mu_n - \mu|(A) = 0$. The following example will show that the weak-star topology is indeed weaker than the norm topology, that is, sequences that converge in the weak-star topology may not converge in the norm topology.

Let A be the unit interval $[0, 1] \subset \mathbb{R}^1$ and let

$$\mu_n := \frac{1}{n} \sum_{i=1}^{n} \delta_{i/n}.$$

For each natural number n, μ_n distributes n Dirac-delta measures evenly along the interval

$[0,1]$ where each is scaled by $1/n$. We have

$$\lim_{n\to\infty}\int f d\mu_n = \lim_{n\to\infty}\frac{1}{n}\sum_{i=1}^{n}\int f d\delta_{i/n} = \lim_{n\to\infty}\frac{1}{n}\sum_{i=1}^{n} f(i/n) = \int_0^1 f(x)dx.$$

The integral with respect to dx is integration with respect to the one-dimensional Lebesgue measure $\mathcal{L}^1$ which in this case equals $\mathcal{H}^1$. We conclude that $\{\mu_n\}_{n=1}^{\infty}$ converges to $\mathcal{H}^1$ in the weak-star topology. (From this point forward we shall denote weak-star convergence with a starred arrow e.g. we write $\mu_n \overset{*}{\to} \mathcal{H}^1$.)

However, $\{\mu_n\}_{n=1}^{\infty}$ does not converges to $\mathcal{H}^1$ in the norm topology because $|\mu_n - \mathcal{H}^1|([0,1])$ does not converge to zero. For each n we may decompose $\mathbb{R}^1$ into two sets $A = \mathbb{R}^1\backslash\{1/n, 2/n, \ldots, 1\}$ and $B = \{1/n, 2/n, \ldots, 1\}$. Trivially $A \cap B = \varnothing$. Further $\mathcal{H}^1(B) = 0$ and $\mu_n(A) = 0$. Therefore the Jordan decomposition of $\mathcal{H}^1 - \mu_n$ is just $\mathcal{H}^1 - \mu_n$, thus $|\mathcal{H}^1 - \mu_n|([0,1]) = \mathcal{H}^1([0,1]) + \mu_n([0,1]) = 2$ for every n.

Consequently it is not in general true that if a sequence of measures $\{\mu_n\}_{n=1}^{\infty} \subset \mathcal{M}^+(A)$ converges in the weak-star topology to $\mu \in \mathcal{M}^+(A)$, then $\mu_n(E) \to \mu(E)$ for a Borel set E. (Let $E = [0,1]\backslash\mathbb{Q}$ in the previous example, then $\mu_n(E) = 0$ for all n and $\mathcal{H}^1(E) = 1$.) Under certain conditions on the set E one does have that $\mu_n(E) \to \mu(E)$.

The topological boundary of a set $E \subset \mathbb{R}^p$ is given by $\partial E = \overline{E}\backslash E^o$, where $\overline{E}$ is the closure of E and E^o is the interior of E. A set E is said to be *μ-almost clopen* if $\mu(\partial E) = 0$.[2]

Proposition 2.2.2. *Let $\mu \in \mathcal{M}^+(A)$ and $\{\mu_n\}_{n=1}^{\infty} \subset \mathcal{M}^+(A)$ be a sequence of measures so that $\mu_n \overset{*}{\to} \mu$. Then for any μ-almost clopen set E, $\mu_n(E) \to \mu(E)$.*

Proof. Let E be μ-almost clopen, then $\mu(\overline{E}) = \mu(E^o)$. Let $\varepsilon > 0$ be arbitrary.

By Proposition 2.1.1 we may find an open set O so that $\overline{E} \subset O$ and $\mu(O\backslash\overline{E}) < \varepsilon$. Since $\mathbb{R}^p\backslash O$ and $\overline{E}$ are disjoint and closed, we may find a Urysohn function ψ that is 1 on $\overline{E}$ and

[2] A set is said to be clopen if it is closed and open. Since closed sets contain their boundary and open sets do not, a clopen set has no boundary. Almost clopen sets are a measure theoretic extension of this.

0 on $\mathbb{R}^p \backslash \mathcal{O}$, then

$$\limsup_{n\to\infty} \mu_n(E) \leq \lim_{n\to\infty} \int \psi d\mu_n = \int \psi d\mu \leq \mu(\overline{E}) + \varepsilon = \mu(E) + \varepsilon.$$

Similarly we may find a compact set $K \subset E^o$ so that $\mu(E^o \backslash K) < \varepsilon$. Since K and $\mathbb{R}^p \backslash E^o$ are closed, we may find a Urysohn function ϕ that is 1 on K and 0 on $\mathbb{R}^p \backslash E^o$, then

$$\liminf_{n\to\infty} \mu_n(E) \geq \lim_{n\to\infty} \int \phi d\mu_n = \int \phi d\mu \geq \mu(E^o) - \varepsilon = \mu(E) - \varepsilon.$$

Since ε is arbitrary, the claim holds. □

While the weak-star topology admits convergent sequences that other topologies do not, it has the advantage that the closed ball $B(0, R) \subset V^*$ is sequentially compact in the weak-star topology. More precisely if $\Lambda := \{L \in V^* : \|L\| \leq R\}$, then for any sequence $\{L_n\}_{n=1}^{\infty} \subset \Lambda$ there is a subsequence $\{L_m\}_{m=1}^{\infty} \subset \{L_n\}_{n=1}^{\infty}$ and an $L' \in \Lambda$ such that $L_m \overset{*}{\to} L'$. This follows from the Alaoglu Theorem (cf. [9]) although in the special case when $V = C(A)$ and $V^* = \mathcal{M}(A)$ this is known as Helly's Selection Theorem.

Theorem 2.2.3 (Helly's Selection Theorem). *Let $A \subset \mathbb{R}^p$ be compact and $R \in (0, \infty)$. The set $\Lambda := \{\mu \in \mathcal{M}(A) : |\mu|(A) \leq R\}$ is sequentially compact in the weak-star topology.*

The weak-star compactness of bounded subsets will be an invaluable tool for addressing optimization problems on measures. Given an objective function $W : \mathcal{M}^+(A) \to \mathbb{R}$ one may seek to minimize W over $\mathcal{M}_1^+(A)$. A common technique is essentially as follows:

(1) Show that the subset of $\mathcal{M}_1^+(A)$ for which W is finite is non-empty.

(2) Show that $W(\mu)$ is bounded below independently of $\mu \in \mathcal{M}_1^+(A)$.

(3) Let $\{\mu_n\}_{n=1}^{\infty} \subset \mathcal{M}_1^+(A)$ be such that

$$\lim_{n\to\infty} W(\mu_n) = \inf\{W(\mu) : \mu \in \mathcal{M}_1^+(A)\}.$$

(4) Let ν be a weak-star cluster point of $\{\mu_n\}_{n=1}^{\infty}$. The existence of such a weak-star cluster point is guaranteed by Helly's Selection Theorem. Replace $\{\mu_n\}_{n=1}^{\infty}$ with a subsequence converging in the weak-star topology to ν.

(5) Demonstrate a relationship between $\lim_{n\to\infty} W(\mu_n)$ and $W(\nu)$, that is, that ν is the minimizing measure.

The following proof of Helly's Selection Theorem is taken from [45] and, as the authors of that text note, proving the Alaoglu theorem in this case requires nothing more advanced than the Weierstrass Approximation Theorem.

Proof. Let $\{\mu_n\}_{n=1}^{\infty}$ be a sequence of measures in $\mathcal{M}(A)$ such that $|\mu_n|(A) < R$ for all n. By the Weierstrass Approximation Theorem (cf. [9]), we may find a countable collection of polynomials $\{p_n\}_{n=1}^{\infty}$ that are dense in the sup-norm topology on $C(A)$. Define

$$a_n^1 := \int p_1 d\mu_n.$$

Since p_1 is bounded on A and $|\mu_n|(A) < R$ for all n, we may conclude that $\{a_n^1\}_{n=1}^{\infty} \subset \mathbb{R}$ is bounded, and hence has a cluster point. Let $\{\mu_n^1\}_{n=1}^{\infty} \subset \{\mu_n\}_{n=1}^{\infty}$ be a subsequence of measures that generates a convergent subsequence $\{a_n^1\}_{n=1}^{\infty}$. Define

$$a_n^2 := \int p_2 d\mu_n^1.$$

By prior argument, $\{a_n^2\}_{n=1}^{\infty}$ has a cluster point. Let $\{\mu_n^2\}_{n=1}^{\infty} \subset \{\mu_n^1\}_{n=1}^{\infty}$ be a subsequence of measures that generates a convergent subsequence in $\{a_n^2\}_{n=1}^{\infty}$. Inductively we may generate a collection of sequences of measures $\{\{\mu_n^i\}_{n=1}^{\infty}\}_{i=1}^{\infty}$ that have the property that

$$\lim_{n\to\infty} \int p_j d\mu_n^i$$

exists for every j less than or equal to i. Let μ_i denote the diagonal element μ_i^i, then $\{\mu_i\}_{i=1}^{\infty}$

is a subsequence of $\{\mu_n^i\}_{n=1}^{\infty}$ for all $i \in \mathbb{N}$, and so

$$\lim_{i\to\infty} \int p_n d\mu_i$$

converges for every p_n.

Let f by any element of $C(A)$ and $\varepsilon > 0$. Since $\{p_n\}_{n=1}^{\infty}$ is dense in sup-norm topology on $C(A)$, we may find a $p \in \{p_n\}_{n=1}^{\infty}$ such that $\|p - f\|_{C(A)} < \varepsilon/R$. We have

$$\lim_{n\to\infty} \int p d\mu_n - \varepsilon < \liminf_{n\to\infty} \int f d\mu_n \leq \limsup_{n\to\infty} \int f d\mu_n < \lim_{n\to\infty} \int p d\mu_n + \varepsilon$$

and by subtracting

$$\limsup_{n\to\infty} \int f d\mu_n - \liminf_{n\to\infty} \int f d\mu_n \leq 2\varepsilon.$$

Since ε was chosen arbitrarily we conclude the following

$$L(f) := \lim_{n\to\infty} \int f d\mu_n$$

defines a linear functional on $C(A)$ that is bounded by R. By the Riesz Representation Theorem there is some $\mu \in \mathcal{M}^+(A)$ such that

$$L(f) = \int f d\mu$$

for all $f \in C(A)$, and that $|\mu|(A) \leq R$. Hence $\mu_i \xrightarrow{*} \mu$ as $i \to \infty$. □

2.3 **Fourier Transforms**

In this section we sketch the theory behind the Fourier transform. This material is covered more thoroughly in e.g. [10, 50].

We say that a function f is in L^1, L^2 or L^∞ if $|f|$ is integrable, square integrable or uniformly bounded a.e. with respect to the Lebesgue measure $\mathcal{L}^p$ (i.e. integration with

respect to dx) respectively. For a function f in such a space the norms $\|f\|_1$, $\|f\|_2$ and $\|f\|_\infty$ refer to the integral of $|f|$, the square root of the integral of $|f|^2$ and the lowest number that bounds $|f|$ a.e. The collection of functions in L^p with the associated p-norm forms a topologically complete vector space. Note that L^2 is a Hilbert space.

When the integration is performed with respect to a measure μ other than the Lebesgue measure, we shall specify the vector space of p-integrable functions as $L^p(\mu)$.

2.3.1 L^1 Functions and Inversion

For a function $f \in L^1$ we define the Fourier transform of f as

$$\hat{f}(\xi) := \int f(x) e^{-2\pi i x \cdot \xi} dx \qquad \text{for } \xi \in \mathbb{R}^p. \tag{2.6}$$

Observe that

$$|\hat{f}(\xi)| \leq \int |f(x)||e^{-2\pi i x \cdot \xi}| dx = \|f\|_1.$$

and so $\hat{} : L^1 \to L^\infty$ is bounded and linear. If $\hat{f} \in L^1$, then one may define an inverse transform (cf. [50]) as

$$\check{\hat{f}}(x) := \int \hat{f}(\xi) e^{2\pi i x \cdot \xi} d\xi.$$

In such a case $\check{\hat{f}} = f$ a.e. In general, however, the Fourier transform of an L^1 function is not in L^1. The function defined on $\mathbb{R}^1$ that is one on the interval $[-1, 1]$ and zero elsewhere is such an example.

2.3.2 The Schwartz Space and L^2 Functions

With the motivation of finding a class of functions that is closed under the Fourier transform we introduce the Schwartz Space $\mathcal{S}$ (cf. [10, 50]). This space consists of rapidly decreasing, infinitely smooth complex valued functions, and is defined as

$$\mathcal{S} := \{\varphi \in C^\infty(\mathbb{R}^p) : \| \cdot^\alpha D^\beta \varphi(\cdot)\|_\infty < \infty \text{ for all multi-indices } \alpha \text{ and } \beta\}.$$

An example of a Schwartz function is the Gaussian e^{-x^2}. $\mathcal{S}$ is a topological vector space and has a family of semi-norms $\|\cdot\|_{\alpha,\beta} := \|x^\alpha D^\beta \cdot\|_\infty$ indexed by α and β. This family of semi-norms generates a translation invariant topology; if a linear function on $\mathcal{S}$ is continuous at 0, then it is continuous everywhere on S. As such T is continuous if

$$\lim_{n\to\infty} T(\varphi_n) = 0 \qquad \text{whenever} \qquad \lim_{n\to\infty} \varphi_n = 0.$$

By choosing appropriate semi-norms one can show that $\mathcal{S} \subset L^1$ and hence $\hat{\varphi}$ is well defined for all $\varphi \in \mathcal{S}$.

More significantly the operators $\hat{}$ and $\check{}: \mathcal{S} \to \mathcal{S}$ are linear and continuous with respect to the topology on $\mathcal{S}$. It is straightforward to show that for $\varphi, \phi \in \mathcal{S}$

$$\int \hat{\varphi}(x)\phi(x)dx = \int \varphi(x)\hat{\phi}(x)dx.$$

By choosing ϕ to be $\overline{\hat{\psi}} \in \mathcal{S}$ and verifying the effect of interchanging the order of taking a complex conjugate and taking a Fourier transform one obtains

$$\int \varphi(x)\overline{\psi}(x)dx = \int \hat{\varphi}(x)\overline{\hat{\psi}}(x)dx.$$

By choosing $\varphi = \psi$, it follows that $\|\varphi\|_2 = \|\hat{\varphi}\|_2$. This shall be our starting point for extending the Fourier transform to L^2 functions.

Let $\phi \in \mathcal{S}$ so that $\operatorname{supp}\phi \subset B(0,1)$ [3] and $\|\phi\|_1 = 1$. Let $\phi^\varepsilon = \frac{1}{\varepsilon^p}\phi\left(\frac{\cdot}{\varepsilon}\right)$. As ε decreases the support of ϕ^ε contracts, while ϕ^ε gets scaled so that the L^1-norm is preserved. Let f be a compactly supported function in L^2, then $f \in L^1 \cap L^2$. Define

$$f_\varepsilon := \int f(\cdot - y)\phi^\varepsilon(y)dy.$$

[3] The support of a function is the closure of the set of points where the function is non-zero.

It is a standard result (cf. [9, ch. 5]) that $f_\varepsilon \in C^\infty$, that

$$\lim_{\varepsilon \downarrow 0} \|f - f_\varepsilon\|_1 = 0, \quad \lim_{\varepsilon \downarrow 0} \|f - f_\varepsilon\|_2 = 0$$

and that every point in supp f_ε is within ε of supp f, hence $f_\varepsilon \in \mathcal{S}$.

Since f_ε is converging in L^2 and since $\|f_\varepsilon\|_2 = \|\hat{f}_\varepsilon\|_2$, $\hat{f}_\varepsilon$ is Cauchy with respect to the L^2-norm along any subsequence of decreasing ε. Since L^2 is complete, $\hat{f}_\varepsilon$ is convergent and we denote its limit as $\mathcal{F}f$. Since f_ε is converging in L^1 to f, $\hat{f}_\varepsilon$ is converging in L^∞ to $\hat{f}$, we conclude $\mathcal{F}f = \hat{f}$ a.e. and that $\|f\|_2 = \|\mathcal{F}f\|_2$.

Let f be an arbitrary function in L^2 and let $f_n := f\chi_{B(0,n)}$ (where $\chi_E(x) = 1$ for $x \in E$ and $\chi_E(x) = 0$ for $x \notin E$). Then f_n is compactly supported, is in $L^1 \cap L^2$ and $f_n \to f$ in L^2. Then the limit $\lim_{n\to\infty} \mathcal{F}f_n$ exists and its value is denoted $\hat{f}$. With this we have the following theorem:

Theorem 2.3.1 (cf. [10]). *Let $f \in L^2$, then the limit*

$$\hat{f}(\xi) := \lim_{R\to\infty} \int_{|x|<R} f(x)e^{-2\pi i x\cdot\xi} dx$$

converges in L^2. We call $\hat{f}$ the Fourier transform of f. The Fourier transform defined in this manner is an isometric isomorphism from L^2 to itself with an inverse given by

$$\check{f}(x) := \lim_{R\to\infty} \int_{|\xi|<R} f(\xi)e^{2\pi i x\cdot\xi} d\xi.$$

2.3.3 $L^1 + L^2$ Functions

Note that if a function $f \in L^1 \cap L^2$, then the Fourier transform given by Theorem 2.3.1 agrees with the Fourier transform given by equation (2.6). We consider functions of the form $f = f_1 + f_2$ where $f_1 \in L^1$ and $f_2 \in L^2$. For such an f we may unambiguously define the Fourier transform a.e. as $\hat{f} = \hat{f}_1 + \hat{f}_2$, where $\hat{f}_1 \in L^\infty$ and $\hat{f}_2 \in L^2$. This is independent

of the choice of f_1 and f_2. If $f = f_1' + f_2'$ is another representation of f, then

$$f_1 + f_2 = f_1' + f_2' \qquad \text{hence} \qquad f_1 - f_1' = f_2' - f_2.$$

Then $f_1 - f_1' \in L^1$ and $f_2 - f_2' \in L^2$. Since $\hat{}$ is well defined and linear on $L^1 \cap L^2$, we have

$$\hat{f}_1 - \hat{f}_1' = \hat{f}_2' - \hat{f}_2 \qquad \text{hence} \qquad \hat{f}_1 + \hat{f}_2 = \hat{f}_1' + \hat{f}_2'.$$

The following will be useful for computing the Fourier transform of a particular kernel function.

Proposition 2.3.2 (cf. [50]). *If $f \in L^1 + L^2$ and M is an invertible matrix, then*

$$\widehat{f \circ M} = \frac{1}{|\det M|} \hat{f} \circ (M^{-1})^T.$$

2.3.4 Measures and Tempered Distributions

Let μ be a signed measure such that $|\mu|$ is a compactly supported Radon measure, then we may define the Fourier transform of μ as

$$\hat{\mu}(\xi) := \int e^{-2\pi i x \cdot \xi} d\mu(x).$$

Analogous to the L^1 case, we have that $|\hat{\mu}(\xi)| \leq \mu(\mathbb{R}^p)$.

Theorem 2.3.3. *If μ is a compactly supported Radon measure and $\hat{\mu} \in L^2$, then μ is absolutely continuous with respect to Lebesgue Measure and $d\mu/d\mathcal{L}^p \in L^2$*

The space of tempered distributions is the space of continuous linear functionals on $\mathcal{S}$ and is defined

$$\mathcal{S}^* := \{T : \mathcal{S} \to \mathbb{R} \ : \ T \text{ is linear and } \lim_{n\to\infty} T(\varphi_n) = 0 \text{ whenever } \lim_{n\to\infty} \varphi_n = 0 \text{ in } \mathcal{S}\}.$$

While $\mathcal{S}$ is a not a normed space, we still consider the space of tempered distributions as the dual space of $\mathcal{S}$, hence the notation $\mathcal{S}^*$. We say that $\hat{T}$ is the Fourier transform of T if $\hat{T}\varphi = T\hat{\varphi}$ for all $\varphi \in \mathcal{S}$. With this definition we have the following proposition (cf. [10].)

Proposition 2.3.4 (cf. [10]). *The Fourier transform is a continuous linear bijection from $\mathcal{S}^*$ to $\mathcal{S}^*$.*

The following proposition and corollary will be particularly useful examining a kernel that arises in potential theory.

Proposition 2.3.5. *If $f \in L^1 + L^2$ and $\varphi \in \mathcal{S}$ then*

$$\int f(x)\hat{\varphi}(x)dx = \int \hat{f}(x)\varphi(x)dx.$$

For convenience we introduce the following notation for a function $f : \mathbb{R}^p \to \mathbb{R}$,

$$[f > \alpha] := \{x \in \mathbb{R}^p \ : \ f(x) > \alpha\}.$$

Similarly we define $[f \geq \alpha]$, $[f < \alpha]$ and $[f \leq \alpha]$.

We shall use the notion of weak-convergence in a Hilbert space in the following proof. We say $\{f_n\}_{n=1}^{\infty}$ converges to f weakly in a Hilbert space H if $\langle f_n, g\rangle \to \langle f, g\rangle$ for every $g \in H$. Strong convergence, i.e. $\|f_n - f\|_2 \to 0$ implies weak convergence.

Proof. Let $f \in L^1 + L^2$ and $\varphi \in \mathcal{S}$.

$$\begin{aligned}
\int f(x)\hat{\varphi}(x)dx &= \lim_{n\to\infty} \int_{B(0,n)} f(x)\hat{\varphi}(x)\,dx \\
&= \lim_{n\to\infty} \int_{B(0,n)} f(x) \int \varphi(y)e^{-2\pi i x\cdot y}\,dy\,dx \\
&= \lim_{n\to\infty} \int \varphi(y) \int_{B(0,n)} f(x)e^{-2\pi i x\cdot y}\,dx\,dy \\
&= \lim_{n\to\infty} \int \varphi(y)\left(\int_{B(0,n)} f\chi_{[f\geq 1]}(x)e^{-2\pi i x\cdot y}\,dx + \int_{B(0,n)} f\chi_{[f<1]}(x)e^{-2\pi i x\cdot y}\,dx\right)dy
\end{aligned}$$

Note that

$$\left| \int_{B(0,n)} f(x)\chi_{[f\geq 1]} e^{-2\pi i x\cdot y}\, dx \right| < \|f\chi_{[f\geq 1]}\|_1 < \infty,$$

and by dominated convergence

$$\lim_{n\to\infty} \int \varphi(y) \int_{B(0,n)} f\chi_{[f\geq 1]}(x) e^{-2\pi i x\cdot y}\, dx\, dy = \int \varphi(y)\, \widehat{f\chi_{[f\geq 1]}}(y) dy.$$

Also the functions

$$g_n(y) := \int_{B(0,n)} f\chi_{[f<1]}(x) e^{-2\pi i x\cdot y}\, dx$$

are converging in L^2 to $\widehat{f\chi_{[f<1]}}$ and so

$$\begin{aligned} &\lim_{n\to\infty} \int \varphi(y) \int_{B(0,n)} f\chi_{[f<1]}(x) e^{-2\pi i x\cdot y}\, dx\, dy = \lim_{n\to\infty} \langle \varphi, g_n \rangle \\ = &\int \varphi(y)\, \widehat{f\chi_{[f<1]}}(y) dy, \end{aligned}$$

Here $\langle \cdot, \cdot \rangle$ is the standard inner-product in L^2. We may then combine our limits to obtain the Fourier transform of f. This completes the proof. □

This gives us the following corollary:

Corollary 2.3.6. *If $T_f \in \mathcal{S}^*$ has the representation*

$$T_f \varphi = \int f(x)\varphi(x) dx$$

where $f \in L^1 + L^2$, then $\hat{T}_f = T_{\hat{f}}$.

2.4 Potential Theory

In this section we shall examine classical potential theory as a natural extension of electrostatics. We begin with a discussion of energies and potentials of Radon measures and examine the relationship between potentials and approximate densities. We then consider

the problem of finding the lowest possible energy for a measure of unit mass supported on a compact set A. This leads to the questions of the existence and uniqueness of a measure that achieves this energy. Both these questions have affirmative answers and the latter is established through Hilbert space techniques. We review a characterization the energy minimizing measure in terms of its potential. Finally, we examine results for a related discrete problem.

This material is covered in more depth in [21, 30, 34].

2.4.1 Energies, Potentials of Measures, the Set $\mathcal{E}_s$ and Average Densities

Let μ be a Radon measure with support in $\mathbb{R}^p$ and $s > 0$. The *Riesz (s-)energy of* μ is defined as

$$I_s(\mu) := \iint \frac{1}{|x-y|^s} d\mu(y) d\mu(x).$$

The integrand $\frac{1}{|x-y|^s}$ is referred to as the *Riesz (s)-kernel* and is positive. The measure μ is unsigned and so the quantity $I_s(\mu)$ is well defined and may take on the value $+\infty$. The inner integral

$$U_s^\mu(x) := \int \frac{1}{|x-y|^s} d\mu(y)$$

is called the *(s)-potential of* μ *at* x. We have that

$$I_s(\mu) = \int U_s^\mu d\mu.$$

In $\mathbb{R}^3$ the Riesz kernel of exponent 1 is proportional to the Coloumb kernel and it is natural to consider $U_s^\mu(x)$ as a generalized electrostatic potential at the point x caused by the presence of the charge distribution μ. Following this interpretation $I_s(\mu)$ integrates the potential due to the charge distribution μ against the distribution itself and is a reasonable generalization of the electrostatic energy.

If we let $\nu = \nu^+ - \nu^-$ be the Jordan decomposition of the signed measure ν where $|\nu|$ is

Radon, then formally we may write

$$\begin{aligned} I_s(\nu) &= \iint \frac{1}{|x-y|^s} d(\nu^+ - \nu^-)(y) d(\nu^+ - \nu^-)(x) \\ &= \iint \frac{1}{|x-y|^s} d\nu^+(y) d\nu^+(x) + \iint \frac{1}{|x-y|^s} d\nu^-(y) d\nu^-(x) \qquad (2.7) \\ &- \left(\iint \frac{1}{|x-y|^s} d\nu^+(y) d\nu^-(x) + \iint \frac{1}{|x-y|^s} d\nu^-(y) d\nu^+(x) \right). \qquad (2.8) \end{aligned}$$

This is well defined so long as it is not the difference of two quantities both of which are infinite. Each of the four integrals in (2.7) - (2.8) is well defined for the same reasons the s-energy of a Radon measure μ is. Further each of these integrals is less than or equal to $I_s(|\nu|)$. From this we conclude that if $I_s(|\nu|) < \infty$, then $I_s(\nu)$ is well defined and finite. With this motivation we define the following set of signed measures

$$\mathcal{E}_s := \{\mu \text{ a measure supported on } \mathbb{R}^p \text{ such that } |\mu| \text{ is Radon and } I_s(|\mu|) < \infty\}.$$

One may verify that the set $\mathcal{E}_s$ is closed under addition and multiplication by scalars.

If μ is Radon, then $\mu(B(x,r))$ and the *average d-density* $\mu(B(x,r))/r^d$ are both well defined and finite for all $x \in \mathbb{R}^p$ and all $r > 0$. The average d-density and potential of a measure are related by the following useful application of Tonelli's Theorem (cf. [9, ch. 3].)

Let $f : \mathbb{R}^p \to \mathbb{R}$ be a non-negative Borel-measurable function and μ a Radon measure with support in $\mathbb{R}^p$. We have

$$\begin{aligned} \int f(y) d\mu(y) &= \int \left(\int_0^{f(y)} dt \right) d\mu(y) \\ &= \int \left(\int_0^{\infty} \chi_{[0,f(y)]}(t) dt \right) d\mu(y) \\ &= \int_0^{\infty} \left(\int \chi_{[0,f(y)]}(t) d\mu(y) \right) dt \\ &= \int_0^{\infty} \mu(\{y \,:\, f(y) \geq t\}) dt, \end{aligned}$$

where the interchange of the order of integration is permitted by Tonelli's Theorem.

When the function f is the Riesz kernel the above gives the following:

$$\begin{aligned} U_s^\mu(x) &= \int \frac{1}{|x-y|^s} d\mu(y) \\ &= \int_0^\infty \mu\left(\left\{y \,:\, \frac{1}{|x-y|^s} \geq t\right\}\right) dt \\ &= \int_0^\infty \mu(\{y \,:\, |x-y| \leq t^{-1/s}\}) dt \\ &= s\int_0^\infty \frac{\mu(\{y \,:\, |x-y| \leq r\})}{r^{s+1}} dr \qquad \text{here we make the replacement } r = t^{-1/s} \\ &= s\int_0^\infty \frac{\mu(B(x,r))}{r^{s+1}} dr = s\int_0^\infty \left(\frac{\mu(B(x,r))}{r^d}\right) r^{d-s-1} dr \end{aligned} \tag{2.9}$$

If μ is a compactly supported Radon measure, then $\mu(B(x,r)) \leq \mu(\mathbb{R}^p) < \infty$ for all x and $r > 0$. If in addition μ satisfies the condition that there is a $C < \infty$ so that the average d-density satisfies $\mu(B(x,r))/r^d < C$ for all $x \in \mathbb{R}^p$ and all $r > 0$, then

$$\begin{aligned} U_s^\mu(x) &= s\int_0^1 \left(\frac{\mu(B(x,r))}{r^d}\right) r^{d-s-1} dr + s\int_1^\infty \left(\frac{\mu(B(x,r))}{r^d}\right) r^{d-s-1} dr \\ &< s\int_0^1 C\, r^{d-s-1} dr + s\int_1^\infty \left(\frac{\mu(\mathbb{R}^p)}{r^d}\right) r^{d-s-1} dr \\ &= \frac{sC}{d-s} + \mu(\mathbb{R}^p) < \infty. \end{aligned}$$

We conclude that if a compactly supported Radon measure satisfies the condition that $\mu(B(x,r)) < Cr^d$ for all $x \in \mathbb{R}^p$ and all $r > 0$, then U_s^μ is uniformly bounded in $\mathbb{R}^p$. *Note that on the last line the expression* $1/(d-s)$ *appears. This factor will play a significant role in the next chapter.*

The condition $\mu(B(x,r)) < Cr^d$ is commonly referred to as a *growth condition on* μ. There are many common cases where this condition occurs. Let L be a line in $\mathbb{R}^p$, then $\mathcal{H}_L^1$ satisfies this growth condition for $d = 1$. Similarly if P is a two-dimensional hyper-plane in $\mathbb{R}^p$, then $\mathcal{H}_P^2$ satisfies this growth condition for $d = 2$. More generally, given a compact

d-dimensional manifold X embedded in $\mathbb{R}^p$, then $\mathcal{H}^d_X$ satisfies this growth condition. The Dirac-delta measure does not satisfy this condition for any $d > 0$.

2.4.2 Capacity, The Principle of Descent and the Existence of a Minimizing Measure

Let $A \subset \mathbb{R}^p$ be a compact set. The s-capacity of A is defined[4] as

$$\mathrm{Cap}_s(A) := \sup\{1/I_s(\mu) \,:\, \mu \in \mathcal{M}_1^+(A)\},$$

where $\mathrm{Cap}_s(A)$ is defined to be 0 if $\mathcal{M}_1^+(A) \cap \mathcal{E}_s = \varnothing$. As is shown below if $\mathcal{H}^d(A) > 0$, then $\mathcal{M}_1^+(A) \cap \mathcal{E}_s = \varnothing$ if, and only if, $s \geq d$. This fact follows from Theorem 2.4.1 and Lemma 2.4.2. Note that $I_s(\mu) > (\operatorname{diam} A)^{-s}$ for every $\mu \in \mathcal{M}_1^+(A)$ so $\mathrm{Cap}_S(A) < \infty$ for every s and every compact set A.

In the case $s < d$ we have Frostman's lemma (cf. [34]).

Theorem 2.4.1 (Frostman's Lemma). *Let A be a Borel set in $\mathbb{R}^p$. $\mathcal{H}^d(A) > 0$ if and only if there exists a non-trivial measure $\mu \in \mathcal{M}^+(A)$ such that $\mu(B(x,r)) < r^d$ for μ-a.a. $x \in \mathbb{R}^p$ and $r > 0$.*

An immediate corollary is that if $\mathcal{H}^d(A) > 0$, then there is a measure $\mu \in \mathcal{M}_1^+(A)$ and a constant $C < \infty$ so that $\mu(B(x,r)) < Cr^d$ for all $x \in \mathbb{R}^p$ and all $r > 0$. This is precisely the growth condition we need for U^μ_s to be uniformly bounded, and hence for $I_s(\mu)$ to be finite. We can conclude that if $s < d$, then $\mathrm{Cap}_s(A) > 0$.

If $s \geq d$ then $\mathcal{M}_1^+(A) \cap \mathcal{E}_s = \varnothing$. This follows from the next lemma (cf. [34]). While the lemma only makes a statement about the case $s = d$, the result holds for $s > d$ as well for the following reason: If μ is a compactly supported Radon measure so that $I_s(\mu) = \infty$ for

[4]This notion of capacity mirrors the notion of capacity from electrostatics in that both are reciprocals of energy, although in the electrostatic case positive and negative charge are distributed over disjoint regions, typically capacitor plates.

some s, then

$$\infty = I_s(\mu) = \iint_{|x-y|<1} \frac{1}{|x-y|^s} d\mu(y) d\mu(x) + \iint_{|x-y|\geq 1} \frac{1}{|x-y|^s} d\mu(y) d\mu(x)$$

Since A is compact the second integral is finite and hence the first must be infinite. But then for any $t > s$ and any x, y so that $|x - y| < 1$, we have that

$$\frac{1}{|x-y|^s} < \frac{1}{|x-y|^t}.$$

This is enough to show that $I_t(\mu) = \infty$ as well.

Lemma 2.4.2 (cf. [34]). *Let A be a compact subset of $\mathbb{R}^p$ such that $\mathcal{H}^d(A) < \infty$. Then $I_d(\mu) = \infty$ for every $\mu \in \mathcal{M}_1^+(A)$.*

Proof. For sake of contradiction assume that $I_d(\mu) < \infty$ for some $\mu \in \mathcal{M}_1^+(A)$. Then $U_d^\mu(x)$ is finite for μ-a.e x. For such an x

$$\lim_{r \downarrow 0} \int_{B(x,r)} \frac{1}{|x-y|^d} d\mu(y) = 0.$$

By Egorov's Theorem we can select a set A_0 such that $\mu(A_0) > 1/2$ and the above limit is uniform in A_0. Fix $\varepsilon > 0$ and find an $r_0 = r_0(\varepsilon)$ such that for all $x \in A_0$ and all $r < r_0$

$$\mu(B(x,r)) r^{-d} \leq \int_{B(x,r)} \frac{1}{|x-y|^d} d\mu(y) < \varepsilon,$$

allowing us to conclude that for all $x \in A_0$ and all $r < r_0$,

$$\mu(B(x,r)) < \varepsilon r^d.$$

From the definition of the Hausdorff measure, we may find a collection of sets $\{Q_i\}_{i=1}^\infty$ such that

(a) $A_0 \subset \bigcup_{i=1}^{\infty} Q_i$

(b) $A_0 \cap Q_i \neq \varnothing$ for all $i \in 1, 2, \ldots$

(c) $\operatorname{diam} Q_i < r_0$ for all $i \in 1, 2, \ldots$

(d) $\sum_{i=1}^{\infty} (\operatorname{diam} Q_i)^d < \mathcal{H}^d(A_0) + 1$.

For each Q_i, select an $x_i \in Q_i \cap A_0$ and let $r_i := \operatorname{diam} Q_i$. Then

$$\frac{1}{2} < \mu(A_0) \leq \sum_{i=1}^{\infty} \mu(B(x_i, r_i) \leq \varepsilon \sum_{i=1}^{\infty} r_i^d < \varepsilon(\mathcal{H}^d(A_0) + 1).$$

Since ε is arbitrarily small, $\mathcal{H}^d(A_0)$ cannot be finite and hence $\mathcal{H}^d(A)$ cannot be finite. □

One might think of the preceding lemma as an extension of the fact that in $\mathbb{R}^d$

$$\int_{B(0,1)} \frac{1}{|x|^s} dx$$

is finite only when $s < d$. The preceding lemma is quite general, however, in that it holds for non-integral values of d.

With this one may define a *capacitary dimension* (cf. [34]) as

$$\dim_C(A) := \sup\{s \in \mathbb{R}_+ \,:\, I_s(\mu) < \infty \text{ for some } \mu \in \mathcal{M}_1^+(A)\}$$

Theorem 2.4.1 and Lemma 2.4.2 prove the following:

Proposition 2.4.3. *Let A be a compact set in $\mathbb{R}^p$ such that the Hausdorff dimension of A ($\dim A$) is d. If $\mathcal{H}_A^d$ is a σ-finite measure – that is to say, $\mathcal{H}_A^d$ can be subdivided into a countable sum of finite measures, then $\dim A$ agrees with the capacitary dimension $\dim_C(A)$.*

Having established the conditions ($s < d = \dim A$) for which the s-capacity of A is non-zero, we show that there is at least one measure whose s-energy is the reciprocal of the

s-capacity, that is, there is a measure μ' such that

$$I_s(\mu') = \inf\{I_s(\mu) \,:\, \mu \in \mathcal{M}_1^+(A)\}. \tag{2.10}$$

To prove this we shall employ some further results regarding the weak-star convergence of measures.

Lemma 2.4.4. *Let A be a compact subset of $\mathbb{R}^p$ and let $\{\mu_n\}_{n=1}^{\infty} \subset \mathcal{M}^+(A)$ be a sequence of measures converging in the weak-star topology to $\nu \in \mathcal{M}^+(A)$, then*

$$\lim_{n\to\infty} \iint f(x,y)d\mu_n(x)d\mu_n(y) = \iint f(x,y)d\nu(x)d\nu(y)$$

for any $f \in C(A \times A)$.

A sketch of a proof of this lemma is as follows: Consider the case when f is a polynomial on $\mathbb{R}^p \times \mathbb{R}^p$, then f may be written as a sum of monomials on $A \times A$. The integral of each monomial on $A \times A$ is the product of integrals of monomials on A, and the weak-star convergence $\mu_n \xrightarrow{*} \nu$ applied to a polynomial restricted to A ensures that the claim holds for such an f. By the Weierstrass Approximation Theorem polynomials on $\mathbb{R}^p \times \mathbb{R}^p$ are dense in set $C(A \times A)$ with regards to the topology induced by the sup-norm.

Our next tool is the *Principle of Descent* which is expressed in the following lemma:

Lemma 2.4.5. *Let A be a compact subset of $\mathbb{R}^p$. Let $\{\mu_n\}_{n=1}^{\infty} \subset \mathcal{M}^+(A)$ such that $\mu_n \xrightarrow{*} \nu \in \mathcal{M}^+(A)$. Then*

$$I_s(\nu) \leq \liminf_{n\to\infty} I_s(\mu_n).$$

Proof. Define the following continuous function from $\mathbb{R}_+$ to $\mathbb{R}_+$:

$$k_s^{\delta}(r) := \begin{cases} \frac{1}{r^s} & r \geq \delta \\ \delta^{-s} & r < \delta. \end{cases} \tag{2.11}$$

For each pair of distinct x and y $k_s^\delta(|x-y|) \leq |x-y|^{-s}$ and

$$\lim_{\delta \downarrow 0} \left(\frac{1}{|x-y|^s} - k_s^\delta(|x-y|) \right) = 0.$$

We have

$$\begin{aligned} \iint \frac{1}{|x-y|^s} d\nu(y) d\nu(x) &\leq \liminf_{\delta \downarrow 0} \iint k_s^\delta(|x-y|) d\nu(y) d\nu(x) \quad \text{(by Fatou's Lemma)} \\ &= \liminf_{\delta \downarrow 0} \lim_{n \to \infty} \iint k_s^\delta(|x-y|) d\mu_n(y) d\mu_n(x) \quad (\text{since } \mu_n \overset{*}{\to} \nu) \\ &\leq \liminf_{n \to \infty} \iint \frac{1}{|x-y|^s} d\mu_n(y) d\mu_n(x) \end{aligned}$$

□

We are now prepared to show the existence of a measure μ' satisfying (2.10). This argument is presented in a variety of texts including [30].

Proposition 2.4.6. *Let $A \subset \mathbb{R}^p$ be compact. Let $s < d := \dim A$. There is a measure $\mu' \in \mathcal{M}_1^+(A)$ such that $I_s(\mu') = \inf\{I_s(\mu) : \mu \in \mathcal{M}_1^+(A)\}$.*

Proof. Let $W_s = \inf\{I_s(\mu) : \mu \in \mathcal{M}_1^+(A)\}$, as already noted $W_s > 0$. Let $\{\mu_n\}_{n=1}^\infty$ be a sequence so that

$$\lim_{n \to \infty} I_s(\mu_n) = W_s.$$

By Helly's Selection Theorem we may chose a cluster point $\psi \in \mathcal{M}_1^+(A)$ of $\{\mu_n\}_{n=1}^\infty$ and a subsequence $\{\mu_k\}_{k=1}^\infty \subset \{\mu_n\}_{n=1}^\infty$ so that $\mu_k \overset{*}{\to} \psi$. By the Principle of Descent we have

$$W_s \leq I_s(\psi) \leq \liminf_{k \to \infty} I_s(\mu_k) = \lim_{n \to \infty} I_s(\mu_n) = W_s.$$

This implies $I_s(\psi) = W_s$ and so our claimed measure μ' is ψ. To see that ψ is of unit mass, choose the continuous function to be the constant 1. □

2.4.3 **Hilbert Space Techniques and The Uniqueness of the Minimizing Measure**

The proof of the existence of a minimizing measure for the Riesz s-energy in the previous section relied on two facts about the Riesz s-kernel. First, the arguments presented in section 2.4.1 showed that if a measure had a certain growth condition, then the singularity in the Riesz s-kernel was integrable with respect to that measure. Frostman's lemma ensures there is a measure with this growth condition, and so there is at least one measure with finite energy. Second, in the proof of the Principle of Descent we used the fact that the Riesz s-kernel can be approximated pointwise from below by continuous functions. In this section we will use another feature of the Riesz s-kernel, namely that it forms an inner product on the set $\mathcal{E}_s$, to show that the energy minimizing measure we identified in the previous section is unique.

The set $\mathcal{E}_s$ is the vector space of all signed measures of finite energy. As such the bi-linear form

$$\langle \mu, \nu \rangle_s := \iint \frac{1}{|x-y|^s} d\mu(x) d\nu(y)$$

is well-defined. Intuitively this is the amount of energy required to assemble the charge distribution μ in the presence of the charge distribution ν. For $\langle \cdot, \cdot \rangle_s$ to be an inner product it must also satisfy the positivity requirement that $\langle \mu, \mu \rangle_s = 0$ if, and only if, $\mu \equiv 0$. We reproduce arguments (cf. [30]) based on Fourier techniques to show this.

The function $f(x) := |x|^{-s}$ defines a functional on $\mathcal{S}$ as follows

$$T_f(\varphi) := \int \frac{1}{|x|^s} \varphi(x) dx.$$

If $s \in (0, p)$, then this integral is absolutely convergent as follows:

$$\begin{aligned} \int \frac{1}{|x|^s} |\varphi(x)| dx &= \int_{B(0,1)} \frac{1}{|x|^s} |\varphi(x)| dx + \int_{\mathbb{R}^p \setminus B(0,1)} \frac{1}{|x|^s} |\varphi(x)| dx \\ &\leq \|\varphi\|_\infty \int_{B(0,1)} \frac{1}{|x|^s} dx + \int_{\mathbb{R}^p \setminus B(0,1)} |\varphi(x)| dx < \infty. \end{aligned}$$

From this we may conclude that T_f is linear as well. To show that T_f is continuous, let $\{\varphi_n\}_{n=1}^{\infty} \subset \mathcal{S}$ be a sequence converging to 0 in $\mathcal{S}$. This implies that

$$\lim_{n\to\infty} \|\varphi_n\|_\infty = 0 \qquad \text{and} \qquad \lim_{n\to\infty} \left\| |\cdot|^{p+1}\varphi_n \right\|_\infty = 0.$$

Choose an N large enough so that for all $n > N$ we have $\|\varphi_n\|_\infty < 1$ and $\left\| |\cdot|^{p+1}\varphi_n \right\|_\infty < 1$. For such n we have the following bound

$$\frac{1}{|x|^s}|\varphi_n(x)| \le g(x) := \begin{cases} |x|^{-s} & |x| \le 1 \\ |x|^{-(s+p+1)} & |x| > 1. \end{cases}$$

One may quickly see that g is integrable, and so we appeal to dominated convergence and conclude that

$$\lim_{n\to\infty} T_f(\varphi_n) = 0.$$

This establishes that $T_f \in \mathcal{S}^*$ and we may consider its Fourier transform in the sense of distributions.

We shall not compute the Fourier transform of $|x|^{-s}$ directly, but rather infer it based on properties of T_f. The following arguments are taken from [10, 50][5]. Proofs of this fact are also presented in [23, 34]. Consider the case when $s > p/2$. The function $f(x) := |x|^{-s}$ may be written as $f = f\chi_{B(0,1)} + f\chi_{\mathbb{R}^p \setminus B(0,1)}$. Because $s < p$, $f\chi_{B(0,1)} \in L^1$ and because $s > p/2$, $f\chi_{\mathbb{R}^p\setminus B(0,1)} \in L^2$, thus $f \in L^1 + L^2$.

If we consider Proposition 2.3.2 where M is chosen to be a rotation matrix, then because $f \circ M = f$ we have

$$\hat{f} = \widehat{f \circ M} = \hat{f} \circ (M^{-1})^T,$$

and we conclude that $\hat{f}$ is a radial function.

[5] In [10] these arguments are presented quite concisely by tacitly equating properties of the Fourier transform of a tempered distribution T_f with properties of f. We shall provide those details.

A tempered distribution T is said to be *homogenous of degree a* if

$$T\left(\frac{\varphi(\cdot/\lambda)}{\lambda^p}\right) = \lambda^a T\varphi,$$

for all $\varphi \in \mathcal{S}$ and all $\lambda > 0$. With this definition we have the following:

Proposition 2.4.7. *If $T \in \mathcal{S}^*$ is homogeneous of degree a, then $\hat{T}$ is homogeneous of degree $-p - a$.*

The proof follows from the definition of $\hat{T}$ and an application of Proposition 2.3.2 to $\varphi(\cdot/\lambda)$.

One may verify that T_f is homogeneous of degree $-s$ and so $\hat{T}_f$ is homogenous of degree $s - p$. From this and Corollary 2.3.6 it follows that

$$\int \left[\hat{f}(\lambda x) - \lambda^{s-p}\hat{f}(x)\right]\varphi(x)dx = 0, \tag{2.12}$$

for every $\varphi \in \mathcal{S}$.

We now employ arguments similar to those used in Section 2.3.2. Let $g := \hat{f}(\lambda\cdot) - \lambda^{s-p}\hat{f}$ and let $\phi \in \mathcal{S}$ be compactly supported such that $\|\phi\|_1 = 1$. Define $\phi^\varepsilon := \frac{1}{\varepsilon^p}\phi\left(\frac{\cdot}{\varepsilon}\right)$. By choosing φ in equation (2.12) as $\phi^\varepsilon(y - \cdot)$, we have

$$g * \phi^\varepsilon(y) = 0 \qquad \text{for all } y \in \mathbb{R}^p.$$

If we let $K \subset \mathbb{R}^p$ be a compact set, then (cf. [9, ch.5] for details.)

$$\lim_{\varepsilon \downarrow 0} \|(g\chi_K) * \phi^\varepsilon - g\chi_K\|_p = 0,$$

for $1 \leq p < \infty$. (This is the essential argument used in [9] to prove the density of $\mathcal{S} \subset L^p$.)

This implies g must be zero a.e. and so

$$\hat{f}(\lambda x) = \lambda^{s-p}\hat{f}(x) \qquad \text{for a.a. } x \in \mathbb{R}^p, \tag{2.13}$$

Since $\hat{f}$ is radial there is a function $\underline{f}$ such that $\hat{f}(x) = \underline{f}(|x|)$ for a.a. $x \in \mathbb{R}^p$. Integrating both sides of (2.13) over the ball $B(0,R)$ gives

$$\int_0^R \underline{f}(\lambda r) r^{p-1} dr = \lambda^{s-p} \int_0^R \underline{f}(r) r^{p-1} dr,$$

Letting $u = \lambda r$ gives

$$\frac{1}{\lambda^p} \int_0^{\lambda R} \underline{f}(u) u^{p-1} du = \lambda^{s-p} \int_0^R \underline{f}(r) r^{p-1} dr.$$

Choose $R = 1$ and let

$$C = \int_0^1 \underline{f}(r) r^{p-1} dr,$$

and then

$$\int_0^{\lambda} \underline{f}(u) u^{p-1} du = \lambda^s C. \tag{2.14}$$

By the absolute continuity of the integral we may differentiate both sides with respect to λ and conclude

$$\underline{f}(\lambda)\lambda^{p-1} = \lambda^{s-1} C$$

Hence $\hat{f}(x) = c(s,p)|x|^{s-p}$ for some constant $c(s,p)$ depending on s and p. By proposition 2.3.5 and the fact that the Gaussian $e^{-\pi|x|^2}$ is its own Fourier transform we obtain

$$\int e^{-\pi|x|^2} |x|^{-s} dx = c(s,p) \int e^{-\pi|x|^2} |x|^{s-p} dx. \tag{2.15}$$

Converting to radial coordinates and making the substitution $u = \sqrt{\pi r}$ both sides may be

written as Gamma functions and we see that

$$c(s,p) = 2\pi^{s-\frac{p}{2}} \frac{\Gamma\left(\frac{p-s}{2}\right)}{\Gamma\left(\frac{s}{2}\right)}. \tag{2.16}$$

In the following chapters we shall be interested in the case when $s \in (p/2, p)$. However this result can be extended to all $s \in (0, p)$. The case $s \in (0, p/2)$ is handled roughly as follows: If $f_s := |\cdot|^{-s}$, then $\hat{f}_s = \check{f}_s$ where $\hat{}$ and $\check{}$ are considered in the sense of $L^1 + L^2$ functions. We then have

$$\hat{T}_{f_s} = T_{\hat{f}_s} = T_{\check{f}_s} = \check{T}_{f_s}.$$

From the previous calculations we have

$$\check{T}_{f_s} = \hat{T}_{f_s} = c(s,p) T_{f_{p-s}}.$$

Taking the Fourier transform of the leftmost and rightmost expressions gives

$$\hat{T}_{f_{p-s}} = \frac{1}{c(s,p)} T_{f_s}. \tag{2.17}$$

Equation (2.17) holds for $s \in (p/2, p)$ and hence for $p - s \in (0, p/2)$. The case $s = p/2$ is handled by continuity arguments.

Having established the Fourier transform in the distributional sense of the function $|\cdot|^{-s}$, we refer to a result in [50] that the energy $I_s(\mu)$ for $\mu \in \mathcal{E}_s$ can be expressed as

$$I_s(\mu) = c(s,p) \int |\xi|^{s-p} |\hat{\mu}(\xi)|^2 \, d\xi = \langle \mu, \mu \rangle_s. \tag{2.18}$$

This is sufficient to establish positivity of $\langle \cdot, \cdot \rangle_s$. If $\langle \mu, \mu \rangle_s = 0$, then $\hat{\mu}$ is zero a.e. and by Theorem 2.3.3, $\mu \equiv 0$. [6]

[6] In [22] M. Gotz provides an alternate proof of the positivity of the Riesz kernel using geometric arguments that avoid the Fourier transform.

This shows that $(\mathcal{E}_s, \langle\cdot,\cdot\rangle_s)$ is a pre-Hilbert space. The norm arising from this Hilbert space is $\|\cdot\|_s := \sqrt{I_s(\cdot)}$ and is referred to as the *(s-)energy norm*. The following theorem is central to the proof of a unique minimizing measure and potential theory in general. The proof is technical and we omit it. The interested reader should consult [21] or [30, p.90].

Theorem 2.4.8. *The positive cone of (unsigned) measures in $\mathcal{E}_s$ is topologically complete with respect to the metric induced from the norm $\|\cdot\|_s$. The space $\mathcal{E}_s$ with the same norm is not.*

We shall also need the following:

Proposition 2.4.9 (cf [30]). *Let $s \in (0, p)$. If $f : \mathbb{R}^p \to \mathbb{R}$ has compact support and continuous derivatives up to order $p + 2$ then there is a signed measure ν so that*

$$f = U_s^\nu.$$

Further, ν is absolutely continuous with respect to Lebesgue measure.

We sketch the proof for the case $s = p - 2$, a complete proof may be found in [30]. The Riesz kernel for $s = p - 2$ is proportional to the fundamental solution of Laplace's equation given by (cf. [8]):

$$F(x; y) := \frac{1}{(p-2)\omega_p} \frac{1}{|x-y|^{p-2}}$$

(Here and in the rest of this document ω_p will denote the "area" of the $(p-1)$-sphere in $\mathbb{R}^p$) For sufficiently smooth and integrable functions, ϕ and ρ, the following:

$$\phi = \frac{1}{(p-2)\omega_p} \int \frac{\rho(y)}{|\cdot - y|^{p-2}} dy$$

and

$$\rho = -\Delta\phi$$

are equivalent. If ϕ is the smooth compactly supported potential we desire, then $\frac{-\Delta\phi}{(p-2)\omega_p}$ will be the Radon-Nikodým derivative of the claimed measure ν.

The immediate consequence relevant to the topic at hand is the following:

Proposition 2.4.10. *If a sequence of measures $\{\mu_n\}_{n=1}^{\infty}$ converge in the strong topology on the pre-Hilbert space $(\mathcal{E}_s, \langle\cdot,\cdot\rangle_s)$ to μ, then the measures converge to μ in the weak-star topology on $\mathcal{M}(A)$ for any compact set $A \subset \mathbb{R}^p$.*

Again we sketch the proof and refer the interested reader to [30]. Strong convergence in a Hilbert space immediately implies weak convergence in the Hilbert space, observing that for any $\nu \in \mathcal{E}_s$

$$\int U_s^{\nu} d\mu = \langle \mu, \nu \rangle_s = \lim_{n\to\infty} \langle \mu_n, \nu \rangle_s = \lim_{n\to\infty} \int U_s^{\nu} d\mu_n,$$

that any compactly supported smooth function function f can be represented as a potential of the form U_s^{ν}, and that smooth compactly supported functions are dense in $C(A)$, we conclude weak-star convergence of $\{\mu_n\}_{n=1}^{\infty}$.

With these tools we present a proof of the uniqueness of the energy minimizing measure. (cf. [30, pp.132-133])

Theorem 2.4.11. *Let $A \in \mathbb{R}^p$ be compact so that $\mathcal{H}^d(A) > 0$, and let $s \in (0, d)$. There is a measure $\mu^{s,A} \in \mathcal{M}_1^+(A)$ such that $I_s(\mu^{s,A}) < I_s(\nu)$ for all $\nu \in \mathcal{M}_1^+(A)\backslash\{\mu^{s,A}\}$.*

Proof. As in the proof of the existence of the equilibrium measure let $\{\mu_n\}_{n=1}^{\infty} \subset \mathcal{M}_1^+(A)$ be a sequence of measures such that $\lim_{n\to\infty} I_s(\mu_n) = W_s := \inf\{I_s(\mu) : \mu \in \mathcal{M}_1^+(A)\}$. Proposition 2.4.6 and in particular Frostman's lemma ensures that $W_s < \infty$ and without lose of generality we may choose $\{\mu_n\}_{n=1}^{\infty} \subset \mathcal{M}_1^+(A) \cap \mathcal{E}_s$. Then $\sqrt{W_s} \leq \|\frac{1}{2}(\mu_m + \mu_n)\|_s$ for any m and $n \in \mathbb{N}$, and by the polarization identity

$$\|\mu_m - \mu_n\|_s^2 = 2\|\mu_m\|_s^2 + 2\|\mu_n\|_s^2 - \|\mu_m + \mu_n\|_s^2,$$

hence

$$\|\mu_m - \mu_n\|_s^2 \leq 2\|\mu_m\|_s^2 + 2\|\mu_n\|_s^2 - 4W_s.$$

For every $\varepsilon > 0$, there is an $N \in \mathbb{N}$ so that $\|\mu_n\|_s^2 - W_s < \varepsilon/2$ whenever $n > N$. If $n, m > N$ then $\|\mu_m - \mu_n\|_s^2 \leq \varepsilon$ and so $\{\mu_n\}_{n=1}^{\infty}$ is a Cauchy sequence with respect to the norm $\|\cdot\|_s$. By the completeness of $\mathcal{M}^+(A) \cap \mathcal{E}_s$, $\{\mu_n\}_{n=1}^{\infty}$ converges in the strong topology on $\mathcal{E}_s$ to a measure λ. By proposition 2.4.10, $\mu_n \xrightarrow{*} \lambda$ and hence $\lambda \in \mathcal{M}_1^+(A)$ (Choose the constant 1 as the continuous test function to see that $\lambda(A) = 1$.)

Let $\lambda_1 \in \mathcal{M}_1^+(A)$ be another measure such that $I_s(\lambda_1) = W_s$, then by the Cauchy-Schwarz inequality

$$W_s \leq \left\| \frac{\lambda + \lambda_1}{2} \right\|_s^2 = \frac{1}{4}\left[\|\lambda\|_s^2 + \|\lambda_1\|_s^2 + 2\langle \lambda, \lambda_1 \rangle_s\right] \leq \frac{1}{4}\left[\|\lambda\|_s^2 + \|\lambda_1\|_s^2 + 2\|\lambda\|_s\|\lambda_1\|_s\right] = W_s.$$

Hence

$$\langle \lambda, \lambda_1 \rangle_s = \|\lambda\|_s \|\lambda_1\|_s.$$

Which implies that $\lambda_1 = C\lambda$. Since $\lambda, \lambda_1 \in \mathcal{M}_1^+(A)$, $C = 1$. □

Note that the positive-definiteness of $\langle \cdot, \cdot \rangle_s$ allows us to use the Cauchy-Schwartz inequality. This unique probability measure λ shall be denoted $\mu^{s,A}$ and referred to as the *(s-)equilibrium measure on A*

Finally we note that by taking an appropriate limit as $s \downarrow 0$ one may replace the Riesz s-kernel with the logarithmic kernel $-\log|x - y|$. In this case there is a unique equilibrium measure as well. This is referred to as the "$s = 0$" case, although it is not obtained by using a value of zero for the parameter s. The limit of the gradient of the s-potential as $s \downarrow 0$ will give the gradient of the logarithmic or "$s = 0$" kernel.

2.4.4 **Constant Potential of $\mu^{s,A}$**

When electrostatics is studied as a physical phenomenon, one encounters the following standard argument that the potential is constant across a conductor: Suppose the potential was not constant, then the gradient of the potential would give a non-zero field that would induce the mobile electrons to move in opposition to that field. Any steady-state must therefore have a field of zero and hence constant potential.

This argument assumes a signed measure of fixed net mass to represent a charge distribution and takes for granted that the potential is differentiable. Nevertheless, there is an important idea: If the potential of a measure is non-constant, then the measure does not have minimal energy. This idea continues to hold in the setting of potential theory in a modified form: The potential of the equilibrium measure is constant approximately everywhere on the support of the equilibrium measure; where we say a condition holds *(s-)approximately everywhere* (cf. [30, pg. 135]) if the set of points N where the condition does not hold contains no compact sets of positive (s-)capacity.

To prove and use this concept we introduce the notion of lower semicontinuity. Let $A \subset \mathbb{R}^p$ be compact. We say that $f : A \to \mathbb{R} \cup \{\infty\}$ is *lower semicontinuous on A* if for every $x \in A$ and $\alpha < f(x)$ there is a neighborhood O of x that is open in the subspace topology on A such that for all $y \in O$ we have $f(y) > \alpha$.

The following may be found in the introduction of [45].

Lemma 2.4.12. *Let $A \subset \mathbb{R}^p$ be compact and let $f : A \to \mathbb{R} \cup \{\infty\}$ have the property that there is an increasing sequence of functions $\{f_n\}_{n=1}^{\infty} \subset C(A)$ such that for each $x \in K$,*

$$\lim_{n\to\infty} f_n(x) = f(x),$$

where the limit is infinite whenever $f(x)$ is. Then f is lower-semicontinuous.

Proof. Let A, f and $\{f_n\}_{n=1}^{\infty}$ be as provided in the hypothesis of the lemma. Let $x \in A$ and

$\alpha < f(x)$. Let N so that for all $n \geq N$ $f_n(x) > \alpha$. Let

$$O := \{y \in A : f_N(y) > \alpha\} \subset \{y \in A : f(y) > \alpha\},$$

then O is open in the subspace topology on A by the continuity of f_N. □

Lemma 2.4.13. *Let μ be a Radon measure with support in a compact set $A \subset \mathbb{R}^p$, then $U_s^\mu : A \to \mathbb{R} \cup \{\infty\}$ is lower-semicontinuous.*

Proof. Define a truncated Riesz s-kernel $k_s^n : \mathbb{R}^p \to \mathbb{R} \cup \{\infty\}$ as

$$k_s^n(x) := \begin{cases} |x|^s & \text{when } |x|^s < n \\ n & \text{when } |x|^s \geq n. \end{cases}$$

Define an analogous s-potential as

$$U_{s,n}^\mu(x) := \int k_s^n(|x-y|)d\mu(y).$$

By dominated convergence

$$\lim_{x \to x_0} \int k_s^n(|x-y|)d\mu(y) = \int k_s^n(|x_0-y|)d\mu(y),$$

and so $U_{s,n}^\mu$ is continuous. By monotone convergence

$$\lim_{n \to \infty} \int k_s^n(|x-y|)d\mu(y) = \int \frac{1}{|x-y|^s} d\mu(y).$$

Lemma 2.4.12 completes the proof. □

An important consequence is that for a measure $\mu \in \mathcal{M}^+(A)$ the set $[U_s^\mu > \alpha]$ is open and hence (cf. [9, ch. 3]) the sets $[U_s^\mu \geq \alpha]$, $[U_s^\mu < \alpha]$ and $[U_s^\mu \leq \alpha]$ are Borel-measurable.

The proof of the following proposition is taken from [21].

Proposition 2.4.14. *Let $A \subset \mathbb{R}^p$ be compact so that $\mathcal{H}^d(A) > 0$. Then*

(1) $U_s^{\mu^{s,A}} \geq I_s(\mu^{s,A})$ approximately everywhere on A.

(2) $U_s^{\mu^{s,A}} \leq I_s(\mu^{s,A})$ everywhere on the support of $\mu^{s,A}$.

Proof. Let $\nu \in \mathcal{M}_1^+(A) \cap \mathcal{E}_s$ and let $a \in [0,1]$, then by the minimality of $I_s(\mu^{s,A})$

$$\|\mu^{s,A}\|_s^2 \leq \|a\mu^{s,A} + (1-a)\nu\|_s^2 = a^2\|\mu^{s,A}\|_s^2 + (1-a)^2\|\nu\|_s^2 + 2a(1-a)\langle\mu^{s,A}, \nu\rangle_s,$$

hence

$$\|\mu^{s,A}\|_s^2 = \lim_{a\uparrow 1} \frac{(1-a^2)\|\mu^{s,A}\|_s^2 - (1-a)^2\|\nu\|_s^2}{2a - 2a^2} \leq \langle\mu^{s,A}, \nu\rangle_s.$$

The linearity of the inner product allows us to conclude that $\|\mu^{s,A}\|_s^2\nu(A) \leq \langle\mu^{s,A}, \nu\rangle_s$ for all $\nu \in \mathcal{M}^+(A) \cap \mathcal{E}_s$.

Let $N := \{x \in A : U_s^{\mu^{s,A}}(x) < \|\mu^{s,A}\|_s^2\}$. Suppose $\nu \in \mathcal{M}^+(A)$ such that $\nu(N) > 0$ (N.B. We use the measurability of N for this supposition.) Then there is a $K \subset N$ so that K is compact and $\nu(K) > \nu(N)/2 > 0$. Let ν_K be the restriction of ν to K, in this case

$$\langle\nu_K, \mu^{s,A}\rangle_s = \int U_s^{\mu^{s,A}} d\nu_K < \|\mu^{s,A}\|_s^2\nu_K(A),$$

implying that $\nu_K \notin \mathcal{E}_s$ and hence $\nu \notin \mathcal{E}_s$. This proves the first claim. In particular

$$\mu^{s,A}([U_s^{\mu^{s,A}} < \|\mu^{s,A}\|_s^2]) = 0,$$

hence

$$\|\mu^{s,A}\|_s^2 = \int_{[U_s^{\mu^{s,A}} = \|\mu^{s,A}\|_s^2]} U_s^{\mu^{s,A}} d\mu^{s,A} + \int_{[U_s^{\mu^{s,A}} > \|\mu^{s,A}\|_s^2]} U_s^{\mu^{s,A}} d\mu^{s,A}.$$

Which implies $\mu^{s,A}([U_s^{\mu^{s,A}} > \|\mu^{s,A}\|_s^2]) = 0$. Because $[U_s^{\mu^{s,A}} > \|\mu^{s,A}\|_s^2]$ is open, it is disjoint from the support of $\mu^{s,A}$. This proves the second claim. □

From this we have an immediate corollary.

Corollary 2.4.15. *Let $A \subset \mathbb{R}^p$ be compact such that $\mathcal{H}^d(A) > 0$, let $s \in (0, d)$. Then $U_s^{\mu^{s,A}} = I_s(\mu^{s,A})$ $\mu^{s,A}$-a.e.*

2.5 Discrete Minimal Energy Problems

The previous sections of this chapter developed a mathematical model for arranging a continuous fixed amount of charge over an object so as to minimize a generalized electrostatic energy. The notion of a continuous charge density arises in physics as a continuum limit of letting the number of electrons grow. In this section we shall see that for $s < d$ this continuum limit is justified if the electrons or point charges minimize a discrete minimal energy problem.

Let $\omega_N := \{x_1, \ldots, x_N\}$ denote a configuration of N distinct points in $\mathbb{R}^p$. The *discrete s-energy* of ω_N is

$$E_s(\omega_N) := \sum_{i=1}^{N} \sum_{j=1\, j\neq i}^{N} \frac{1}{|x_i - x_j|^s}.$$

If we let $A \subset \mathbb{R}^p$ be an infinite and compact set, then we may consider the constrained problem of choosing a configuration $\omega_N \subset A$ that minimizes E_s over all N-point subsets of A. We first establish that this problem has a solution.

Proposition 2.5.1. *Let $A \subset \mathbb{R}^p$ be an infinite compact set. Let $s > 0$. Then there is a configuration $\omega_N^{s,A}$, which is sometimes denoted ω_N^s when the set A may be inferred, so that $E_s(\omega_N^s) \leq E_s(\omega_N)$ for any N-point configuration ω_N.*

Proof. Let

$$k_s^{(\varepsilon)}(x) := \begin{cases} |x|^{-s} & |x| \geq \varepsilon \\ \varepsilon^{-s} & |x| < \varepsilon \end{cases}$$

and $E_s^{(\varepsilon)}$ denote the energy where the kernel $|x - y|^{-s}$ is replaced by $k_s^{(\varepsilon)}$ for some value of $\varepsilon > 0$. For a given N, we may choose an arbitrary configuration of distinct points on A denoted ω_N^0. We then choose an $\varepsilon > 0$ such that $1/\varepsilon^s > E_s(\omega_N^0)$. Any configuration

with lesser energy must contain points that are separated by at least ε. For configurations whose points are separated by ε, the quantities E_s and $E_s^{(\varepsilon)}$ agree. A is compact, and $E_s^{(\varepsilon)} : A^N \to \mathbb{R}$ is continuous so we may find a configuration $\omega_N^s \subset A^N$, that minimizes $E_s^{(\varepsilon)}$. This configuration also minimizes E_s. □

It should be noted that a minimizing configuration may not be unique. For example, if we let A be a circle and ω_N be a minimal configuration on the circle, then any rotation of ω_N is also minimal. Further, there is no restriction on s other than it be positive, the dimension of A does not play a role in the existence of a minimizing configuration. With this in mind we define, for a compact set A,

$$\mathcal{E}_s(A, N) := E_s(\omega_N^{s,A}).$$

An early formulation of this problem is Thomson's Problem (cf. [48]) which is to arrange N-electrons on the unit sphere so as to minimize the electrostatic ($s = 1$, $d = 3$) energy. Under the reasonable assumption that the electrons are separated, the energy is a differentiable function of the positions of the electrons. One may write down the equations necessary for a configuration to be at a local minimum and attempt to solve them. There are two obstacles to this problem: strong evidence that there are many configurations that are local minima but not the global minimum, equations which are intractable even for modest value of N.

In the appropriate limit as $s \to \infty$ one recovers the best-packing problem or Tammes' problem [47].

An alternative approach is to examine more qualitative behaviors of energy minimizing configurations. The questions that have been of interest are:

(1) What is the asymptotic distribution (or continuum limit) of the energy minimizing configurations? How does it depend on s or A?

(2) How does the minimal discrete energy grow with N, and what factors contribute to the nature of the growth?

The techniques for addressing these questions depend to a large degree on whether $s < \dim A$.

2.5.1 The Potential Theory Case

Here we consider a compact set $A \subset \mathbb{R}^p$ of positive $\mathcal{H}^d$ measure and assume $s < d$. One may define the following measure based on an energy minimizing configuration ω_N^s of A. Let

$$\gamma_s^{(N)} := \frac{1}{N} \sum_{x \in \omega_N^s} \delta_x. \tag{2.19}$$

We consider the asymptotic distribution of points by examining the limit of $\gamma_s^{(N)}$ as $N \to \infty$. The central tools are the integrability for the Riesz s-kernel on A and the existence of a unique equilibrium measure $\mu^{s,A}$.

The setting for this next proposition is Riesz potentials in $\mathbb{R}^p$, however the proof hinges on the uniqueness of the equilibrium measure, the minimality of the s-energy of ω_N^s and the fact that the kernel can be approximated by continuous functions. These conditions hold in more general settings (cf. [21]) and related results in these more general settings are obtained in [17].

Proposition 2.5.2 (cf. [30] pp 160-162). *Let ω_N^s denote the configuration of points that minimizes E_s over all N point subsets of A and $\gamma_s^{(N)}$ denote the measure derived from ω_N^s. Let $\mu^{s,A}$ be the unique measure that minimizes I_s. If $s < d := \dim A$, then*

$$\gamma_s^{(N)} \xrightarrow{*} \mu^{s,A} \qquad \text{and} \qquad \frac{\mathcal{E}_s(A,N)}{N^2} \to I_s(\mu^{s,A}).$$

as $N \to \infty$.

Proof. We show that the limit

$$\lim_{N\to\infty} \frac{2}{N(N-1)} E_s(\omega_N^s) \tag{2.20}$$

exists. For sake of clarity, if a point x belongs to ω_N^s, then we shall append a superscript of the form, $x^{(N)}$. By creating sums in which one point is omitted we have

$$\sum_{i<j} \frac{1}{\left|x_i^{(N)} - x_j^{(N)}\right|^s} = \frac{1}{N-2} \sum_{k=1}^{N} \sum_{i<j,\, i\neq k,\, j\neq k} \frac{1}{\left|x_i^{(N)} - x_j^{(N)}\right|^s}.$$

The inner sum on the right hand side is $E_s(\omega_N^s \backslash \{x_k^{(N)}\})$. By the minimality of $E_s(\omega_N^s)$, this must be greater than or equal to $E_s(\omega_{N-1}^s)$, giving

$$\sum_{i<j} \frac{1}{\left|x_i^{(N)} - x_j^{(N)}\right|^s} \geq \frac{N}{N-2} \sum_{i<j} \frac{1}{\left|x_i^{(N-1)} - x_j^{(N-1)}\right|^s},$$

which implies that

$$\frac{2}{N(N-1)} \sum_{i<j} \frac{1}{\left|x_i^{(N)} - x_j^{(N)}\right|^s} \geq \frac{2}{(N-1)(N-2)} \sum_{i<j} \frac{1}{\left|x_i^{(N-1)} - x_j^{(N-1)}\right|^s}.$$

This is sufficient to show that the quantity in (2.20) is increasing with N and thus the limit, finite or infinite, exists.

Now we let $\{y_i\}_{i=1}^N$ be an arbitrary set of points on A, and $\{x_i\}_{i=1}^N$ denote the points in ω_N^s. By minimality we have

$$\sum_{i<j} \frac{1}{|x_i - x_j|^s} \leq \sum_{i<j} \frac{1}{|y_i - y_j|^s}$$

where we replace $|y_i - y_j|^{-s}$ with ∞ if $y_i = y_j$. We let $\mu \in \mathcal{M}_1^+(A)$. We shall integrate both sides with respect to $d\mu(y_1) \dots d\mu(y_N)$. Since the left hand side does not depend on y_i, it is unchanged. On the right hand side, we see that integrating against $d\mu(y_i)$ only affects the

terms containing y_i, and leaves $N(N-1)/2$ copies of the same integral giving

$$\sum_{i<j} \frac{1}{|x_i - x_j|^s} \leq \sum_{i<j} \iint \frac{1}{|y_i - y_j|^s} d\mu(y_i) d\mu(y_j) = \frac{N(N-1)}{2} \iint \frac{1}{|y_a - y_b|^s} d\mu(y_a) d\mu(y_b)$$

Since the above holds for any probability measure, it holds for the unique equilibrium measure $\mu^{s,A}$. Further, since it holds for all N, it holds in the limit and we obtain

$$\lim_{N\to\infty} \frac{2}{N(N-1)} \sum_{i<j} \frac{1}{|x_i - x_j|^s} \leq \iint \frac{1}{|y_a - y_b|^s} d\mu^{s,A}(y_a) d\mu^{s,A}(y_b).$$

We fix $\varepsilon > 0$ and consider the integral

$$\iint k_s^{(\varepsilon)}(x,y) d\gamma_s^{(N)}(y) d\gamma_s^{(N)}(x).$$

The above integral is similar to the discrete sum with two exceptions. The terms resulting from pairs of distinct points are bounded above by ε^{-s}, and we now include pairs where both points are the same. With this in mind the following bound may be established where the first term is the bound on the terms where $i \neq j$ and the second term bounds the terms where $i = j$.

$$\iint k_s^{(\varepsilon)}(x,y) d\gamma_s^{(N)}(y) d\gamma_s^{(N)}(x) \leq \frac{2}{N(N-1)} \sum_{i<j} \frac{1}{|x_i - x_j|^s} + \frac{\varepsilon^{-s}}{N}$$

Let γ_s denote any weak-star cluster point of $\gamma_s^{(N)}$, and let $\{N_i\}_{i=1}^{\infty}$ be such that $\gamma_s^{(N_i)} \xrightarrow{*} \gamma_s$, as $i \to \infty$. We take the limit $N_i \to \infty$ and obtain

$$\iint k_s^{(\varepsilon)}(x-y) d\gamma_s(y) d\gamma_s(x) \leq \iint \frac{1}{|y_a - y_b|^s} d\mu^{s,A}(y_a) d\mu^{s,A}(y_b)$$

The integrability of the Riesz kernel for $s < d$ and the fact that ε is independent of N give

$$I_s(\gamma_s) \leq I_s(\mu^{s,A}).$$

The uniqueness of the equilibrium measure ensures $\gamma_s = \mu^{s,A}$. □

Related to the potential theory case are the cases when $s < 0$. In this setting one considers a maximization problem. In general one does not have a positive definite kernel for $s < 0$. Results are obtained in [2]

2.5.2 **The Singular Case**

The first order growth of $\mathcal{E}_s(A, N)$ and the weak-star limit of $\gamma_s^{(N)}$ were obtained in the last section from a potential-theoretic approach. Such an approach is not available in the case $s \geq d$ and new techniques are required to make progress. Significant results were obtained by Kuijlaars and Saff in [29] describing the energy of configurations which minimized the d-energy on the sphere $\mathcal{S}^d$. Results for the 1-energy for minimal energy configurations on rectifiable curves were obtained by Martínez-Finkelshtein, Maymeskul, Rakhmanov, and Saff in [33].

Recent results for $s \geq d$ can be found in [24] by Hardin and Saff. These results were extended by Borodachov, Hardin and Saff in [3, 4]. The results apply to configurations on d-rectifiable sets and manifolds. The precise definitions of these classes of sets are left to the next chapter. Because we omit the (technical) proofs of the following results, it is enough to understand that d-rectifiable sets and manifolds have a local structure, which in a measure-theoretic sense, is d-dimensional for a natural number d. Some of the more significant results for the case $s \geq d$ are presented here.

(1) Borodachov, Hardin and Saff show in [3] that for a d-rectifiable set A, and $s > d$ the sequence of N-point minimal energy configurations becomes asymptotically, uniformly distributed in the limit $N \to \infty$. That is to say, if $\gamma_s^{(N)}$ is as defined in the previous section, then

$$\gamma_s^{(N)} \xrightarrow{*} \frac{\mathcal{H}_A^d}{\mathcal{H}^d(A)}$$

as $N \to \infty$.

(2) Hardin and Saff show in [24] that if $s = d$ and A is a d-rectifiable manifold and also a subset of a C^1 manifold, then the same results holds.

(3) In [24] separation results are obtained for $A \subset \mathbb{R}^d$ where $\mathcal{H}^d(A) \in (0, \infty)$. Note that the dimension of A is the same as that of the embedding space. In this setting there is a constant C depending only on A so that

$$\min_{i \neq j} |x_i - x_j| > CN^{-1/d}$$

when $s > d$ and

$$\min_{i \neq j} |x_i - x_j| > C(N \log N)^{-1/d}$$

when $s = d$. It is strongly believed that this second result is not sharp, and that the factor of $\log N$ is not needed. Further, the proof of these results relies on growth estimates for $\mathcal{H}^d_A$ that are satisfied for $A \subset \mathbb{R}^d$. However, a similar result holds when $A \subset \mathbb{R}^p$ is such that $\mathcal{H}^d_A$ satisfies the same growth conditions.

(4) In [3] it is shown for a d-rectifiable set and $s > d$ that

$$\lim_{N \to \infty} \frac{\mathcal{E}_s(A, N)}{N^{1+s/d}} = \frac{C_{s,d}}{\mathcal{H}^d(A)^{s/d}},$$

where the constant $C_{s,d}$ depends only on s and d. It is known that $C_{s,1}$ is twice the Riemann Zeta Function of s (cf. [33]), and it is conjectured that $C_{s,2}$ is the Zeta Function associated with the hexagonal lattice in $\mathbb{R}^2$ (cf. [29]).

(5) In [24] it is shown for a d-rectifiable manifold A, which is also a compact subset of a d-dimensional C^1 manifold, that, in the case $s = d$ we have

$$\lim_{N \to \infty} \frac{\mathcal{E}_d(A, N)}{N^2 \log N} = \frac{\mathcal{H}^d(B^d)}{\mathcal{H}^d(A)}$$

where B^d is the closed unit ball in $\mathbb{R}^d$. We note that in this result $\mathcal{H}^d$ is normalized so that $\mathcal{H}^d$ restricted to $\mathbb{R}^d$ is d-dimensional Lebesgue measure.

(6) In [3] we have the following result about weighted energy problems. If we modify the quantity to minimize by introducing a symmetric weight function $w : A \times A \to \mathbb{R}_+$ to get

$$E_s^{(w)}(\omega_N) := \sum_{x_i \neq x_j \in \omega_N} \frac{w(x_i, x_j)}{|x_i - x_j|^s}$$

and if the function $w(x, y)$ satisfies the CPD property (cf. [3]), then the N-point configurations will converge in the weak-star sense to a density derived from w.

(7) In [4] the limiting case when $s \to \infty$ is examined. Further a construction is provided for a fractal set A so that

$$0 < \liminf_{N\to\infty} \frac{\mathcal{E}_s(A, N)}{N^{1+s/d}} < \limsup_{N\to\infty} \frac{\mathcal{E}_s(A, N)}{N^{1+s/d}} < \infty.$$

We remark that items four and six and their proofs suggest that for $s > d$ the behavior of $\mathcal{E}_s(A, N)$ results from local properties of $\omega_N^{s,A}$ which in turn are derived from local properties of the set A.

CHAPTER 3

A NORMALIZED d-ENERGY

This chapter presents a limiting Riesz d-energy that is derived from the limit of Riesz s-energies as $s \uparrow d$. This result is of value in that potential theory has broad physical application and deep connections with other branches of mathematics. We are further motivated by connections between the equilibrium measure and the discrete problem discussed in Chapter 2.

When $s < d$ and A is merely compact and of positive d-dimensional Hausdorff measure, the first order growth in discrete minimal energy and the asymptotic distribution of minimal s-energy points are addressed by Proposition 2.5.2. Further, given a collection of minimal energy configurations $\{\omega_N^{s,A}\}_{s\in[s_0,d)}$ indexed by s, one can find a sequence $s_n \uparrow d$ such that $\{\omega_N^{s_n,A}\}_{n=1}^{\infty}$ has a cluster point in A^N, and that cluster point achieves the minimal N-point d-energy. In light of these facts it is reasonable to investigate the behavior of the equilibrium measures as $s \uparrow d$ with the hope that one can learn about the asymptotic behavior of minimal d-energy configurations.

As an example consider the case when A is the interval $[-1,1] \subset \mathbb{R}^1$. In this case the Hausdorff dimension d of A is 1. It is well-known (cf. [25]) that the equilibrium measure $\mu^{s,[-1,1]}$ is given by the following Radon-Nikodým derivative $c_s(1-x^2)^{\frac{s-1}{2}}$ where c_s is chosen so that $\mu^{s,[-1,1]}$ is a probability measure. From proposition 2.5.2 the weak-star limit as $N \to \infty$ of the discrete minimal s-energy configurations is $\mu^{s,[-1,1]}$ when $s < 1$. One may verify that $\mu^{s,[-1,1]} \xrightarrow{*} \mathcal{H}^1_{[-1,1]}/2$. This indicates that the weak-star limit as $N \to \infty$ of the discrete minimal energy points is converging in the weak-star topology to the uniform probability measure on A as $s \uparrow d$. From [24] we also know that $\omega_N^d \xrightarrow{*} \mathcal{H}^1_{[-1,1]}/2^1$.

[1]When we say a sequence of configurations converges in the weak-star topology we mean that the measures derived from the configurations by (2.19) converge in the weak-star topology.

To put this concisely we know that

$$\begin{aligned} \lim_{s\uparrow d} \mu^{s,[-1,1]} &= \mathcal{H}^1_{[-1,1]}/2 \qquad \text{and} \qquad (3.1) \\ \lim_{N\to\infty} \omega_N^s &= \mu^{s,[-1,1]} \qquad \text{hence} \\ \lim_{s\uparrow d}\left(\lim_{N\to\infty} \omega_N^s\right) &= \mathcal{H}^1_{[-1,1]}/2 \qquad (3.2) \end{aligned}$$

where all the limits are considered in the weak-star sense. We also know

$$\lim_{N\to\infty} \omega_N^d = \mathcal{H}^1_{[-1,1]}/2. \qquad (3.3)$$

It is not surprising that the right hand sides of (3.1) and (3.3) agree, however the technique used to prove (3.3) did not rely on potential theory and (3.3) has been shown to hold only for a compact d-rectifiable manifolds which are also subsets of d-dimensional C^1 manifolds. We take this as motivation to study the minimal discrete d-energy as a limit of potential theory.

A potential theoretic approach to the discrete minimal d-energy problem requires addressing the following questions.

(1) Under what conditions on A does a limit such as the one in (3.1) exist?

(2) For what conditions on A and in what sense can we interchange the limits in (3.2) to conclude that the right hand sides of (3.1) and (3.3) agree?

This and the following chapter address the first question. We hope to address the second question in future work. The approach is to develop a normalized d-energy that is analogous to the s-energy I_s. This normalized d-energy is

$$\tilde{I}_d(\mu) := \lim_{s\uparrow d}(d-s)I_s(\mu),$$

and the related normalized d-potential is

$$\tilde{U}_d^{\mu}(x) := \lim_{s \uparrow d}(d-s)U_s^{\mu}(s).$$

using a combination of density arguments and Fourier analysis, we shall show for measures supported on a set belonging to appropriate classes of sets that these two quantities are well defined and that this normalized energy gives rise to a minimization problem with a unique solution. This is done in this chapter. In the following chapter we show that, for certain classes of sets, any weak-star cluster point as $s \uparrow d$ of $\mu^{s,A}$ has d-energy less than or equal to that of the unique solution, and hence must be the unique solution (this is done in the following chatper.) This will be sufficient to show weak-star convergence of the equilibrium measures.

The rest of this chapter will present classes of sets related that shall be examined, review some notions of density necessary to study this normalized d-energy, and finally characterize this d-energy in terms of the Radon-Nikodým derivative.

3.1 **Classes of Sets**

We shall begin by defining several classes of subset of $\mathbb{R}^p$. Roughly speaking the sets described in Sections 3.1.1, 3.1.2 and 3.1.3 can be assembled from bi-Lipschitz images of compact subsets of $\mathbb{R}^d$. From Corollary 2.1.6 properties of the d-dimensional Hausdorff measure restricted to these sets will be similar to the d-dimensional Hausdorff measure on $\mathbb{R}^d$. Further, image measures associated with bi-Lipschitz maps have energies bounded by the original measure. More concretely, if μ is a measure, and φ is a bi-Lipschitz map with constant L, then

$$I_s(\varphi_{\#}\mu) = \iint \frac{1}{|x-y|^s} d\varphi_{\#}\mu(y) d\varphi_{\#}\mu(x) = \iint \frac{1}{|\varphi(x)-\varphi(y)|^s} d\mu(y) d\mu(x).$$

Since the denominator of the Riesz kernel can be bounded by

$$L^{-1}|x-y| \leq |\varphi(x)-\varphi(y)| \leq L|x-y|,$$

we have that

$$L^{-s}I_s(\mu) \leq I_s(\varphi_{\#}\mu) \leq L^s I_s(\mu). \tag{3.4}$$

This fact coupled with Corollary 2.1.6 provide a means to look at these sets as if they were a collection of subsets of $\mathbb{R}^d$. In broad terms, this approach works if the energy in consideration can be shown to be localized; by this we mean that the interaction energy of the charge on different bi-Lipschitz images interacting with charge on other bi-Lipschitz images is small relative to the energy of the charges on the bi-Lipschitz images interacting with themselves.

The fourth class of set is a type of fractal. These fractals cannot be assembled from bi-Lipschitz images of $\mathbb{R}^d$, but by their construction they have the desired localization property for certain types of energy. Further, their self similar nature ensures that the measure and potential theoretic properties at each scale are proportional to these properties for the whole set.

A set $A \subset \mathbb{R}^p$ is said to be Ahlfors d-regular if there are constants C_1, and C_2 so that for all $x \in A$ and all $r \in (0, \operatorname{diam} A)$

$$C_1 < \frac{\mathcal{H}^d_A(B(x,r))}{r^d} < C_2 \tag{3.5}$$

A set $A \subset \mathbb{R}^p$ is said to be upper(lower) Ahlfors d-regular if the upper(lower) bound in (3.5) holds.

3.1.1 d-Rectifiable and $(\mathcal{H}^d, d)$-Rectifiable Sets

A set $A \subset \mathbb{R}^p$ is *d-rectifiable* (cf. [18, §3.2.14]) if it is the Lipschitz image of a bounded set in $\mathbb{R}^d$. If we consider such a definition in measure theoretic terms we have the following: A set $A \subset \mathbb{R}^p$ is *$(\mathcal{H}^d, d)$-rectifiable* (cf. [18, §3.2.14]) if $\mathcal{H}^d(A) < \infty$ and there exists a countable collection $E_1, E_2, \ldots$ of d-rectifiable sets that cover $\mathcal{H}^d$-almost all of A. That is, there exists a countable collection of bounded subsets of $\mathbb{R}^d$ $K_1, K_2, \ldots$ and a corresponding collection of Lipschitz maps, $\varphi_1 : K_1 \to \mathbb{R}^p, \varphi_2 : K_2 \to \mathbb{R}^p, \ldots$ such that

$$\mathcal{H}^d\left(A \setminus \bigcup_{i=1}^{\infty} \varphi_i(K_i)\right) = 0.$$

Moreover, it is a result of Federer [18, §3.2.18]) that if A is $(\mathcal{H}^d, d)$-rectifiable then for every $\varepsilon > 0$, the Lipschitz maps and the bounded sets may be chosen such that each φ_i is bi-Lipschitz with constant less than $1+\varepsilon$, each K_i is compact and the sets $\varphi_1(K_1), \varphi_2(K_2), \ldots$ are pairwise disjoint. For such a choice of the φ_i and K_i there is an $N = N(\varepsilon)$ such that

$$\mathcal{H}^d\left(A \setminus \bigcup_{i=1}^{N} \varphi_i(K_i)\right) < \varepsilon.$$

This class of set arose in the study of geometric measure theory, one of whose motivations was to generalize differential geometry from smooth manifolds to sets satisfying certain measure theoretic properties. While the results in this dissertation do not reference $(\mathcal{H}^d, d)$-rectifiable sets, this definition and the results due to Federer provide the basis for the next two classes of sets.

3.1.2 Strongly $(\mathcal{H}^d, d)$-Rectifiable Sets

The following definition of strong $(\mathcal{H}^d, d)$-rectifiability strengthens this condition in that for each $\varepsilon > 0$ there must be a finite collection of the mappings as above such that the portion of A not covered by the union is of strictly lower dimension. We say that a set $A \subset \mathbb{R}^p$ is *strongly $(\mathcal{H}^d, d)$-rectifiable* if, for every $\varepsilon > 0$, there is a finite collection of

compact subsets of $\mathbb{R}^d$ $K_1, \ldots, K_N$ and a corresponding set of bi-Lipschitz maps $\varphi_1 : K_1 \to \mathbb{R}^p, \ldots, \varphi_N : K_N \to \mathbb{R}^p$ such that

1. The bi-Lipschitz constant of each map is less than $1 + \varepsilon$,
2. $\mathcal{H}^d(\varphi_i(K_i) \cap \varphi_j(K_j)) = 0$ for all $i \neq j$,
3. $\dim\left(A \setminus \bigcup_{i=1}^N \varphi_i(K_i)\right) < d$.

Note that compact subsets of d-dimensional C^1 manifolds are strongly $(\mathcal{H}^d, d)$-rectifiable and any strongly $(\mathcal{H}^d, d)$-rectifiable set is $(\mathcal{H}^d, d)$-rectifiable. Further note that any strongly $(\mathcal{H}^d, d)$-rectifiable set is of finite $\mathcal{H}^d$-measure.

This definition was first presented in [6]. The requirements that the $\mathcal{H}^d_A$ measure of the intersection of the bi-Lipshcitz images is zero, and that any portion of A that is not covered be of lower dimension are needed for energy localization as $s \uparrow d$.

Proposition 3.1.1. *Let $A \subset \mathbb{R}^p$ be strongly $(\mathcal{H}^d, d)$-rectifiable. Then A is upper Ahlfors d-regular.*

Proof. Let $K_1, \ldots, K_N$ and $\varphi_1 : K_1 \to \mathbb{R}^p, \ldots, \varphi_N : K_N \to \mathbb{R}^p$ be the compact subsets of $\mathbb{R}^d$ and the corresponding maps with bi-Lipschitz constant less than 2 provided by the strong $(\mathcal{H}^d, d)$-rectifiability of A. Since $\mathcal{H}^d(A) = \mathcal{H}^d(\bigcup_{i=1}^N \varphi_i(K_i))$ and since each φ_i is bijective, we have

$$\frac{\mathcal{H}^d_A(B(x,r))}{r^d} \leq \sum_{i=1}^N \frac{\mathcal{H}^d(\varphi_i(K_i) \cap B(x,r))}{r^d}$$

$$= \sum_{i=1}^N \frac{\mathcal{H}^d(\varphi_i(K_i \cap \varphi_i^{-1}(B(x,r))))}{r^d} \leq \sum_{i=1}^N \frac{2^d \mathcal{H}^d(K_i \cap \varphi_i^{-1}(B(x,r)))}{r^d},$$

where the last inequality follows from Corollary 2.1.6. Since $\mathcal{H}^d(K_i \cap \varphi_i^{-1}(B(x,r))) \leq 2^{2d} r^d$, the claim holds with $C = 2^{3d} N$. □

3.1.3 d-Rectifiable Manifolds

A set A is said to be a *d-rectifiable manifold* if

$$A = \bigcup_{i=1}^{N} \varphi_i(K_i),$$

where each K_i is a compact subset of $\mathbb{R}^d$ and $\varphi_i : O_i \to \mathbb{R}^p$ is bi-Lipschitz on some open set $O_i \supset K_i$. This class of sets was introduced in [24] in a broad examination of discrete minimal (s)-energy problems for $s > d$. As with strongly $(\mathcal{H}^d, d)$-rectifiable sets, d-rectifiable manifolds are $(\mathcal{H}^d, d)$ rectifiable sets.

3.1.4 Strictly Self-Similar d-Dimensional Fractals

We say a compact set $A \subset \mathbb{R}^p$ is a *strictly self-similar d-fractal* if

$$A = \bigcup_{i=1}^{N} \varphi_i(A),$$

where the union is disjoint and the maps (which we shall also refer to as similitudes) $\varphi_1, \ldots, \varphi_N$ are of the form $\varphi(x) = L_i A_i x + b_i$ where A_i is an isometry, L_i is a scale factor and b_i describes the translation. We require $L_i \in (0, 1)$. In [35] Moran shows for strictly self-similar d-fractals the Hausdorff dimension is also the unique value of d that satisfies the equation

$$\sum_{i=1}^{N} L_i^d = 1,$$

and that $\mathcal{H}^d(A) \in (0, \infty)$. Moran shows this result for fractals satisfying the broader *open set condition* (cf. [15]), however we use the strict separation in the proofs of the following results.

An example of such a set would be the middle third Cantor set in $\mathbb{R}^1$. In this case there are two similitudes $\varphi_1(x) := x/3$ and $\varphi_2(x) = 2/3 + x/3$, $L_1 = L_2 = 1/3$, and the Hausdorff dimension is $\log 2 / \log 3$.

The following proposition is proven by Hutchinson in [27, §5.3], although Hutchinson does not explicitly state the result that sets he considers are Ahlfors d-regular. We will need the intermediate result given in Lemma 3.1.3, and so for completeness we include our own proof based on techniques employed in [27].

For the rest of the paper we shall order our maps $\{\varphi_1, \ldots, \varphi_N\}$ so that the scaling factors satisfy $L_1 \leq L_2 \leq \ldots \leq L_N$.

Proposition 3.1.2. *Let $A \subset \mathbb{R}^p$ be a strictly self-similar d-fractal, then A is Ahlfors d-regular.*

The intermediate result we need is:

Lemma 3.1.3. *Let A be a strictly self-similar d-fractal then, for each $x \in A$ and $r > 0$ there is a subset $A' \subset A$ so that*

1. $B(x, r) \cap A \subset A'$.
2. $A' = \varphi(A)$ *for some similitude* φ.
3. $\operatorname{diam} A' < Wr$ *where W depends only on the set A.*

Proof. Choose $x \in A$ and $r > 0$. Let $\tilde{K} = \min_{i \in 1,\ldots,N}\{\operatorname{dist}(\varphi_i(A), A \backslash \varphi_i(A))\}$. If $r \geq L_1\tilde{K}$, let $A' = A$ and then trivially $A \cap B(x, r) \subset A'$ and $\operatorname{diam} A' < r(2 \operatorname{diam} A)/(L_1\tilde{K})$.

We now consider the case when $r < L_1\tilde{K}$. Because the images of A under each φ_i are disjoint, we may assign to every $y \in A$ a unique infinite sequence $\{j_1, j_2 \ldots\} \in \{1, \ldots, N\}^{\mathbb{N}}$ so that $\{y\} = \bigcap_{n=1}^{\infty} \varphi_{j_n}(\varphi_{j_{n-1}}(\ldots \varphi_{j_1}(A) \ldots))$. If $\{i_1, i_2, \ldots\}$ is the sequence identifying x, let M be the smallest natural number so that $L_{i_1} L_{i_2} \ldots L_{i_M} \tilde{K} < r$ (note that $M \geq 2$), then

$$r \leq L_{i_1} L_{i_2} \ldots L_{i_{M-1}} \tilde{K} < \frac{r}{L_{i_M}} < \frac{r}{L_1}.$$

Let $A' = \varphi_{i_{M-1}}(\varphi_{i_{M-2}}(\ldots \varphi_{i_1}(A) \ldots))$, hence $\operatorname{diam} A' = L_{i_1} L_{i_2} \ldots L_{i_{M-1}} \operatorname{diam} A < r \operatorname{diam} A/(L_1\tilde{K})$. To complete the proof we shall show $B(x, r) \cap A \subset A'$.

Choose $y \in B(x,r) \cap A$. If $y = x$, then $y \in A'$, otherwise let $\{j_1, j_2 \ldots\}$ be the sequence identifying $y \in A$ and m the smallest natural number so that $j_m \neq i_m$. We have that

$$L_{i_1} L_{i_2} \ldots L_{i_{m-1}} \tilde{K} \leq \operatorname{dist}(x,y) \leq r \leq L_{i_1} L_{i_2} \ldots L_{i_{M-1}} \tilde{K},$$

from which we conclude $m \geq M$ forcing $y \in \varphi_{i_{M-1}}(\varphi_{i_{M-2}}(\ldots \varphi_{i_1}(A)\ldots)) = A'$.

The claimed constant W is $(2 \operatorname{diam} A)/(L_1 \tilde{K})$. □

Proof of Proposition 3.1.2. We shall prove the lower bound first. Let $x \in A$, $\{i_1, i_2, \ldots\}$ be the identifying sequence for x and $r \in (0, \operatorname{diam} A)$. Let M be a the smallest natural number so that $L_{i_1} L_{i_2} \ldots L_{i_M} \operatorname{diam} A < r$. Then $rL_1 \leq L_{i_1} L_{i_2} \ldots L_{i_M} \operatorname{diam} A$ and $\varphi_{i_M}(\varphi_{i_{M-1}}(\ldots \varphi_{i_1}(A)\ldots)) \subset B(x,r)$, hence

$$\mathcal{H}^d_A(B(x,r)) \geq \mathcal{H}^d(\varphi_{i_M}(\varphi_{i_{M-1}}(\ldots \varphi_{i_1}(A)\ldots)))$$

$$= (L_{i_1} L_{i_2} \ldots L_{i_M})^d \mathcal{H}^d(A) \geq r^d \mathcal{H}^d(A) \left(\frac{L_1}{\operatorname{diam} A}\right)^d.$$

This proves that A is lower Ahlfors d-regular with constant $\mathcal{H}^d(A)\left(\frac{L_1}{\operatorname{diam} A}\right)^d$.

Let $A' \subset A$ be as provided by Lemma 3.1.3, then $B(x,r) \subset A'$, and $\operatorname{diam} A' < Wr$. We have

$$\mathcal{H}^d_A(B(x,r)) \leq \mathcal{H}^d(A') = \left(\frac{\operatorname{diam} A'}{\operatorname{diam} A}\right)^d \mathcal{H}^d(A) < r^d \left(\frac{W}{\operatorname{diam} A}\right)^d \mathcal{H}^d(A).$$

where W is the constant from Lemma 3.1.3. This proves that A is upper Ahlfors d-regular with constant $\left(\frac{W}{\operatorname{diam} A}\right)^d \mathcal{H}^d(A)$. □

3.2 **Generalized Densities**

Section 2.4.1 discussed the (r)-average d-density of a measure μ at a point x as it related to the potential of μ at x. Here we assign the following symbol to the average density

$$\Theta^r_d(\mu, x) := \frac{\mu(B(x,r))}{r^d}.$$

The traditional point density of a measure μ at a point x is the limit

$$\Theta_d(\mu, x) := \lim_{r \downarrow 0} \Theta_d^r(\mu, x).$$

This limit need not exist and the following two results (cf. [34]) indicate that the existence of this limit on a set of positive μ-measure is a strong condition.

Theorem 3.2.1 (Marstrand [32]). *Let μ be a Radon measure supported on $\mathbb{R}^p$ and d be a positive number. If $\Theta_d(\mu, x)$ exists and is positive and finite on a set of positive μ-measure, then $d \in \mathbb{N}$.*

If one choses μ to be $\mathcal{H}_A^d$ for some set A of fractional dimension, then $\mathcal{H}_A^d$-a.e. the point densities $\Theta_d(\mathcal{H}_A^d, \cdot)$ do not exist. Put another way fractional dimensional sets do not have a traditional point density. As an example the non-existence of $\Theta(\mathcal{H}_A^d, 0)$ where A is the middle third Cantor set in $\mathbb{R}^1$ with one end at 0 can be seen by choosing two sequences indexed by n of decreasing radii $\left(\frac{1}{3}\right)^n \frac{1}{3}$ and $\left(\frac{1}{3}\right)^n \frac{2}{3}$.

A stronger result due to Priess (cf. [34]) indicates that if the point density exists and is positive and finite on a set of positive μ-measure, then μ is concentrated on an $(\mathcal{H}^d, d)$-rectifiable set.

Theorem 3.2.2 (Preiss [39]). *Let μ be a Radon measure supported on $\mathbb{R}^p$ and d be a positive number. If $\Theta_d(\mu, x)$ exists and is positive and finite μ-a.e., then there is an $(\mathcal{H}^d, d)$-rectifiable set A so that $\mu(\mathbb{R}^p \backslash A) = 0$.*

A related result (cf. [34, ch.16,17])[2] indicates that for a $(\mathcal{H}^d, d)$-rectifiable set A the density $\Theta_d(\mathcal{H}_A^d, \cdot)$ exists and is constant $\mathcal{H}_A^d$-a.e.

Theorem 3.2.3. *Let A be a $(\mathcal{H}^d, d)$-rectifiable set, then $\Theta_d(\mathcal{H}_A^d, x) = 2^d$ for $\mathcal{H}_A^d$-a.a. x.*

[2]Note that Mattila uses the term d-rectifiable to describe what we refer to as $(\mathcal{H}^d, d)$-rectifiable.

We conclude that, if A belongs to one of the first three classes of sets, $\Theta_d(\mathcal{H}^d_A, x) = 2^d$ for $\mathcal{H}^d_A$-a.a x, but that if A is a strictly self similar d-fractal then, at $\mathcal{H}^d_A$-a.a. x the limit $\Theta_d(\mathcal{H}^d_A, x)$ does not exist.

3.2.1 The Order-Two Density

Bedford and Fisher in [1] consider the following averaging integral:

$$D^2_d(\mu, x) := \lim_{\varepsilon \downarrow 0} \frac{1}{|\log \varepsilon|} \int_\varepsilon^1 \frac{1}{r} \Theta^r_d(\mu, x) dr,$$

which they call an *order-two density* of μ at x. It is known (cf. [16, 38, 51]) that for a class of sets including strictly self-similar d-fractals $D^2_d(\mathcal{H}^d_A, x)$ is positive, finite and constant $\mathcal{H}^d_A$-a.e. We shall denote this $\mathcal{H}^d_A$-a.e. constant as $D^2_d(A)$. The next proposition shows that this order-two density agrees with the traditional density whenever the traditional density exists.

Proposition 3.2.4. *Let μ be a Radon measure supported on $\mathbb{R}^p$ and $x \in \mathbb{R}^p$ such that $\Theta_d(\mu, x)$ exists, then $D^2_d(\mu, x) = \Theta_d(\mu, x)$.*

Proof. Let μ be a Radon measure supported on $\mathbb{R}^p$ and $x \in \mathbb{R}^p$ such that $\Theta_d(\mu, x)$ exists. Let $\delta > 0$ and choose an $R > 0$ so that for all $r \in (0, R)$

$$|\Theta^r_d(\mu, x) - \Theta_d(\mu, x)| < \delta.$$

We have

$$\begin{aligned} \frac{1}{|\log \varepsilon|} \int_\varepsilon^1 \frac{1}{r} \Theta^r_d(\mu, x) dr &= \Theta_d(\mu, x) \frac{1}{|\log \varepsilon|} \int_\varepsilon^R \frac{1}{r} dr && (3.6) \\ &+ \frac{1}{|\log \varepsilon|} \int_\varepsilon^R \frac{1}{r} \left[\Theta^r_d(\mu, x) - \Theta_d(\mu, x)\right] dr && (3.7) \\ &+ \frac{1}{|\log \varepsilon|} \int_R^1 \frac{1}{r} \Theta^r_d(\mu, x) dr && (3.8) \end{aligned}$$

The limit as $\varepsilon \downarrow 0$ of the right hand side of (3.6) is $\Theta_d(\mu, x)$. The limit superior as $\varepsilon \downarrow 0$ of the absolute value of (3.7) is less than δ. The limit as limit as $\varepsilon \downarrow 0$ of (3.8) is zero. The choice of δ was arbitrary and this completes the proof. □

From this we conclude that for a set A in any of the classes described in section 3.1 $D_d^2(A)$ exists and is positive and finite. With this we present our first theorem regarding the normalized d-energy $\tilde{I}_d$.

3.3 Results for a Normalized d-Energy

Theorem 3.3.1 ensures that the normalized d-energy $\tilde{I}_d$ is well defined on all of $\mathcal{M}^+(A)$, and generates a minimization problem whose solution is unique.

Theorem 3.3.1. *Let A be a strictly self-similar d-fractal or a strongly $(\mathcal{H}^d, d)$-rectifiable set of positive $\mathcal{H}^d$ measure and let $\lambda^d := \mathcal{H}_A^d / \mathcal{H}^d(A)$, then*

(1) The limit $\tilde{I}_d(\mu)$ exists for all $\mu \in \mathcal{M}^+(A)$ and

$$\tilde{I}_d(\mu) = \begin{cases} dD_d^2(A) \int \left(\frac{d\mu}{d\mathcal{H}_A^d} \right)^2 d\mathcal{H}_A^d & \text{if } \mu \ll \mathcal{H}_A^d, \\ \infty & \text{otherwise.} \end{cases}$$

(2) If $\tilde{I}_d(\mu) < \infty$, then the limit $\tilde{U}_d^\mu$ equals $\frac{d\mu}{d\mathcal{H}_A^d}$ μ-a.e. and

$$\tilde{I}_d(\mu) = \int \tilde{U}_d^\mu d\mu.$$

(3) $\tilde{I}_d(\lambda^d) < \tilde{I}_d(\nu)$ for all $\nu \in \mathcal{M}_1^+(A) \backslash \left\{ \lambda^d \right\}$.

We shall accomplish the proof of Theorem 3.3.1 in several steps. We shall first show that if $\mu \in \mathcal{M}^+(A)$ and $\mu \not\ll \mathcal{H}_A^d$, then $\tilde{I}_d(\mu) = \infty$. We shall then relate the Radon-Nikodým of a measure with finite normalized d-energy to the normalized d-potential of the measure. We shall use the maximal function in conjunction with dominated convergence to show that

second result in Theorem 3.3.1 implies the first. Finally, we shall appeal to Hilbert space techniques to show the third result.

3.4 $\mu \not\ll \mathcal{H}^d_A$ Implies $\tilde{I}_d(\mu) = \infty$

In this section we shall show that if A is a strictly self-similar d-fractal or a strongly $(\mathcal{H}^d, d)$-rectifiable set and if $\mu \in \mathcal{M}^+(A)$ is such that $\mu \not\ll \mathcal{H}^d_A$, then $I_d(\mu) = \infty$.

3.4.1 Case I: A is a Strongly $(\mathcal{H}^d, d)$-Rectifiable Set

Given a compactly supported Radon measure μ on $\mathbb{R}^d$ and $s \in (0, d)$ the Riesz s-energy of μ may be expressed via (2.18) as

$$I_s(\mu) = c(s, d) \int_{\mathbb{R}^d} |\xi|^{s-d} |\hat{\mu}(\xi)|^2 d\xi,$$

where the constant $c(s, d)$ is given by

$$c(s, d) = \pi^{s-\frac{d}{2}} \frac{\Gamma(\frac{d-s}{2})}{\Gamma(\frac{s}{2})}.$$

Observe that (cf. [30, ch. 1])

$$\lim_{s \uparrow d} (d - s) c(s, d) = \omega_d, \tag{3.9}$$

where ω_d is the surface area of the $d-1$ sphere in $\mathbb{R}^d$.

Lemma 3.4.1. *Let $K \subset \mathbb{R}^d$ be compact. For a measure $\mu \in \mathcal{M}(K)$ we have*

$$\tilde{I}_d(\mu) = \omega_d \|\hat{\mu}\|^2_{2, \mathcal{L}^d}.$$

Further, if $\tilde{I}_d(\mu) < \infty$, then $\mu \ll \mathcal{L}^d$.

Proof. For any measure $\mu \in \mathcal{M}(K)$ the Riesz s-energy can be expressed as

$$I_s(\mu) = c(s,d) \int_{|\xi|\leq 1} |\xi|^{s-d} |\hat{\mu}(\xi)|^2 d\xi + c(s,d) \int_{|\xi|>1} |\xi|^{s-d} |\hat{\mu}(\xi)|^2 d\xi.$$

By dominated convergence

$$\lim_{s \uparrow d} \int_{|\xi|\leq 1} |\xi|^{s-d} |\hat{\mu}(\xi)|^2 d\xi = \int_{|\xi|\leq 1} |\hat{\mu}(\xi)|^2 d\xi,$$

and by monotone convergence

$$\lim_{s \uparrow d} \int_{|\xi|>1} |\xi|^{s-d} |\hat{\mu}(\xi)|^2 d\xi = \int_{|\xi|>1} |\hat{\mu}(\xi)|^2 d\xi.$$

From (3.9) the first statement is proven, and hence $\hat{\mu} \in L^2$. Theorem 2.3.3 completes the proof. □

Lemma 3.4.2. *Let $A \subset \mathbb{R}^p$ be a compact and strongly $(\mathcal{H}^d, d)$-rectifiable and let $\mu \in \mathcal{M}^+(A)$ be such that $\mu \ll \mathcal{H}^d_A$, then $\tilde{I}_d(\mu)$ exists and is infinite.*

Proof. Let $\mu \in \mathcal{M}^+(A)$ such that $\mu \ll \mathcal{H}^d_A$. Let $\mu = \mu^\perp + \mu^\ll$ be the Lebesgue decomposition of μ with respect to $\mathcal{H}^d_A$. Let $K_1, \ldots, K_N$ and $\varphi_1 : K_1 \to \mathbb{R}^p, \ldots, \varphi_N : K_N \to \mathbb{R}^p$ be the compact subsets of $\mathbb{R}^d$ and the corresponding maps with bi-Lipschitz constant less than 2 provided by the strong $(\mathcal{H}^d, d)$-rectifiability of A. Let $B = A \setminus \bigcup_{i=1}^N \varphi_i(K_i)$ and $s_0 = \dim B$. If $\mu(B) > 0$, then, by the equality of the capacitory and Hausdorff dimensions (see Proposition 2.4.3), $I_s(\mu) = \infty$ for all $s \in (s_0, d)$. Hence $\tilde{I}_d(\mu) = \infty$.

If $\mu(B) = 0$, then

$$0 < \mu^\perp(A) \leq \sum_{i=1}^N \mu^\perp(\varphi_i(K_i)).$$

Choose $j \in 1, \ldots, N$ such that $\mu^\perp(\varphi_j(K_j)) > 0$, and define $\nu_j := \mu^\perp_{\varphi_j(K_j)}$. Since $\nu_j \perp \mathcal{H}^d_{\varphi_j(K_j)}$, it follows that $\varphi^{-1}_{j\#}\nu_j \perp \mathcal{H}^d$ and hence $\varphi^{-1}_{j\#}\nu_j \perp \mathcal{L}^d$. By Lemma 3.4.1 we have that $\tilde{I}_d(\varphi^{-1}_{j\#}\nu_j) = \infty$ and by (3.4) it follows that $\infty = \tilde{I}_d(\varphi_{j\#}\varphi^{-1}_{j\#}\nu_j) = \tilde{I}_d(\nu_j) \leq \tilde{I}_d(\mu)$. □

3.4.2 Case II: A is a Strictly Self-Similar d-Fractal

Lemma 3.4.3. *Let A be a compact strictly self-similar d-fractal and let $\mu \in \mathcal{M}^+(A)$ such that $\mu \ll \mathcal{H}_A^d$. Then $\tilde{I}_d(\mu) = \infty$.*

Proof. Let A be a compact strictly self-similar d-fractal and let $\mu \in \mathcal{M}^+(A)$ such that $\mu \ll \mathcal{H}_A^d$. Let $\mu = \mu^{\ll} + \mu^{\perp}$ be the Lebesgue decomposition of μ with respect to $\mathcal{H}_A^d$. The Radon-Nikodým theorem ensures that for $\mu^{\perp}$-a.a. x,

$$\lim_{r \downarrow 0} \frac{\mu^{\perp}(B(x,r))}{\mathcal{H}_A^d(B(x,r))} = \infty.$$

For such an x, let $M \in \mathbb{R}$ be arbitrary and $R > 0$ such that for all $r \in (0, R)$ we have $\mu^{\perp}(B(x,r))/\mathcal{H}_A^d(B(x,r)) > M$. It then follows from the technique presented in (2.9) that

$$\begin{aligned}
\liminf_{s \uparrow d}(d-s)\int \frac{1}{|x-y|^s} d\mu^{\perp}(y) &= \liminf_{s \uparrow d}(d-s)s\int_0^{\infty} \frac{\mu^{\perp}(B(x,r))}{r^{s+1}} dr \\
&\geq \left(\inf_{r \in (0,R)} \frac{\mu^{\perp}(B(x,r))}{\mathcal{H}_A^d(B(x,r))}\right) \liminf_{s \uparrow d}(d-s)s\int_0^{R} \frac{\mathcal{H}_A^d(B(x,r))}{r^{s+1}} dr \\
&\geq M \liminf_{s \uparrow d}(d-s)sC_1 \frac{1}{d-s} R^{d-s} = C_1 M d,
\end{aligned}$$

where C_1 is the lower bound from the Ahlfors d-regularity of A. M is arbitrary. Hence $\tilde{U}_d^{\mu^{\perp}}(x) = \infty$ for $\mu^{\perp}$-a.a. x.

By Fatou's lemma

$$\begin{aligned}
\infty &= \int \tilde{U}_d^{\mu^{\perp}} d\mu^{\perp} = \int \liminf_{s \uparrow d}(d-s) U_s^{\mu^{\perp}} d\mu^{\perp} \\
&\leq \liminf_{s \uparrow d}(d-s) \int U_s^{\mu^{\perp}} d\mu^{\perp} = \tilde{I}_d(\mu^{\perp}) \leq \tilde{I}_d(\mu).
\end{aligned}$$

□

3.5 The Order-Two Density, $\tilde{U}_d^\mu$ and $\frac{d\mu}{d\mathcal{H}_A^d}$ for a Measure $\mu \in \mathcal{M}^+(A)$

One of the central results used to examine the functional $\tilde{I}_d$ is the fact that if the order-two density of a measure μ at a point x ($D_d^2(\mu, x)$) exists, then the normalized d-potential of μ at x ($\tilde{U}_d^\mu(x)$) exists as well, and the two agree. This relationship between the order-two density and the limiting potential is examined by Zähle in the context of stochastic differential equations in [52] and also by Hinz, in [26]. We include a proof of this relationship from [26].

Proposition 3.5.1. *Let μ be a finite Borel measure with support in $\mathbb{R}^p$, $x \in \operatorname{supp}\mu$, $d \in (0, p]$. If $D_d^2(\mu, x)$ exists and is finite, then*

$$\tilde{U}_d^\mu(x) = dD_d^2(\mu, x).$$

Proof. One may verify that the function $k_\varepsilon(t) := \varepsilon^2 \chi_{(0,1]}(t) t^{\varepsilon - 1} |\log t|$ is an approximate identity in the following sense: If $f : \mathbb{R} \to \mathbb{R}$ is right continuous at 0 and is bounded on $(0, 1)$, then

$$\lim_{\varepsilon \downarrow 0} \int_0^\infty k_\varepsilon(t) f(t) dt = f(0).$$

Define the following function:

$$f(t) := \begin{cases} \frac{1}{|\log t|} \int_t^1 \frac{1}{r} \Theta_d^r(\mu, x) dr & \text{when } t > 0 \\ D_d^2(\mu, x) & \text{when } t = 0 \end{cases}$$

If $D_d^2(\mu, x)$ exists and is finite, then f is right-continuous at 0 and bounded on $(0, 1)$ thus

$$\begin{aligned} D_d^2(\mu, x) &= \lim_{\varepsilon \downarrow 0} \int_0^\infty k_\varepsilon(t) f(t) dt \\ &= \lim_{\varepsilon \downarrow 0} \varepsilon^2 \int_0^1 t^{1-\varepsilon} \int_0^1 \frac{\chi_{[t,1]}(r)}{r} \Theta_d^r(\mu, x) dr dt \\ &= \lim_{\varepsilon \downarrow 0} \varepsilon^2 \int_0^1 \frac{1}{r} \Theta_d^r(\mu, x) \int_0^r t^{\varepsilon - 1} dt dr \\ &= \lim_{\varepsilon \downarrow 0} \varepsilon \int_0^1 \frac{1}{r} \Theta_d^r(\mu, x) r^\varepsilon dr \\ &= \lim_{s \uparrow d} (d - s) \int_0^1 \Theta_d^r(\mu, x) \frac{1}{r^{1-(d-s)}} dr = \frac{1}{d} \tilde{U}_d^\mu(x). \end{aligned}$$

The final equivalence is an application of (2.9). □

We define a modified normalized energy as follows: For a measure $\mu \in \mathcal{M}^+(A)$, let

$$\underline{\tilde{I}_d}(\mu) := \liminf_{s \uparrow d} (d - s) \iint \frac{1}{|x - y|^s} d\mu(y) d\mu(x).$$

With this definition we shall provide a characterization of measures for which $\underline{\tilde{I}_d}$ is finite.

Proposition 3.5.2. *Let $A \subset \mathbb{R}^p$ be a compact set such that $D_d^2(A)$ exists and is $\mathcal{H}_A^d$-a.e. constant. Let $\mu \in \mathcal{M}^+(A)$ so that $\underline{\tilde{I}_d}(\mu) < \infty$. Then,*

(1) $\tilde{U}_d^\mu(x) = d D_d^2(A) \frac{d\mu}{d\mathcal{H}_A^d}(x)$ for μ-a.a. x and

(2) $\frac{d\mu}{d\mathcal{H}_A^d} \in L^2(\mathcal{H}_A^d)$.

Proof. Note that for all $R > 0$

$$\lim_{s \uparrow d} (d - s) s \int_R^\infty \Theta_d^r(\mu, x) \frac{1}{r^{1-(d-s)}} dr = 0.$$

From this we conclude that if $\tilde{U}_d^\mu(x)$ exists, then

$$\tilde{U}_d^\mu(x) = \lim_{s \uparrow d} (d - s) s \int_0^R \Theta_d^r(\mu, x) \frac{1}{r^{1-(d-s)}} dr,$$

for any $R > 0$.

We begin with the following equality for an arbitrary $R > 0$:

$$(d-s)s\int_0^R \frac{\mu(B(x,r))}{r^{s+1}}dr \tag{3.10}$$

$$= \frac{d\mu}{d\mathcal{H}_A^d}(x)(d-s)s\int_0^R \frac{\mathcal{H}_A^d(B(x,r))}{r^{s+1}}dr \tag{3.11}$$

$$+ (d-s)s\int_0^R \left(\frac{\mu(B(x,r))}{\mathcal{H}_A^d(B(x,r))} - \frac{d\mu}{d\mathcal{H}_A^d}(x)\right)\frac{\mathcal{H}_A^d(B(x,r))}{r^{s+1}}dr. \tag{3.12}$$

By Proposition 3.5.1 the limit as $s \uparrow d$ of the summand in (3.11) is $\frac{d\mu}{d\mathcal{H}_A^d}(x)dD_d^2(A)$ for $\mathcal{H}_A^d$-a.a. x. The absolute value of the limit superior of the summand in (3.12) is bounded for $\mathcal{H}_A^d$-a.a. x by

$$\sup_{r\in(0,R)}\left|\frac{\mu(B(x,r))}{\mathcal{H}_A^d(B(x,r))} - \frac{d\mu}{d\mathcal{H}_A^d}(x)\right| dD_d^2(A),$$

which can be made arbitrarily small by choosing R sufficiently small. Thus the limit as $s \uparrow d$ of (3.10) exists $\mathcal{H}_A^d$-a.e. and hence $\tilde{U}_d^\mu$ does as well.

Arguing as we did in the proof of Lemma 3.4.3 we appeal to Fatou's lemma to obtain

$$\int \liminf_{s\uparrow d}(d-s)U_s^\mu d\mu \le \underline{\tilde{I}_d}(\mu) < \infty.$$

This implies that $\liminf_{s\uparrow d}(d-s)U_s^\mu$ is finite μ-a.e. and, by Lemmas 3.4.3 and 3.4.1, $\mu \ll \mathcal{H}_A^d$. By the first claim in this proposition and by the previous equation

$$\int\left(\frac{d\mu}{d\mathcal{H}_A^d}\right)^2 d\mathcal{H}_A^d = \int\left(\frac{d\mu}{d\mathcal{H}_A^d}\right)d\mu = \int \frac{1}{dD_2^d(A)}\tilde{U}_d^\mu d\mu < \infty.$$

□

3.6 **Proof of Theorem 3.3.1**

With the preceding results we may now prove Theorem 3.3.1.

Proof of Theorem 3.3.1. Let $\mu \in \mathcal{M}^+(A)$ so that $\underline{\tilde{I}_d}(\mu) < \infty$, then $\mu \ll \mathcal{H}_A^d$ and $d\mu/d\mathcal{H}_A^d \in$

$L^2(\mathcal{H}^d_A)$. The maximal function of μ with respect to $\mathcal{H}^d_A$ is

$$M_{\mathcal{H}^d_A}\mu(x) := \sup_{r>0} \frac{\mu(B(x,r))}{\mathcal{H}^d_A(B(x,r))} = \sup_{r>0} \frac{1}{\mathcal{H}^d_A(B(x,r))} \int_{B(x,r)} \frac{d\mu}{d\mathcal{H}^d_A} d\mathcal{H}^d_A.$$

The maximal function is bounded on $L^2(\mathcal{H}^d_A)$ and so $M_{\mathcal{H}^d_A}\mu \in L^2(\mathcal{H}^d_A)$. We shall use this to provide a μ-integrable bound for $(d-s)U^\mu_s$ that is independent of s and appeal to dominated convergence. We begin with the point-wise bound

$$\begin{aligned}
& (d-s)\int \frac{1}{|x-y|^s} d\mu(y) \\
= \;& (d-s)s \int_0^\infty \frac{\mu(B(x,r))}{\mathcal{H}^d_A(B(x,r))} \frac{\mathcal{H}^d_A(B(x,r))}{r^{s+1}} dr \\
\leq \;& M_{\mathcal{H}^d_A}\mu(x)(d-s)s \left[\int_0^{\operatorname{diam} A} \frac{\mathcal{H}^d_A(B(x,r))}{r^{s+1}} dr + \int_{\operatorname{diam} A}^\infty \frac{\mathcal{H}^d_A(B(x,r))}{r^{s+1}} dr \right] \\
\leq \;& M_{\mathcal{H}^d_A}\mu(x) \left[(d-s)s \int_0^{\operatorname{diam} A} \frac{C_2 r^d}{r^{s+1}} dr + (d-s)s \int_{\operatorname{diam} A}^\infty \frac{1}{r^{s+1}} dr \right], \qquad (3.13)
\end{aligned}$$

where C_2 is the constant in the upper bound of the Ahlfors d-regularity of A. The quantity in brackets in (3.13) may be maximized over $s \in (0,d)$ and we denote this maximum by K. Then, by the Cauchy-Schwarz inequality,

$$\int K M_{\mathcal{H}^d_A}\mu \, d\mu < K \int \left(M_{\mathcal{H}^d_A}\mu\right) \left(\frac{d\mu}{d\mathcal{H}^d_A}\right) d\mathcal{H}^d_A < K \left\| M_{\mathcal{H}^d_A}\mu \right\|_{2,\mathcal{H}^d_A} \left\| \frac{d\mu}{d\mathcal{H}^d_A} \right\|_{2,\mathcal{H}^d_A} < \infty.$$

By dominated convergence the second claim follows. The first claim follows from the second and from Proposition 3.5.2

The final claim of the theorem follows from a straightforward Hilbert space argument. Let ν denote the finite measure $dD_d^2(A)^{-1}\mathcal{H}^d_A$. By Proposition 3.5.2 the set of measures with finite normalized d-energy is identified with the non-negative cone in $L^2(\nu)$ (denoted $L^2(\nu)_+$) via the map $\mu \leftrightarrow d\mu/d\nu$. Under this map we have $\tilde{I}_d(\mu) = \|d\mu/d\nu\|^2_{2,\nu}$. A measure μ of finite d-energy is a probability measure if and only if $\|d\mu/d\nu\|_{1,\nu} = 1$. We seek a unique

non-negative function f that minimizes $\|\cdot\|_{2,\nu}$ subject to the constraint $\|f\|_{1,\nu} = 1$. The non-negative constant function $1/\nu(\mathbb{R}^p)$ satisfies the constraint $\|1/\nu(\mathbb{R}^p)\|_{1,\nu} = 1$. Let $f \in L^2(\nu)_+$ such that $\|f\|_{1,\nu} = 1$ and $\|f\|_{2,\nu} \leq \|1/\nu(\mathbb{R}^p)\|_{2,\nu}$, then

$$\frac{1}{\nu(\mathbb{R}^p)} = \left\| \frac{f}{\nu(\mathbb{R}^p)} \right\|_{1,\nu} = \left\langle f, \frac{1}{\nu(\mathbb{R}^p)} \right\rangle_\nu \leq \|f\|_{2,\nu} \left\| \frac{1}{\nu(\mathbb{R}^p)} \right\|_{2,\nu} \leq \left\| \frac{1}{\nu(\mathbb{R}^p)} \right\|_{2,\nu}^2 = \frac{1}{\nu(\mathbb{R}^p)}.$$

Thus

$$\left\langle f, \frac{1}{\nu(\mathbb{R}^p)} \right\rangle_\nu = \|f\|_{2,\nu} \left\| \frac{1}{\nu(\mathbb{R}^p)} \right\|_{2,\nu}.$$

From the Cauchy-Schwarz inequality $f = 1/\nu(\mathbb{R}^p)$ ν-a.e. By the identification above the measure $\lambda^d := \mathcal{H}_A^d / \mathcal{H}^d(A) \in \mathcal{M}_1^+(A)$, uniquely minimizes $\tilde{I}_d$ over $\mathcal{M}_1^+(A)$. □

CHAPTER 4

THE BEHAVIOR OF $\mu^{s,A}$ AS $s \uparrow d$

The previous chapter showed that the normalized d-energy is well defined and gives rise to a minimization problem with a unique solution. In this chapter we use properties of the normalized d-energy to show that the (s-)equilibrium measures on appropriate classes of sets converge in the weak-star sense to the minimizer of the normalized d-energy as $s \uparrow d$.

4.1 Results Regarding the Behavior of $\mu^{s,A}$ as $s \uparrow d$

Theorems 4.1.1 and 4.1.2 establish the weak-star convergence of the equilibrium measures to normalized Hausdorff measure as $s \uparrow d$. While the statements of the theorems are nearly the same, the methods used in their proofs are quite different and hence we provide two different theorems.

Theorem 4.1.1. *Let $A \subset \mathbb{R}^p$ be a compact strongly $(\mathcal{H}^d, d)$-rectifiable set such that $\mathcal{H}^d(A) > 0$. Let $\lambda^d := \mathcal{H}^d_A/\mathcal{H}^d(A)$. Then $\mu^{s,A} \xrightarrow{*} \lambda^d$ as $s \uparrow d$.*

Theorem 4.1.2. *Let $A \subset \mathbb{R}^p$ be a compact strictly-self similar d-fractal. Let $\lambda^d := \mathcal{H}^d_A/\mathcal{H}^d(A)$. Then $\mu^{s,A} \xrightarrow{*} \lambda^d$ as $s \uparrow d$.*

Theorem 4.1.3 ensures that the equilibrium measure or charge distribution on strictly self-similar d-fractals cannot be too concentrated. Any growth condition with exponent less than d allows the measure to be concentrated on a lower dimensional subset of A.

Theorem 4.1.3. *Let A be a compact strictly self-similar d-fractal, then there is a constant K depending only on A, so that for any $s \in (0, d)$, $\mu^{s,A}(B(x,r)) \leq Kr^s$ for $\mu^{s,A}$-a.a. $x \in A$ and $r > 0$.*

A bound similar to that in Theorem 4.1.3 is presented in [34, Ch. 8]. This result differs in that the constant K does not depend on s.

4.2 The Behavior of $\mu^{s,A}$ on Strongly $(\mathcal{H}^d, d)$-Rectifiable Sets

We begin with an estimate obtained via the Fourier transform which will be of considerable value in examining strongly $(\mathcal{H}^d, d)$-rectifiable sets.

Lemma 4.2.1. *Let $K \subset \mathbb{R}^d$ be a compact set. Then, for every $\eta > 0$, there is an $s_0 = s_0(\eta)$ such that, for any s and t satisfying $s_0 < s < t < d$ and any measure $\mu \in \mathcal{M}(K)$,*

$$(d-s)I_s(\mu) \leq (1+\eta)\left[(d-t)I_t(\mu) + \eta\mu(\mathbb{R}^d)^2\right].$$

Proof. Without loss of generality assume $\operatorname{diam} A < 1$. If $I_s(\mu) = \infty$, then $I_t(\mu) = \infty$ for $t > s$ and the lemma holds trivially. Now suppose that $I_s(\mu) < \infty$ for some s such that $(d-t)c(t,d) > \omega_d/2$ for all $t \in (s,d)$ (recall (3.9) to see why there is such a t) and observe that

$$\begin{aligned}(d-s)I_s(\mu) &= (d-s)c(s,d)\int_{\mathbb{R}^d} |\xi|^{s-d}|\hat{\mu}(\xi)|^2 d\xi \\ &= \frac{(d-s)c(s,d)}{(d-t)c(t,d)}(d-t)c(t,d)\int_{\mathbb{R}^d} |\xi|^{s-d}|\hat{\mu}(\xi)|^2 d\xi. \end{aligned} \tag{4.1}$$

We may approximate the integral in (4.1) as follows.

$$\begin{aligned}&\int_{\mathbb{R}^d} |\xi|^{s-d}|\hat{\mu}(\xi)|^2 d\xi \\ =\ &\int_{|\xi|\leq 1} |\xi|^{s-d}|\hat{\mu}(\xi)|^2 d\xi + \int_{|\xi|>1} |\xi|^{s-d}|\hat{\mu}(\xi)|^2 d\xi \\ \leq\ &\int_{|\xi|\leq 1} (|\xi|^{s-d} - |\xi|^{t-d})|\hat{\mu}(\xi)|^2 d\xi + \int_{|\xi|\leq 1} |\xi|^{t-d}|\hat{\mu}(\xi)|^2 d\xi + \int_{|\xi|>1} |\xi|^{t-d}|\hat{\mu}(\xi)|^2 d\xi \\ \leq\ &\mu(\mathbb{R}^d)^2 \int_{|\xi|\leq 1} (|\xi|^{s-d} - |\xi|^{t-d}) d\xi + \int_{\mathbb{R}^d} |\xi|^{t-d}|\hat{\mu}(\xi)|^2 d\xi. \end{aligned}$$

By (3.9) we may pick $s_0 \in (0,d)$ high enough so that, for any s and t satisfying $s_0 < s < t < d$

$$\frac{(d-s)c(s,d)}{(d-t)c(t,d)} < 1+\eta, \qquad (d-t)c(t,d) < 2\omega_d,$$

and

$$\left| \int_{|\xi| \leq 1} (|\xi|^{s-d} - |\xi|^{t-d}) d\xi \right| < \frac{\eta}{2\omega_d}.$$

□

The following generalization of Lemma 4.2.1 will be applied repeatedly to measures supported on the bi-Lipschitz image of a compact set, $K \subset \mathbb{R}^d$. Let $\mu \in \mathcal{M}(\varphi(K))$ be such a measure. Using (3.4) to bound the s-energy of $\varphi_{\#}^{-1}\mu$, applying Lemma 4.2.1 to $\varphi_{\#}^{-1}\mu$, and then using (3.4) again to bound the t-energy of the measure $\varphi_{\#}\varphi_{\#}^{-1}\mu = \mu$ we obtain the following.

Corollary 4.2.2. *Let $K \subset \mathbb{R}^d$ be a compact set and suppose $\varphi : K \to \mathbb{R}^p$ is bi-Lipschitz with constant L. Then, for every $\eta > 0$ there is an $s_0 = s_0(\eta)$ such that for any s and t satisfying $s_0 < s < t < d$ and any measure $\mu \in \mathcal{M}(\varphi(K))$, we have*

$$(d - s) I_s(\mu) \leq L^d (1 + \eta) \left[L^d (d - t) I_t(\mu) + \eta \mu(\mathbb{R}^p)^2 \right].$$

The intuition that led to Corollary 4.2.2 is as follows: Lemma 4.2.1 relies on the Fourier transform of a measure supported on a set of dimension equal to the dimension of the embedding space, and in particular on (3.9). If one takes a d-dimensional set and bends it (and the charge sitting on it) slightly so that it can no longer be embedded in $\mathbb{R}^d$, the Fourier approach breaks down because (3.9) holds only when one is taking the Fourier transform in a space of the same dimension as the set A. However, since the bending is slight, the relative distances are mostly preserved and the energy shouldn't change too much. The parameter L in Corollary 4.2.2 indicates the degree of the bending.

In Proposition 4.2.3 we prove a simple case of Theorem 4.1.1. Its proof illustrates the approach used in the proof of Theorem 4.1.1.

Proposition 4.2.3. *Let $A \subset \mathbb{R}^d$ be a compact set such that $\mathcal{H}^d(A) > 0$. Let μ^s denote the s-equilibrium measure supported on A. Then $\mu^{s,A} \xrightarrow{*} \lambda^d := \mathcal{H}_A^d / \mathcal{H}^d(A)$ as $s \uparrow d$.*

Proof. Let $\psi \in \mathcal{M}_1^+(A)$ be a weak-star cluster point of $\mu^{s,A}$ as $s \uparrow d$. Let $\{s_n\}_{n=1}^{\infty} \uparrow d$ such that $\mu^{s_n,A} \xrightarrow{*} \psi$ as $n \to \infty$. Let $\eta > 0$ be arbitrary, s_0 be as provided by Lemma 4.2.1, and let $s \in (s_0, d)$. We have

$$\begin{aligned}
(d-s)I_s(\psi) &\leq \liminf_{n\to\infty} (d-s)I_s(\mu^{s_n,A}) \\
&\leq \liminf_{n\to\infty} (1+\eta)\left[(d-s_n)I_{s_n}(\mu^{s_n,A}) + \eta\right] \\
&\leq \liminf_{n\to\infty} (1+\eta)\left[(d-s_n)I_{s_n}(\lambda^d) + \eta\right] \\
&= (1+\eta)\left[\tilde{I}_d(\lambda^d) + \eta\right],
\end{aligned}$$

where the first inequality is an application of the Principle of Descent. The second inequality follows from Lemma 4.2.1 where t in the statement of the lemma is chosen to be s_n, and the third from the minimality of $I_{s_n}(\mu^{s_n})$.

The variable s may be taken arbitrarily close to d, and so $\tilde{I}_d(\psi) \leq (1+\eta)[\tilde{I}_d(\lambda^d) + \eta]$. The variable η was also chosen arbitrarily and we conclude $\tilde{I}_d(\psi) \leq \tilde{I}_d(\lambda^d)$. Theorem 3.3.1 ensures that λ^d is the unique probability measure that minimizes $\tilde{I}_d$, and so $\psi = \lambda^d$. Since this holds for any weak-star cluster point, the proposition is proven. □

The only technical hurdle to extending the proof of Proposition 4.2.3 to a proof of Theorem 4.1.1 is to establish an analog of Lemma 4.2.1 for the case when A is strongly $(\mathcal{H}^d, d)$-rectifiable and of lower dimension than that of the embedding space, $\mathbb{R}^p$. This is accomplished by breaking A into near isometries of compact subsets of $\mathbb{R}^d$, establishing the desired estimate on each piece, and showing that the pieces can be glued back together without affecting the estimate. This is the content of Lemmas 4.2.4, 4.2.5 and 4.2.6.

These lemmas are somewhat technical and so the reader may want to keep the following example in mind while reading them. Let A be a one dimensional subset of $\mathbb{R}^2$ consisting of the following union of two intervals

$$\{(x,0) \in \mathbb{R}^2 \,:\, x \in [-1,1]\} \cup \{(0,y) \in \mathbb{R}^2 \,:\, y \in [-1,1]\}.$$

In this case A is a union of two bi-Lipschitz (in fact isometric) images of the interval $[-1, 1]$. Our goal is to establish an estimate like that of Lemma 4.2.1 for strongly $(\mathcal{H}^d, d)$-rectifiable sets such as our example A.

When applied to our example set A Lemma 4.2.4 considers the energy of the charge lying in the intersection of a single image of the interval $[-1, 1]$ and an $\mathcal{H}^d_A$ almost clopen set B. Roughly speaking the limiting energies on this intersection are proportional to the $\mathcal{H}^d_A$-measure of the intersection.

Lemma 4.2.4. *Let $A \subset \mathbb{R}^p$ be a compact, strongly $(\mathcal{H}^d, d)$-rectifiable set such that $\mathcal{H}^d(A) > 0$. Let $K \subset \mathbb{R}^d$ be compact, and $\varphi : K \to \mathbb{R}^p$ a bi-Lipschitz map such that $\varphi(K) \subset A$. Then, for every $\varepsilon > 0$, there is an $s_0 = s_0(\varepsilon)$ and a constant $C_{K,\varphi} = C_{K,\varphi}(A, K, \varphi)$ such that, for any Borel set $B \subset \mathbb{R}^p$ satisfying $\mathcal{H}^d_A(\partial B) = 0$ and any $s \in (s_0, d)$,*

$$\limsup_{t \uparrow d} (d - s) I_s\left(\mu^{t,A}_{B\cap\varphi(K)}\right) \leq C_{K,\varphi} \sqrt{\mathcal{H}^d_A(B)} + \varepsilon.$$

The boundary, ∂B, is computed in the usual topology on $\mathbb{R}^p$.

Proof. Without loss of generality assume $\varepsilon \in (0, 1)$. Let $B \subset \mathbb{R}^p$ be a Borel set such that $\mathcal{H}^d_A(\partial B) = 0$. Observe that

$$I_t\left(\mu^{t,A}_{B\cap\varphi(K)}\right) = \int_{B\cap\varphi(K)} U_t^{\mu^{t,A}_{B\cap\varphi(K)}} d\mu^{t,A} \leq \int_{B\cap\varphi(K)} U_t^{\mu^{t,A}} d\mu^{t,A} = I_t(\mu^{t,A})\mu^{t,A}(B \cap \varphi(K)). \tag{4.2}$$

We bound the quantity $\limsup_{t\uparrow d} \mu^{t,A}(B \cap \varphi(K))$ as follows. Let $\psi \in \mathcal{M}^+(A)$ be a weak-star cluster point of $\mu^{t,A}_{B\cap\varphi(K)}$ as $t \uparrow d$, and let $\{t_n\}_{n=1}^\infty \uparrow d$ such that $\mu^{t_n,A}_{B\cap\varphi(K)} \xrightarrow{*} \psi$ as $n \to \infty$. Let L denote the bi-Lipschitz constant of φ. Choose $\tilde{s}_0$ so that Corollary 4.2.2 applied to Radon measures with supported in $\varphi(K)$ holds for $\eta = 1$. Let $\lambda^d := \mathcal{H}^d_A/\mathcal{H}^d(A)$ denote the

minimizer of $\tilde{I}_d$ over $\mathcal{M}_1^+(A)$. For any $s \in (\tilde{s}_0, d)$,

$$\begin{aligned}(d-s)I_s(\psi) &\leq \liminf_{n\to\infty} (d-s)I_s\left(\mu^{t_n,A}_{B\cap\varphi(K)}\right)\\ &\leq \liminf_{n\to\infty}\ 2L^d\left[(d-t_n)L^d I_{t_n}(\mu^{t_n,A})+1\right]\\ &\leq \liminf_{n\to\infty}\ 2L^d\left[(d-t_n)L^d I_{t_n}(\lambda^d)+1\right]\\ &= 2L^{2d}\tilde{I}_d(\lambda^d)+2L^d =: M<\infty.\end{aligned}$$

The first inequality follows from the Principle of Descent, the second from Corollary 4.2.2 and the inequality, $I_s(\mu^{t_n,A}_{B\cap\varphi(K)}) \leq I_s(\mu^{t_n,A})$, and the third from the minimality of $I_{t_n}(\mu^{t_n,A})$. Letting $s \uparrow d$ we see that, for any weak-star cluster point ψ of $\mu^{t,A}_{B\cap\varphi(K)}$ (as $t \uparrow d$), $\tilde{I}_d(\psi) \leq M$. Theorem 3.3.1 ensures that $\psi \ll \mathcal{H}^d_A$, and so $\psi(\partial B) = 0$, implying $\mu^{t_n,A}(B\cap\varphi(K)) = \mu^{t_n,A}_{B\cap\varphi(K)}(B) \to \psi(B)$ as $n\to\infty$.

The set $\overline{B}\cap A$ is strongly d-rectifiable, and if $\psi(B) > 0$, then $\mathcal{H}^d_A(B) > 0$, implying $\mathcal{H}^d\left(\overline{B}\cap A\right) > 0$ and by Theorem 3.3.1, $\tilde{I}_d$ is minimized over $\mathcal{M}_1\left(\overline{B}\cap A\right)$ by $\lambda^{d,\overline{B}\cap A} := \mathcal{H}^d_{\overline{B}\cap A}/\mathcal{H}^d\left(\overline{B}\cap A\right)$. We then have

$$\frac{2^d d}{\mathcal{H}^d_A(B)} = \frac{2^d d}{\mathcal{H}^d_A\left(\overline{B}\right)} = \frac{2^d d}{\mathcal{H}^d\left(\overline{B}\cap A\right)} = \tilde{I}_d\left(\lambda^{d,\overline{B}\cap A}\right) \leq \tilde{I}_d\left(\frac{\psi}{\psi\left(\overline{B}\right)}\right) = \tilde{I}_d\left(\frac{\psi}{\psi(B)}\right) \leq \frac{M}{\psi(B)^2},$$

and we may conclude

$$\psi(B) \leq \sqrt{\frac{M}{2^d d}\mathcal{H}^d_A(B)}.$$

(If $\psi(B) = 0$, then the above inequality holds trivially.) It follows from the above inequality and (4.2) that for any Borel set $B \subset \mathbb{R}^p$ with $\mathcal{H}^d_A(\partial B) = 0$ we have

$$\begin{aligned}\limsup_{t\uparrow d}(d-t)I_t\left(\mu^{t,A}_{B\cap\varphi(K)}\right) &\leq \limsup_{t\uparrow d}(d-t)I_t(\mu^{t,A})\limsup_{t\uparrow d}\ \mu^{t,A}(B\cap\varphi(K))\\ &\leq \tilde{I}_d(\lambda^d)\sqrt{\frac{M}{2^d d}}\sqrt{\mathcal{H}^d_A(B)}. \qquad (4.3)\end{aligned}$$

We complete the proof of this lemma by appealing to Corollary 4.2.2 applied to

measures supported on $\varphi(K)$ with $\eta = \varepsilon/2L^d$. If s_0 is chosen so that Corollary 4.2.2 holds, then, for any $s \in (s_0, d)$ and $t \in (s, d)$,

$$\begin{aligned}(d-s)I_s\left(\mu^{t,A}_{B\cap\varphi(K)}\right) &\leq L^d\left[\left(1+\frac{\varepsilon}{2L^d}\right)\left(L^d(d-t)I_t\left(\mu^{t,A}_{B\cap\varphi(K)}\right)+\frac{\varepsilon}{2L^d}\right)\right]\\ &\leq 2L^{2d}(d-t)I_t\left(\mu^{t,A}_{B\cap\varphi(K)}\right)+\varepsilon.\end{aligned}$$

Taking the limit superior of both sides as $t \uparrow d$ and appealing to (4.3) completes the proof with $C_{K,\varphi} = 2L^{2d}\tilde{I}_d(\lambda^d)\sqrt{M/2^d d}$. □

Lemma 4.2.5 uses Lemma 4.2.4 to excise a small neighborhood around the crossing of the two intervals in our example set A. The limiting energy due to this excised portion is small and the remaining pieces of A can be embedded into $\mathbb{R}$ and are disjoint.

Lemma 4.2.5. *Let $A \subset \mathbb{R}^p$ be a compact, strongly $(\mathcal{H}^d, d)$-rectifiable set such that $\mathcal{H}^d(A) > 0$. Then, for every $\varepsilon > 0$, there exists a finite collection of compact subsets of $\mathbb{R}^d$ $\tilde{K}_1, \ldots, \tilde{K}_N$ and a corresponding set of bi-Lipschitz maps $\tilde{\varphi}_1 : \tilde{K}_1 \to \mathbb{R}^p, \ldots, \tilde{\varphi}_N : \tilde{K}_N \to \mathbb{R}^p$ each with bi-Lipschitz constant less than $1+\varepsilon$, such that*

1. *$\tilde{\varphi}_i(\tilde{K}_i) \cap \tilde{\varphi}_j(\tilde{K}_j) = \varnothing$ for $i \neq j$, and*
2. *there is an $s_0 = s_0(\varepsilon) \in (0, d)$, such that for $\tilde{B} := A \setminus \bigcup_{i=1}^N \tilde{\varphi}_i(\tilde{K}_i)$ and all $s \in (s_0, d)$ we have*

$$\limsup_{t\uparrow d}\,(d-s)I_s(\mu^{t,A}_{\tilde{B}}) \leq \frac{\varepsilon}{N}.$$

Proof. Without loss of generality assume $\varepsilon \in (0,1)$. Since A is strongly $(\mathcal{H}^d, d)$-rectifiable, we may find a set, $A_0 \subset \mathbb{R}^p$, compact sets $K_1, \ldots, K_N \subset \mathbb{R}^d$ and bi-Lipschitz maps $\varphi_1 : K_1 \to \mathbb{R}^p, \ldots, \varphi_N : K_N \to \mathbb{R}^p$ with constant less than $1+\varepsilon$ such that $A = \bigcup_{i=1}^N \varphi_i(K_i) \cup A_0$, where $\dim A_0 < d$, and $\mathcal{H}^d(\varphi_i(K_i) \cap \varphi_j(K_j)) = 0$. Let $\delta = \varepsilon^2/4N^2 \in (0,1)$. The set $E = \bigcup_{i\neq j}\left(\varphi_i(K_i) \cap \varphi_j(K_j)\right)$ is a compact set of $\mathcal{H}^d_A$-measure 0. Since $\mathcal{H}^d_A$ is Radon, there is an open set O such that $E \subset O$ and $\mathcal{H}^d_A(O) < \delta N^{-4}\left(\max\left\{C_{K_1,\varphi_1}, \ldots, C_{K_N,\varphi_N}\right\}\right)^{-2}$ where C_{K_i,φ_i} is the constant provided by Lemma 4.2.4 applied to $\varphi_i(K_i) \subset A$.

For any point $x \in E$, we may find a non-empty open ball $B(x,R)^0 \subset O$. Since $\partial B(x,r_1) \cap \partial B(x,r_2) = \varnothing$ for any $r_1 \neq r_2$ and since $\mathcal{H}_A^d$ is a finite measure, all but a countable set of values of $r \in (0,R)$ must be such that $\mathcal{H}_A^d(\partial B(x,r)) = 0$. Construct an open cover of E as follows.

$$\Omega = \left\{ B(x,r)^0 : x \in E,\ B(x,r)^0 \subset O,\ \mathcal{H}_A^d(\partial B(x,r)) = 0 \right\}.$$

Choose a finite sub-cover $\Omega' \subset \Omega$, of E. Let $B = \bigcup_{b \in \Omega'} b$. Since $\partial B \subset \bigcup_{b \in \Omega'} \partial b$, we have that $\mathcal{H}_A^d(\partial B) = 0$. Let $B_i = B \cap \varphi_i(K_i)$. For any $s,\ t \in (0,d)$ with $t > \max\{s, \dim A_0\}$ we have, by the equality of the Hausdorff and capacitory dimensions (Proposition 2.4.3), that $\mu^{t,A}(A_0) = 0$ and hence

$$(d-s)I_s(\mu_B^{t,A}) \leq (d-s)I_s\left(\mu_{A_0}^{t,A} + \sum_{i=1}^{N} \mu_{B_i}^{t,A}\right) = \sum_{i,j=1}^{N} (d-s)I_s(\mu_{B_i}^{t,A}, \mu_{B_j}^{t,A}).$$

By Jensen's inequality followed by the Cauchy-Schwarz inequality applied to the inner-product $I_s(\cdot,\cdot)$ we have

$$\begin{aligned} \left[\frac{1}{N^2}\sum_{i,j=1}^{N} (d-s)I_s(\mu_{B_i}^{t,A}, \mu_{B_j}^{t,A})\right]^2 &\leq \frac{1}{N^2}\sum_{i,j=1}^{N} \left[(d-s)I_s(\mu_{B_i}^{t,A}, \mu_{B_j}^{t,A})\right]^2 \\ &\leq \frac{1}{N^2}\sum_{i,j=1}^{N} (d-s)I_s(\mu_{B_i}^{t,A})(d-s)I_s(\mu_{B_j}^{t,A}). \end{aligned}$$

Let $s_0 = \max\{\dim A_0, s_{0,1}, \ldots, s_{0,N}\}$, where $s_{0,i}$ is the value of s_0 provided by Lemma 4.2.4 applied to $\varphi_i(K_i) \subset A$, and where the value of ε in the statement of Lemma 4.2.4 is chosen

to be δ/N^2. Combining the previous bounds gives, for $s \in (s_0, d)$,

$$\begin{aligned}
\left[\limsup_{t\uparrow d}(d-s)I_s(\mu_B^{t,A})\right]^2 &\leq N^2\sum_{i,j=1}^{N}\limsup_{t\uparrow d}(d-s)I_s(\mu_{B_i}^{t,A})\limsup_{t\uparrow d}(d-s)I_s(\mu_{B_j}^{t,A}) \\
&\leq N^2\sum_{i,j=1}^{N}\left(C_{K_i,\varphi_i}\sqrt{\frac{\delta}{N^4\left(C_{K_i,\varphi_i}\right)^2}}+\frac{\delta}{N^2}\right)\left(C_{K_j,\varphi_j}\sqrt{\frac{\delta}{N^4\left(C_{K_j,\varphi_j}\right)^2}}+\frac{\delta}{N^2}\right) \\
&= N^2\sum_{i,j=1}^{N}\left(\frac{\sqrt{\delta}+\delta}{N^2}\right)^2 \\
&\leq 4\delta = \left(\frac{\varepsilon}{N}\right)^2.
\end{aligned}$$

The value of s_0, the set $\tilde{B} := (B \cap A) \cup A_0$, the compact sets $\tilde{K}_i := K_i \backslash \varphi_i^{-1}(B)$, and the bi-Lipschitz maps $\tilde{\varphi}_i := \varphi_i|_{\tilde{K}_i}$ satisfy the properties claimed in the lemma for the value of ε given. □

At this point we are ready to establish an analog of Lemma 4.2.1 for our example set A. We consider the limiting energy on our set A in the following four categories:

(1) The limiting energy of the excised portion around the intersection of the two intervals: By Lemma 4.2.5 this may be made small.

(2) The limiting energy from the interactions between the excision and the interaction with remaining portions of A: By Cauchy-Schwarz applied to the inner product $I_s(\cdot,\cdot)$ this can be made small as well.

(3) The interaction energy between the disjoint pieces of A that weren't excised: This can be made small because the limiting energy is localized.

(4) The limiting energy of the disjoint pieces of A: Because each of them can be embedded into $\mathbb{R}$ we may appeal to Lemma 4.2.2 to establish the desired estimate.

Lemma 4.2.6. *Let $A \subset \mathbb{R}^p$ be a strongly $(\mathcal{H}^d, d)$-rectifiable, compact set such that $\mathcal{H}^d(A) > 0$. Then, for every $\eta > 0$, there is an $s_0 = s_0(\eta)$, such that for all $s \in (s_0, d)$ we have*

$$\limsup_{t\uparrow d} (d-s) I_s(\mu^{t,A}) \leq (1+\eta) \limsup_{t\uparrow d} (d-t) I_t(\mu^{t,A}) + \eta.$$

Proof. Let $\lambda^d := \mathcal{H}^d_A / \mathcal{H}^d(A)$ denote the unique minimizer of $\tilde{I}_d$ over $\mathcal{M}_1^+(A)$. Let $\eta > 0$. Choose $\varepsilon \in (0,1)$ such that

$$\max\left\{\left(\varepsilon\left[2 + (1+\varepsilon)^{d+1}\right] + 2\sqrt{\varepsilon(1+\varepsilon)^{2d+1}\tilde{I}_d(\lambda^d) + \varepsilon^2(1+\varepsilon)^{d+1}}\right), \left((1+\varepsilon)^{2d+1} - 1\right)\right\} < \eta. \tag{4.4}$$

From Lemma 4.2.5 there is an $s_1 \in (0,d)$, a sequence of compact sets $\tilde{K}_1, \ldots, \tilde{K}_N \subset \mathbb{R}^d$ and a sequence of bi-Lipschtiz maps $\tilde{\varphi}_1 : \tilde{K}_1 \to \mathbb{R}^p, \ldots, \tilde{\varphi}_N : \tilde{K}_N \to \mathbb{R}^p$ each with constant less than $1+\varepsilon$ such that $\tilde{\varphi}_i(\tilde{K}_i) \cap \tilde{\varphi}_j(\tilde{K}_j) = \varnothing$ for $i \neq j$, and $\tilde{B} := A \setminus \bigcup_{i=1}^N \tilde{\varphi}_i(\tilde{K}_i)$ satisfies the following for all $s \in (s_1, d)$

$$\limsup_{t\uparrow d} (d-s) I_s(\mu^{t,A}_{\tilde{B}}) \leq \frac{\varepsilon}{N}.$$

For $s \in (s_1, d)$ we have

$$\begin{aligned}
\limsup_{t\uparrow d} (d-s) I_s(\mu^{t,A}) &= \limsup_{t\uparrow d} (d-s) I_s\left(\mu^{t,A}_{\tilde{B}} + \sum_{i=1}^N \mu^{t,A}_{\tilde{\varphi}_i(\tilde{K}_i)}\right) \\
&\leq \limsup_{t\uparrow d} (d-s) I_s\left(\mu^{t,A}_{\tilde{B}}\right) && (4.5) \\
&+ 2\limsup_{t\uparrow d} \sum_{i=1}^N (d-s) I_s\left(\mu^{t,A}_{\tilde{B}}, \mu^{t,A}_{\tilde{\varphi}_i(\tilde{K}_i)}\right) && (4.6) \\
&+ \limsup_{t\uparrow d} \sum_{\substack{i,j=1 \\ i\neq j}}^N (d-s) I_s\left(\mu^{t,A}_{\tilde{\varphi}_i(\tilde{K}_i)}, \mu^{t,A}_{\tilde{\varphi}_j(\tilde{K}_j)}\right) && (4.7) \\
&+ \limsup_{t\uparrow d} \sum_{i=1}^N (d-s) I_s\left(\mu^{t,A}_{\tilde{\varphi}_i(\tilde{K}_i)}\right). && (4.8)
\end{aligned}$$

We next find upper bounds for each of the terms in (4.5–4.8). First, Lemma 4.2.5 implies that, for $s \in (s_1, d)$, expression (4.5) is less than ε/N .

Second, using Jensen's inequality and the Cauchy-Schwarz inequality in the same manner as in the proof of Lemma 4.2.5 we have

$$\sum_{i=1}^{N}(d-s)I_s\left(\mu_{\tilde{B}}^{t,A},\mu_{\tilde{\varphi}_i(\tilde{K}_i)}^{t,A}\right) \leq \sqrt{N(d-s)I_s\left(\mu_{\tilde{B}}^{t,A}\right)\sum_{i=1}^{N}(d-s)I_s\left(\mu_{\tilde{\varphi}_i(\tilde{K}_i)}^{t,A}\right)}.$$

Since each $\tilde{\varphi}_i$ is bi-Lipschitz with constant $(1+\varepsilon)$, Corollary 4.2.2 (with the values of η and L as stated in the corollary chosen to be ε and $1+\varepsilon$ respectively) ensures that there is some $s_2 \in (s_1, d)$ such that, for $s_2 < s < t < d$, we have

$$(d-s)I_s\left(\mu_{\tilde{\varphi}_i(\tilde{K}_i)}^{t,A}\right) \leq (1+\varepsilon)^{2d+1}(d-t)I_t\left(\mu_{\tilde{\varphi}_i(\tilde{K}_i)}^{t,A}\right) + \varepsilon(1+\varepsilon)^{d+1}\mu_{\tilde{\varphi}_i(\tilde{K}_i)}^{t,A}(\mathbb{R}^p)^2. \tag{4.9}$$

Then (4.9), together with the bound for (4.5), implies that expression (4.6) is bounded above by

$$2\sqrt{N\frac{\varepsilon}{N}\limsup_{t\uparrow d}\left[(1+\varepsilon)^{2d+1}\sum_{i=1}^{N}(d-t)I_t\left(\mu_{\tilde{\varphi}_i(\tilde{K}_i)}^{t,A}\right)+\varepsilon(1+\varepsilon)^{d+1}\sum_{i=1}^{N}\mu_{\tilde{\varphi}_i(\tilde{K}_i)}^{t,A}(\mathbb{R}^p)\right]}$$

Using

$$\limsup_{t\uparrow d}\sum_{i=1}^{N}(d-t)I_t\left(\mu_{\tilde{\varphi}_i(\tilde{K}_i)}^{t,A}\right) \leq \limsup_{t\uparrow d}(d-t)I_t(\mu^{t,A}) \leq \limsup_{t\uparrow d}(d-t)I_t(\lambda^d) = \tilde{I}_d(\lambda^d)$$

it follows that, for $s \in (s_2, d)$, expression (4.6) is bounded above by

$$2\sqrt{\varepsilon\left[(1+\varepsilon)^{2d+1}\tilde{I}_d(\lambda^d)+\varepsilon(1+\varepsilon)^{d+1}\right]}.$$

We bound (4.7) as follows. For $1 \leq i \neq j \leq N$, let $D_{i,j} = \operatorname{dist}(\tilde{\varphi}_i(\tilde{K}_i), \tilde{\varphi}_j(\tilde{K}_j)) > 0$ and let $s_{i,j} \in (0, d)$ be such that $(d-s)D_{i,j}^{-s} \leq \varepsilon/N^2$ for all $s \in (s_{i,j}, d)$. For such an s, $(d-s)I_s(\nu_1,\nu_2) \leq \nu_1(\mathbb{R}^p)\nu_2(\mathbb{R}^p)\varepsilon/N^2$, for any $\nu_1, \nu_2 \in \mathcal{M}^+(A)$ supported on $\tilde{\varphi}_i(\tilde{K}_i)$ and

$\tilde{\varphi}_j(\tilde{K}_j)$ respectively. Let $s_0 := \max\left\{s_2, s_{i,j} : i \neq j\right\}$. For all $s \in (s_0, d)$,

$$\sum_{\substack{i,j=1 \\ i\neq j}}^{N}(d-s)I_s\left(\mu^{t,A}_{\tilde{\varphi}_i(\tilde{K}_i)}, \mu^{t,A}_{\tilde{\varphi}_j(\tilde{K}_j)}\right) < \varepsilon.$$

From (4.9) we have the following bound for (4.8)

$$\begin{aligned}\sum_{i=1}^{N}(d-s)I_s\left(\mu^{t,A}_{\tilde{\varphi}_i(\tilde{K}_i)}\right) &\leq (1+\varepsilon)^{2d+1}\left(\sum_{i=1}^{N}(d-t)I_t\left(\mu^{t,A}_{\tilde{\varphi}_i(\tilde{K}_i)}\right)\right) + \varepsilon(1+\varepsilon)^{d+1}\left(\sum_{i=1}^{N}\mu^{t,A}_{\tilde{\varphi}_i(\tilde{K}_i)}(\mathbb{R}^p)^2\right) \\ &\leq (1+\varepsilon)^{2d+1}(d-t)I_t(\mu^{t,A}) + \varepsilon(1+\varepsilon)^{d+1}.\end{aligned}$$

For $s \in (s_0, d)$, the preceding estimates, together with (4.4), gives

$$\begin{aligned}\limsup_{t\uparrow d}(d-s)I_s(\mu^{t,A}) &\leq \left[\varepsilon\left[2+(1+\varepsilon)^{d+1}\right] + 2\sqrt{\varepsilon(1+\varepsilon)^{2d+1}\tilde{I}_d(\lambda^d) + \varepsilon^2(1+\varepsilon)^{d+1}}\right] \\ &+ \left[(1+\varepsilon)^{2d+1}\right]\limsup_{t\uparrow d}(d-t)I_t(\mu^{t,A}) \\ &\leq \eta + (1+\eta)\limsup_{t\uparrow d}(d-t)I_t(\mu^{t,A}).\end{aligned}$$

□

4.2.1 **Proof of Theorem 4.1.1**

Proof of theorem 4.1.1. Let A satisfy the hypotheses of Theorem 4.1.1 and hence of Theorem 3.3.1. Let $\lambda^d := \mathcal{H}^d_A/\mathcal{H}^d(A)$ denote the unique minimizer of $\tilde{I}_d$ over $\mathcal{M}_1^+(A)$. Let ψ be any weak-star cluster point of $\mu^{s,A}$ as $s \uparrow d$, and let $\{s_n\}_{n=1}^{\infty} \uparrow d$ such that $\mu^{s_n,A} \xrightarrow{*} \psi$. Let $\eta > 0$ be arbitrary. Let s_0 be the value provided by lemma 4.2.6 for this choice of η.

For any $s \in (s_0, d)$, we have

$$\begin{aligned}(d-s)I_s(\psi) &\leq \liminf_{n\to\infty} (d-s)I_s(\mu^{s_n,A}) \\ &\leq \limsup_{n\to\infty} (d-s_n)I_{s_n}(\mu^{s_n,A})(1+\eta)+\eta \\ &\leq \limsup_{n\to\infty} (d-s_n)I_{s_n}(\lambda^d)(1+\eta)+\eta \\ &= (1+\eta)\tilde{I}_d(\lambda^d)+\eta.\end{aligned}$$

As in the proof of Proposition 4.2.3, the first inequality follows from the Principle of Descent, the second from Lemma 4.2.6, and the third from the minimality of $I_{s_n}(\mu^{s_n,A})$. Since s may be chosen arbitrarily close to d, $\tilde{I}_d(\psi) \leq (1+\eta)\tilde{I}_d(\lambda^d)+\eta$. Since η was also arbitrarily chosen, $\tilde{I}_d(\psi) \leq \tilde{I}_d(\lambda^d)$. The uniqueness of the minimizer λ^d ensured by Theorem 3.3.1 proves that $\psi = \lambda^d$ and is sufficient to prove Theorem 4.1.1. □

4.3 The Behavior of $\mu^{s,A}$ for Strictly Self-Similar d-Fractals

Lemma 4.3.1. *Let A be a compact subset of $\mathbb{R}^p$ such that $\dim A = d$ and $\mathcal{H}^d(A) < \infty$*[1] *, then*

$$\lim_{s\uparrow d} I_s(\mu^{s,A}) = \infty.$$

Proof. Without loss of generality we shall assume that $\operatorname{diam} A \leq 1$, then for $0 < s < t < d$ and any measure $\mu \in \mathcal{M}^+(A)$, $I_s(\mu) \leq I_t(\mu)$. Let $\{s_n\}_{n=1}^{\infty}$ be any sequence increasing to d so that $\mu^{s_n,A} \xrightarrow{*} \nu$ for some $\nu \in \mathcal{M}_1^+(A)$. Then for any $t \in (0,d)$ we have

$$\begin{aligned}I_t(\nu) &\leq \liminf_{n\to\infty} I_t(\mu^{s_n,A}) \quad \text{by the Principle of Descent (Lemma 2.4.5)} \\ &\leq \liminf_{n\to\infty} I_{s_n}(\mu^{s_n,A}) \quad \text{because } \operatorname{diam} A < 1 \text{ and } s_n > t \text{ for } n \text{ large.} \qquad (4.10)\end{aligned}$$

[1] *The author would like to thank Douglas Hardin for reducing the hypotheses necessary for this lemma.*

(4.10) is independent of t and so we may take $t \uparrow d$. Then by monotone convergence

$$\lim_{t\uparrow d} I_t(\nu) = I_d(\nu).$$

By Lemma 2.4.2, $I_d(\nu) = \infty$. Since every sequence of values of s increasing to d has a subsequence which is convergent in the weak-star topology, the claim folows. □

Lemma 4.3.2. *Let A be a compact Ahlfors d-regular set, then*

$$\lim_{s\uparrow d} \sup_{y\in A} \operatorname{dist}(y, \operatorname{supp}\mu^{s,A}) = 0.$$

Proof. Let $s \in (0,d)$ and $\delta = \sup_{y\in A} \operatorname{dist}(y, \operatorname{supp}\mu^{s,A})$. We consider the possibility that $\delta > 0$. Pick $y' \in A$ so that $\operatorname{dist}(y', \operatorname{supp}\mu^{s,A}) > \delta/2$. Let $\nu = \mathcal{H}^d_{A\cap B(y',\delta/4)}/\mathcal{H}^d_A(B(y',\delta/4))$. For $\beta \in [0,1]$ we have $(1-\beta)\mu^{s,A} + \beta\nu \in \mathcal{M}^+_1(A)$. The lower Ahlfors d-regularity ensures that ν is not identically zero and the upper Ahlfors d-regularity ensures that $I_s(\nu) < \infty$ for all $s \in (0,d)$. Define the function

$$f(\beta) := I_s\left((1-\beta)\mu^{s,A} + \beta\nu\right) = (1-\beta)^2 I_s(\mu^{s,A}) + \beta^2 I_s(\nu) + 2\beta(1-\beta) I_s(\mu^{s,A}, \nu).$$

Differentiating gives

$$\frac{1}{2}\frac{df}{d\beta} = \beta\left[I_s(\mu^{s,A} - \nu)\right] - \left[I_s(\mu^{s,A}) - I_s(\mu^{s,A}, \nu)\right] \qquad \text{and} \qquad \frac{1}{2}\frac{d^2 f}{d\beta^2} = \left[I_s(\mu^{s,A} - \nu)\right].$$

Because $I_s(\cdot,\cdot)$ is positive definite, $I_s(\mu^{s,A} - \nu) > 0$. Because $\mu^{s,A}$ is the unique minimizer of I_s, f cannot have a minimum for any $\beta > 0$, hence $I_s(\mu^{s,A}) - I_s(\mu^{s,A}, \nu) \le 0$. We obtain

$$I_s(\mu^{s,A}) \le I_s(\mu^{s,A}, \nu) \le \frac{1}{(\delta/4)^s}, \qquad \text{and hence} \qquad \delta \le \frac{4}{I_s(\mu^{s,A})^{1/s}}.$$

The compactness and the upper Ahlfors d-regularity of A ensure that $\mathcal{H}^d(A) < \infty$. By Lemma 4.3.1 $\delta \downarrow 0$ as $s \uparrow d$. □

4.3.1 **Proof of Theorem 4.1.3**

The remaining proofs will make use of the following fact regarding the behavior of equilibrium measures on scaled sets: If $B' = \varphi(B)$ where φ is a similitude with a scale factor of L, then for any Borel set $E \subset B'$, $\mu^{s,B'}(E) = \mu^{s,B}(\varphi^{-1}(E))$ and $I_s(\mu^{s,B'}) = L^{-s} I_s(\mu^{s,B})$. This follows from scaling properties of the Riesz kernel.

Proof of Theorem 4.1.3. Without loss of generality assume $\operatorname{diam} A \leq 1$. Let $x \in A$ and $r \in (0, \operatorname{diam} A/4)$, then

$$I_s(\mu^{s,A}) = I_s\left(\mu^{s,A}_{B(x,r)} + \mu^{s,A}_{A\setminus B(x,r)}\right) \geq I_s\left(\mu^{s,A}_{B(x,r)}\right) + I_s\left(\mu^{s,A}_{A\setminus B(x,r)}\right). \tag{4.11}$$

By Lemma 4.3.2 there is an $s_0 \in (0, d)$ so that $\mu^{s,A}(A\setminus B(x, \operatorname{diam} A/4)) > 0$ for all $s \in (s_0, d)$. Note that the choice of s_0 depends only on A and not on x. First, consider the case $s \in (s_0, d)$. If $\mu^{s,A}(B(x,r)) = 0$, then the claim is trivially proven. Assume $\mu^{s,A}(B(x,r)) > 0$. We normalize the measures on the right hand side of (4.11) to be probability measures and obtain

$$\begin{aligned} & I_s\left(\mu^{s,A}_{B(x,r)}\right) + I_s\left(\mu^{s,A}_{A\setminus B(x,r)}\right) && (4.12)\\ = \;& \mu^{s,A}(B(x,r))^2 I_s\left(\frac{\mu^{s,A}_{B(x,r)}}{\mu^{s,A}(B(x,r))}\right) \\ + \;& (1-\mu^{s,A}(B(x,r)))^2 I_s\left(\frac{\mu^{s,A}_{A\setminus B(x,r)}}{1-\mu^{s,A}(B(x,r))}\right). && (4.13)\end{aligned}$$

By Lemma 3.1.3 we may find a set $A' \subset A$ so that $B(x,r) \cap A \subset A'$, $\operatorname{diam} A' < Wr$ and A' is a scaling of A. The right hand side of (4.12) is bounded below by

$$\begin{aligned} & \mu^{s,A}(B(x,r))^2 I_s(\mu^{s,A'}) + (1-\mu^{s,A}(B(x,r)))^2 I_s(\mu^{s,A}) \\ = \;& I_s(\mu^{s,A})\left[\mu^{s,A}(B(x,r))^2\left(\frac{\operatorname{diam} A'}{\operatorname{diam} A}\right)^{-s} + (1-\mu^{s,A}(B(x,r)))^2\right] \\ > \;& I_s(\mu^{s,A})\left[\mu^{s,A}(B(x,r))^2\left(\frac{Wr}{\operatorname{diam} A}\right)^{-s} + (1-\mu^{s,A}(B(x,r)))^2\right] && (4.14)\end{aligned}$$

Combining (4.11) and (4.14) and dividing by $I_s(\mu^{s,A})$ gives the following:

$$1 \geq \mu^{s,A}(B(x,r))^2 \left(\frac{Wr}{\operatorname{diam} A}\right)^{-s} + 1 - 2\mu^{s,A}(B(x,r)) + \mu^{s,A}(B(x,r))^2,$$

hence

$$2\mu^{s,A}(B(x,r)) \geq \mu^{s,A}(B(x,r))^2 \left[\left(\frac{Wr}{\operatorname{diam} A}\right)^{-s} + 1\right],$$

and thus

$$\mu^{s,A}(B(x,r)) \leq 2\left(\frac{W}{\operatorname{diam} A}\right)^{s} r^s.$$

Let K_1 be the maximum of $2(W/\operatorname{diam} A)^s$ over $s \in [0,d]$, K_2 the maximum of $(4/\operatorname{diam} A)^s$ over $s \in [0,d]$ and $K_a := \max\{K_1, K_2\}$, then $\mu^{s,A}(B(x,r)) < K_a r^s$ for all $x \in A$, $r > 0$ and $s \in (s_0, d)$.

For $s \in (0, s_0]$ we have the bound (cf. [34, Ch. 8]) $\mu^{s,A}(B(x,r)) \leq U_s^{\mu^{s,A}}(x) r^s = I_s(\mu^{s,A}) r^s$ for $\mu^{s,A}$-a.a. x. Because $\operatorname{diam} A \leq 1$, $I_s(\mu^{s,A}) \leq I_{s_0}(\mu^{s_0,A})$ for all $s \in (0, s_0]$. Let $K = \max\{K_a, 2I_{s_0}(\mu^{s_0,A})\}$, then $\mu^{s,A}(B(x,r)) < Kr^s$ for $\mu^{s,A}$-a.a. $x \in A$ and $r > 0$. □

4.3.2 **Proof of Theorem 4.1.2**

Proof of Theorem 4.1.2. Let $f : A \to \mathbb{R}$ be continuous. Since A is compact f is uniformly continuous on A. Fix $\varepsilon > 0$ and let $\delta > 0$ so that $f(A \cap B(x,\delta)) \subset (f(x) - \varepsilon, f(x) + \varepsilon)$ for all $x \in A$. Let M be a natural number high enough so that $L_N^M \operatorname{diam} A < \delta$.

Let α be a multi-index of length M taking values in $\{1, \ldots, N\}^M$. If $\alpha = (i_1, \ldots, i_M)$, then we denote $\varphi_{i_M}(\varphi_{i_{M-1}}(\ldots(\varphi_{i_1})\ldots))$ by ϕ_α. Let $\tilde{x}$ be any point in A. For any $\nu \in \mathcal{M}_1^+(A)$ we may write

$$\int f d\nu = \sum_\alpha \int f d\nu_{\phi_\alpha(A)} = \sum_\alpha f(\phi_\alpha(\tilde{x}))\nu(\phi_{\alpha(A)}) + \sum_\alpha \int (f - f(\phi_\alpha(\tilde{x}))) \, d\nu_{\phi_\alpha(A)}.$$

(When we write a multi-index α at bottom of a sum we indicate summation over all possible

multi-indices of the specified length.) It follows that

$$\left| \int f d\nu - \sum_{\alpha} f(\phi_\alpha(\tilde{x}))\nu(\phi_{\alpha(A)}) \right| < \varepsilon. \tag{4.15}$$

As in the proof of Lemma 3.1.3 let $\tilde{K} = \min_{i\in 1,\ldots,N}\{\text{dist}(\varphi_i(A), A\backslash\varphi_i(A))\}$. If α and α' are different multi-indices of length M, then $\text{dist}(\phi_\alpha(A), \phi_{\alpha'}(A)) \geq L_N^{M-1}\tilde{K}$. By Lemma 4.3.2 there is an $s_0 < d$ so that for all $s \in (s_0, d)$ we have $\sup_{y\in A} \text{dist}(y, \text{supp}\,\mu^{s,A}) < L_N^{M-1}\tilde{K}$. From this we conclude $\mu^{s,A}(\phi_\alpha(A)) > 0$ for any multi-index α of length M and any $s \in (s_0, d)$. For such a choice of s we have

$$I_s(\mu^{s,A}) > \sum_{\alpha} I_s\left(\mu^{s,A}_{\phi_\alpha(A)}\right) = \sum_{\alpha} \mu^{s,A}(\phi_\alpha(A))^2 I_s\left(\frac{\mu^{s,A}_{\phi_\alpha(A)}}{\mu^{s,A}(\phi_\alpha(A))}\right) \geq \sum_{\alpha} \mu^{s,A}(\phi_\alpha(A))^2 I_s\left(\mu^{s,\phi_\alpha(A)}\right).$$

We shall use the notation L_α to denote $L_{i_1}L_{i_2}\ldots L_{i_M}$. By appealing to the scaling properties of the Riesz energy, the above becomes

$$I_s(\mu^{s,A}) > \sum_{\alpha} \mu^{s,A}(\phi_\alpha(A))^2 L_\alpha^{d-s}\frac{I_s(\mu^{s,A})}{L_\alpha^d}.$$

Let ψ be any weak-star cluster point of $\mu^{s,A}$ as $s \uparrow d$ and let $\{s_n\}_{n=1}^{\infty} \uparrow d$ be a sequence so that $\mu^{s_n,A} \xrightarrow{*} \psi$ and hence so that $(\mu^{s_n,A}(\phi_\alpha(A)))_\alpha$ converges in $[0,1]^{N^M}$, then

$$1 = \lim_{n\to\infty} \frac{1}{(L_1^M)^{d-s_n}} \geq \lim_{n\to\infty} \sum_{\alpha} \frac{\mu^{s_n,A}(\phi_\alpha(A))^2}{L_\alpha^d} = \sum_{\alpha} \frac{[\lim_{n\to\infty} \mu^{s_n,A}(\phi_\alpha(A))]^2}{L_\alpha^d}.$$

We then have that

$$\begin{aligned} 1 &= \sum_{\alpha} \lim_{n\to\infty} \mu^{s_n,A}(\phi_\alpha(A)) = \sum_{\alpha} \frac{\lim_{n\to\infty} \mu^{s_n,A}(\phi_\alpha(A)}{\sqrt{L_\alpha^d}} \sqrt{L_\alpha^d} \\ &\leq \sqrt{\sum_{\alpha} \frac{[\lim_{n\to\infty} \mu^{s_n,A}(\phi_\alpha(A))]^2}{L_\alpha^d}} \sqrt{\sum_{\alpha} L_\alpha^d} = 1. \end{aligned}$$

Note that the sum over α of L_α^d is one because the sum over $i \in 1,\ldots N$ of L_i^d is one. From

this we conclude

$$\lim_{n\to\infty} \mu^{s_n,A}(\phi_\alpha(A)) = L_\alpha^d$$

for every multi-index α of length M. Because $\lambda^d(\phi_\alpha(A)) = L_\alpha^d$, we have that

$$\lim_{n\to\infty} \sum_\alpha f(\phi_\alpha(\tilde{x}))\mu^{s_n,A}(\phi_\alpha(A)) = \sum_\alpha f(\phi_\alpha(\tilde{x}))\lambda^d(\phi_\alpha(A)),$$

and so

$$\left|\lim_{n\to\infty} \int f d\mu^{s_n,A} - \int f d\lambda^d\right| < 2\varepsilon.$$

The choice of ε in (4.15) was arbitrary as was the choice of the continuous function f and so $\lambda^d = \psi$ for any weak-star cluster point ψ, and hence $\mu^{s,A} \xrightarrow{*} \lambda^d$ as $s \uparrow d$. □

CHAPTER 5

NUMERICAL EXPERIMENTS

In this chapter we describe our numerical experiments regarding discrete minimal energy configurations on the 2-dimensional sphere $\mathbb{S}^2 \subset \mathbb{R}^3$. There are a variety of motivations for such experiments. Separation results such as those presented in [7, 24] and weak-star convergence of discrete minimal energy points to the uniform measure suggest these points may be of value for numerical integration or coding theory. Minimizing the logarithmic or "$s = 0$" energy is equivalent to finding a collection of points where the product of the pairwise distances is maximized. In general minimal energy points appear to provide a good sampling set for $\mathbb{S}^2$. The physical underpinning of the problem suggests that numerical results may lead to a better understanding of structures found in spherical seed-pods, virus shells and colloids.

For the purposes of this chapter it will be more convenient to define the s-energy as

$$E_s(\omega_N) := \begin{cases} \sum_{1=i<j=N} \frac{1}{|x_i - x_j|^s} & \text{when } s \neq 0 \\ \sum_{1=i<j=N} \log \frac{1}{|x_i - x_j|} & \text{when } s = 0. \end{cases} \tag{5.1}$$

Note that this is half the value of the discrete energy as presented in 2.5. Recall that

$$\mathcal{E}_s(A, N) := \inf\{E_s(\omega_N) \,:\, \omega_N \subset A \text{ and } \#\omega_N = N\}.$$

Because $\mathbb{S}^2$ has a high degree of symmetry and because it is a manifold without boundary, a variety of numerical techniques are available and certain problems regarding points on a boundary (cf. [37]) are avoided.

In the cases where our experiments can be compared to previous experiments the results are largely in agreement. The new results presented here are:

(1) An accurate energy calculation that computes and minimizes roundoff error.

(2) A technique to compare configurations rapidly that is based on computational geometry and graph theory.

(3) An estimate of the parameters describing exponential growth of the number of stable configurations for a given value of N.

(4) Initial results for the observed minimal discrete energy for $N = 20, \ldots, 200$ and $s = 2, 3$.

5.1 **The Setting**

The following map

$$[0, 2\pi] \times [0, \pi] \ni (\varphi, \theta) \to r(\varphi, \theta) := (\cos(\varphi)\sin(\theta), \sin(\varphi)\sin(\theta), \cos(\theta)) \in \mathbb{S}^2 \subset \mathbb{R}^3 \quad (5.2)$$

takes a point from the rectangle $[0, 2\pi] \times [0, \pi]$ to $\mathbb{S}^2$. The azimuthal angle is φ and the polar angle is θ. A configuration of N points on $\mathbb{S}^2$ may be viewed as the image of a point in the cube $([0, 2\pi] \times [0, \pi])^N$ as follows:

$$([0, 2\pi] \times [0, \pi])^N \ni (\varphi_1, \theta_1, \ldots, \varphi_N, \theta_N) \to (r(\varphi_1, \theta_1), \ldots, r(\varphi_N, \theta_N)) \in (\mathbb{S}^2)^N.$$

The energy we are considering is a function of pairwise distances and so two configurations which are isometric to each other should be identified. As a first step we require that the first point in the configuration lie at the point $(0, 0, 1)$ and that the second point lie in the x-z plane. By appropriate rotations any configuration of $N > 1$ points can meet this requirement, and so the parameterization space we consider is

$$\mathcal{X}_N := [0, 2\pi] \times ([0, 2\pi] \times [0, 2\pi])^{N-1} \ni (\theta_2, \varphi_3, \theta_3, \ldots \varphi_N, \theta_N),$$

where the second point has coordinates $(\sin(\theta_2), 0, \cos(\theta_2))$. We have expanded the range of the polar angle to $[0, 2\pi]$. While this allows multiple representations of a point, it also allows us to identify sections of the boundary of $\mathcal{X}_N$ so that the angles may be considered as elements of $\mathbb{R}/2\pi\mathbb{Z}$.

We shall denote by Φ_N the map from $\mathcal{X}_N$ to $(\mathbb{S}^2)^N$. Note that Φ_N is analytic on $\mathcal{X}_N$. We shall consider E_s in (5.1) as a map from $(\mathbb{S}^2)^N$ to $\mathbb{R}_+ \cup \{\infty\}$. So long as the points making up the configuration $\omega_N \in (\mathbb{S}^2)^N$ are disjoint $E_s : (\mathbb{S}^2)^N \to \mathbb{R}_+ \cup \{\infty\}$ is analytic and hence $E_s(\Phi_N) : \mathcal{X}_N \to \mathbb{R}_+ \cup \{\infty\}$ is analytic. We may then consider the gradient $\nabla E_s(\Phi_N)$ with respect to the coordinate system $\mathcal{X}_N$, and the $2N - 3$ square matrix of mixed second order partials with respect to the same variables i.e. the Hessian of $E_s(\Phi_N)$ which we shall denote $HE_s(\Phi_N)$.

5.2 **Optimization Tools**

Our goal is to minimize $E_s(\Phi_N)$ over the set $\mathcal{X}_N$. Because of the identifications of the boundary this can be considered as an unconstrained minimization problem. The two tools we shall use are nonlinear conjugate gradient with line minimization and Newton's method.

5.2.1 **Nonlinear Conjugate Gradient**

The basis of conjugate gradient is a modified gradient descent algorithm that avoids "zig-zagging" down valleys of positive-definite quadratic forms. It is an iterated method – given a point in $\mathcal{X}_N$, we choose a descent direction, move in that direction and choose a new descent direction. Our scheme for choosing the n-th descent direction d_n is the Polak-Ribière updating scheme(cf. [40]), which is based on the n^{th} point $x^{(n)}$, the previous descent direction d_{n-1} and the previous point $x^{(n-1)}$. It is given by the following formula:

$$d_n = -\nabla E_s(\Phi_N(x^{(n)})) + \left(\frac{\left(\nabla E_s(\Phi_N(x^{(n)})) - \nabla E_s(\Phi_N(x^{(n-1)}))\right) \cdot \nabla E_s(\Phi_N(x^{(n)}))}{\left|\nabla E_s(\Phi_N(x^{(n-1)})\right|^2} \right) d_{n-1}.$$

For the case $n = 1$, d_n is $-\nabla E_s(\Phi_N(x^{(n)}))$.

5.2.2 **Line Minimization**

Given a descent direction d_n we must choose how far to move in this direction. The distance to move α^* should be a minimum of the following function

$$\mathbb{R} \ni \alpha \to f(\alpha) := E_s(\Phi_N(x^{(n)} + \alpha d_n)).$$

The search for α^* begins by choosing α_1 to be the minimum pairwise separation of the points on $\mathbb{S}^2$ as represented by $\Phi_N(x^{(n)})$ divided by 1000 times the largest component of d_n. Because all partial derivatives of the map in (5.2) are bounded above by 1, this initial step size will not decrease the pairwise separation of points in $\Phi_N(x^{(n)})$ by more than $1/1000$. Our motivation is to avoid regions of $\mathcal{X}_N$ where points in the corresponding configuration on $\mathbb{S}^2$ are close together. It is in these regions that the derivatives of E_s become large and derivative-based minimization techniques may become unstable. With α_1 chosen we inductively choose α_{m+1} to be $2\alpha_m$. We stop when the condition

$$f(\alpha_m) < f(\alpha_{m-1}) \qquad \text{and} \qquad f(\alpha_m) < f(\alpha_{m+1}). \tag{5.3}$$

is met. The condition in (5.3) is referred to as having *bracketed a minimum*. Note that if $f(\alpha_1) > f(0)$ we choose α_{m+1} to be $\alpha_m/2$. If α_m drops below the minimum separation divided by $10,000$ times the largest component in d_n, we conclude that the line minimization has failed to bracket a minimum.

Once a minimum has been bracketed we refine our bracket in one of two ways. The first is Brent's Method (cf. [40, §10.2]) where the three bracketing points $(\alpha_{m-1}, f(\alpha_{m-1}))$, $(\alpha_m, f(\alpha_m)$ and $(\alpha_{m+1}, f(\alpha_{m+1})$ are fit to a parabola p. Let $(\tilde{\alpha}, p(\tilde{\alpha}))$ denote the vertex of the parabola, then the center of the refined bracket is chosen to be either α_m or $\tilde{\alpha}$ depending on which makes f less. The edges of the refined bracket are chosen from α_{m-1}, α_{m+1} and α_m

or $\tilde{\alpha}$ (depending on the choice for the new center) that also bracket the new center and are closest to the new center. The second method is the Golden Section Search (cf. [40, §10.1]) which chooses the new center of the bracket as

$$\frac{3-\sqrt{5}}{2}\alpha_m + \left(1 - \frac{3-\sqrt{5}}{2}\right)\alpha_{m\pm1}$$

assuming that $\alpha_{m\pm1}$ is further from α_m than $\alpha_{m\mp1}$. The edges of the bracket are chosen in the same manner as they are in Brent's Method.

We conclude that we have an approximate minimum if the highest and lowest values of f in the bracketing points differ by less than the minimum separation divided by 100 times the largest component in d_n. Note that this relaxes our stopping criteria as the infinity norm of d_n decreases. The line minimization algorithm starts by attempting to obtain an initial bracket, then using Brent's Method for ten iterations or until an approximate minimum is found and then using the Golden Section until an approximate minimum is found.

The rationale for choosing Brent's Method first is that f is differentiable and so the neighborhood around a minimum α^* should be well approximated by a quadratic. Essentially, as is discussed in [40], this is the optimist's approach. If after ten iterations a local minimum has not been found, then the Golden Section search, which is guaranteed to decrease bracket width, is put to use.

5.2.3 **Newton's method**

Newton's method is also an iterative method to find zeros of functions and is based on approximating the derivative with a linear function. We use it to find zeros of the gradient $\nabla E_s(\Phi_N)$, the derivative of which is the Hessian $HE_s(\Phi_N)$. A first-order expansion of the gradient $\nabla E_s(\Phi_N)$ about the point $x^{(n)}$ is

$$\nabla E_s(\Phi_N(x)) \approx \nabla E_s(\Phi_N(x^{(n)})) + HE_s(\Phi_N(x^{(n)}))(x - x^{(n)})$$

If x is a minimum, then $\nabla E_s(\Phi_N(x)) = 0$. Setting our expansion to zero gives

$$0 = \nabla E_s(\Phi_N(x^{(n)})) + HE_s(\Phi_N(x^{(n)}))(x - x^{(n)}),$$

and so

$$HE_s(\Phi_N(x^{(n)}))(x - x^{(n)}) = -\nabla E_s(x^{(n)}) \tag{5.4}$$

The value of x that solves (5.4) is our choice for $x^{(n+1)}$.

Near a minimum the analyticity of $E_s(\Phi_N)$ implies that $E_s(\Phi_N)$ will be well approximated by a quadratic form and hence the derivative will be close to linear. In these cases we expect that Newton's method will converge rapidly.[1] However, unlike conjugate gradient there is no guarantee that a step of Newton's method will decrease the value of $E_s(\Phi_N)$ or bring x_n closer to a local minimum than x_{n-1}.

5.2.4 **Accurate Summations**

It is well known that if a, b and c are double precision floating point numbers differing by many orders of magnitude, then the addition operation performed by most computers can lead to the following error:

$$a + (b + c) \neq (a + b) + c.$$

This is a result of roundoff error where small numbers may individually fall within the roundoff error of the larger numbers, but the sum of the smaller numbers is larger than the roundoff error. The discrete energy of an N-point configuration involves $\frac{N(N-1)}{2}$ summands, the smallest of which is six orders of magnitude smaller than the final sum in the case $N = 500$ and $s = 3$. One goal in these experiments was to minimize this effect. The naive approach of sorting the summands and re-sorting intermediate sums

[1] Conditions under which Newton's method will converge are given in the paper [28] (in Russian) by L. Kantorovich

is prohibitively computationally expensive. In response we developed[2] the following algorithm for summing a finite series of numbers:

Assume that the absolute value of the numbers is bounded away from zero by C. We shall create an array to store summands. Given a summand s we assign it to the bin in the array whose index is $\lfloor \log_2 \frac{s}{C} \rfloor$. If the bin is empty, we place s in that bin. If the bin is not empty, we empty the bin of its content t and we place $t+s$ into the array in the same manner as we placed s into the array. After the last summand has been placed in the array, we add up the contents of the array starting with the lowest indexed bin. This algorithm has several benefits.

(1) Most addition operations occur between numbers that are within a factor of two of each other. It is only in the final sum over the bins in the array that numbers whose ratio is greater than 2 or less than $1/2$ can be added. The number of such addition operations is bounded by $\log_2 \sum_{i=1}^{N} s_i$, where $s_1, s_2, \ldots, s_N$ are the summands.

(2) This algorithm generates a record for how many summations are performed at each scale.

(3) The algorithm completes in $O(N \log_2 \sum_{i=1}^{N} s_i)$ time.

We estimate the error for a single addition operation within a given bin using the following common algorithm: Let b denote the upper bound for a bin. Find the lowest value for n such that the computer's floating point representation returns $(b + 2^{-n}) - b = 0$. If n^* is this lowest exponent then, we say the roundoff error for that bin is 2^{-n^*}. To estimate the error for a sum, we multiply the number of summations performed at each bin by the roundoff error for that bin.

[2]This was done in collaboration with Drew Scoggins.

5.3 Generating Candidate Configurations

The first step is to choose a starting point in $\mathcal{X}_N$. We do this by randomly choosing angles in $[0, \pi] \times [0, 2\pi]$ and making sure that the resulting points on $\mathbb{S}^2$ are separated from all the previous points by at least $\sqrt{\frac{4\pi}{\sqrt{3}N}}$. The rationale for this factor will be discussed in Section 5.6.2; at this point it is sufficient to know that it is possible to choose such points. This gives us our starting configuration and hence our point $x^{(1)} \in \mathcal{X}_N$. Note that the configuration will preferentially place points near the poles of $\mathbb{S}^2$. We then alternate between some number of iterations of conjugate gradient with line minimization and Newton's method. We conclude that we have a candidate for a local minimum when neither method can decrease the energy.

During development this optimization approach appeared to use conjugate gradient with line minimization to get near a local minimum and then use Newton's method to converge rapidly to the minimum. In the cases observed, four or five successive iterations of Newton's method would bring the optimization software to the stopping condition. Because Newton's method was so effective in finding a minimum, we made some effort to choose the number of iterations of conjugate gradient so that Newton's method would be employed as soon as it was likely to converge. However, a single step of Newton's method requires building the Hessian which runs in $O(N^3)$ time, so we also sought to avoiding using Newton's method when it wouldn't converge. In addition, conjugate gradient incorporates information from previous steps to improve the search direction. Running conjugate gradient for too few iterations would mimic steepest descent and was not effective[3]. It is known that conjugate gradient can "lose conjugacy" if run for too many steps and become ineffective. The final choice for the number of consecutive iterations of conjugate gradient was three times the number of points which is roughly 1.5 times the number of degrees of freedom.[4]

[3] In experiments where conjugate gradient was replaced with steepest descent performance dropped dramatically.

[4] The author has since been told that conjugate gradient should not run for more consecutive iterations than there are degrees of freedom.

The algorithm was used in two phases. In the first phase all iterated summations (summations appearing within for-loops) were performed in the natural way. When the stopping condition was met, the program was rerun using the final configuration as the starting point. During this second run a flag was set that caused the program to use the accurate summation technique described in section 5.2.4 for all iterated sums; this includes sums in computing the energy and in building the gradient and the Hessian. For the logarithmic energy there is no lower bound for the magnitude of a summand in the energy calculation. We fixed the constant C as described in section 5.2.4 at $\log \operatorname{diam} \mathbb{S}^2$; any summands of magnitude less than this were added to the zeroth bin.

5.4 Criteria for a Minimum

In an abstract setting the stopping condition – that neither conjugate gradient nor Newton's method can decrease the energy – is only achieved when a point $x \in \mathcal{X}_N$ is precisely at a local minimum of $E_s(\Phi_N)$. It is unlikely that this will occur unless some neighborhood of a stable minimum is exactly a positive quadratic form. We conclude that the stopping condition most likely indicates that possible reductions in energy are smaller than the roundoff error in the energy calculation. Further, we did not make a systematic check to see if the optimization software completed with several successive iterations of Newton's method. To address this we consider the following tests for stability.

5.4.1 A Positive-Definite Hessian

After the optimization software has completed both the initial and final stages, we have a candidate for a local minimum $\tilde{x} \in \mathcal{X}_N$. In a multivariate setting a sufficient condition for a point to be a local minimum is that the Hessian at that point is positive-definite. This requirement is not necessary e.g. the objective function $f(x, y) = x^4 + y^4$ has a local minimum at $(0, 0)$ but the Hessian at that point is all zeroes. Because our goal is to establish

a lower bound on the number of stable configurations we shall require that Hessian with respect to the coordinates of $\mathcal{X}_N$ is positive-definite.

5.4.2 **Lowest Eigenvalue of the Hessian**

In most cases the optimization method stopped with a non-zero gradient indicating that an actual minimum was not achieved. In this section we use some mild assumptions to bound the distance in the space $\mathcal{X}_N$ between the stopping point and the actual minimum.

If $\tilde{x}$ is near an actual local minimum y, then we may write the gradient $\nabla E_s(\Phi_N)$ at $\tilde{x}$ as an expansion about y.

$$\nabla E(\Phi_N(\tilde{x})) \approx \nabla E(\Phi_N(y)) + HE_s(\Phi_N(y))(\tilde{x} - y).$$

By the assumption that y is a local minimum, and that the Hessian at y is nearly the same as the Hessian at $\tilde{x}$, we obtain

$$(\tilde{x} - y) \approx [HE_s(\Phi_N(\tilde{x}))]^{-1} \nabla E_s(\Phi_N(\tilde{x}))$$

Note that $[HE_s(\Phi_N(\tilde{x}))]^{-1}$ exists because the Hessian is positive-definite. If we let $UDU^{-1} = HE_s(\Phi_N(\tilde{x}))$ be the diagonalization of the Hessian at $\tilde{x}$ (i.e. U is unitary and D is a diagonal matrix whose entries are the eiganvalues of $HE_s(\Phi_N(\tilde{x}))$), then we have the following bound on $|\tilde{x} - y|$:

$$|\tilde{x}-y| \approx \left|\left[UDU^{-1}\right]^{-1} \nabla E_s(\Phi_N(\tilde{x}))\right| = \left|UD^{-1}U^{-1}\nabla E_s(\Phi_N(\tilde{x}))\right| \leq \|D^{-1}\| \cdot |\nabla E_s(\Phi_N(\tilde{x}))|. \quad (5.5)$$

Here $\|M\|$ denotes the operator norm of the matrix M acting on Euclidean space and $|x|$ denotes the Euclidian length of a vector in $x \in \mathcal{X}_N$. Because D is diagonal, $\|D^{-1}\|$ is the

inverse of the smallest eigenvalue $d_{\min}$. The bound we obtain is then

$$|\tilde{x} - y| \lesssim \frac{|\nabla E_s(\Phi_N(\tilde{x}))|}{d_{\min}}. \tag{5.6}$$

Note that the Euclidian norm $|\tilde{x} - y|$ is computed in the space $\mathcal{X}_N$.

We require that the right hand side of (5.6) is less than $1/10,000$ the minimum separation between any pair of points in the configuration as represented on $\mathbb{S}^2$. As noted earlier, if one changes a specific angle (i.e. a single component of $x \in \mathcal{X}_N$) by δ, the corresponding change of the location of a point in the configuration on $\mathbb{S}^2$ will be less than δ. It follows from the assumption that the Hessian is constant, that if $|\tilde{x} - y|$ is less than the minimum separation of two points in the configuration divided by $10,000$, then the points will not need to move more than $1/10,000$ of the minimum separation to be positioned at an actual stable minimum.

This condition is probably much more restrictive for the following reasons: First, the quantity $|\tilde{x} - y|$ is likely due to many components of $\tilde{x}$ and y differing, not just one. Second, there is considerable spread in eigenvalues of the Hessian due to the fact that the partial derivatives of $E_s(\Phi_N)$ with respect to the azimuthal angle of points close to the north or south poles will be much smaller than the partial derivatives with respect to the azimuthal angle of points located at the equator. The final inequality of (5.5) chooses the reciprocal of the smallest, thus maximizing our upper bound.

5.4.3 **Comparison of the Lowest Eigenvalue with the Gradient Norm**

It is natural to ask whether the minimum eigenvalue or the gradient norm contributes more to the right hand side of (5.6). For the cases $N = 200$ and $s = 1, 3$, the right hand side of (5.6) is highly correlated with the gradient as is shown in the log-log plot in Figure 5.1. The suggests that the eigenvalue test is in agreement with a similar test requiring that the norm of the gradient be small.

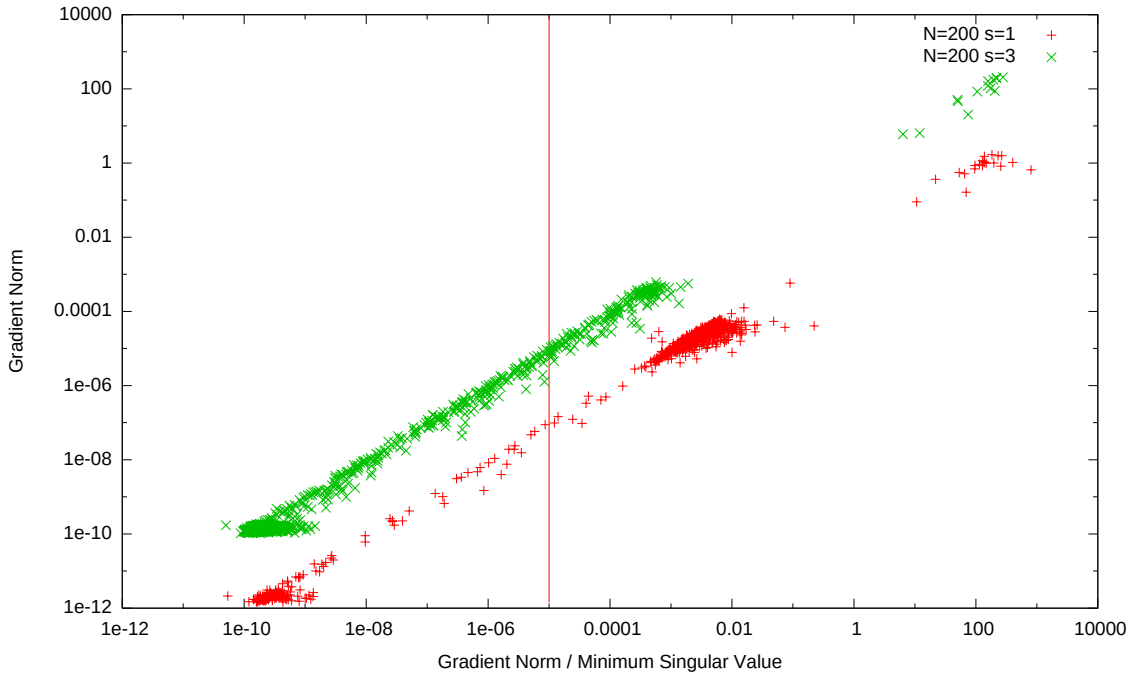

Figure 5.1: A plot of two tests of stability for $N = 200$ and $s = 1$, $s = 3$.

The points in Figure 5.1 appear to be clustered. The lower left of each data set represent points that we accept. In this case we accept every point to the left of the vertical line at 10^{-5}. The points in the upper right indicate cases where the optimization software failed entirely. The middle of the graph suggests that there is a range of gradient norms for the candidate configurations. This poses a question. If the gradient had such a large norm, then conjugate gradient, the first step of which is steepest descent, should have made progress. This suggests that certain descent directions are not explored.

The fraction of candidate configurations that pass both tests is shown in Figure 5.2.

5.5 Implementation of Configuration Generation

The software to implement these algorithms and to test the candidate configurations was written in the C programming language and compiled for AMD Opteron and the IBM PowerPC processors running the CentOS Linux operating system and for the Motorola G4 and Intel Core Duo processors running Apple's OS X operating system. The first phase

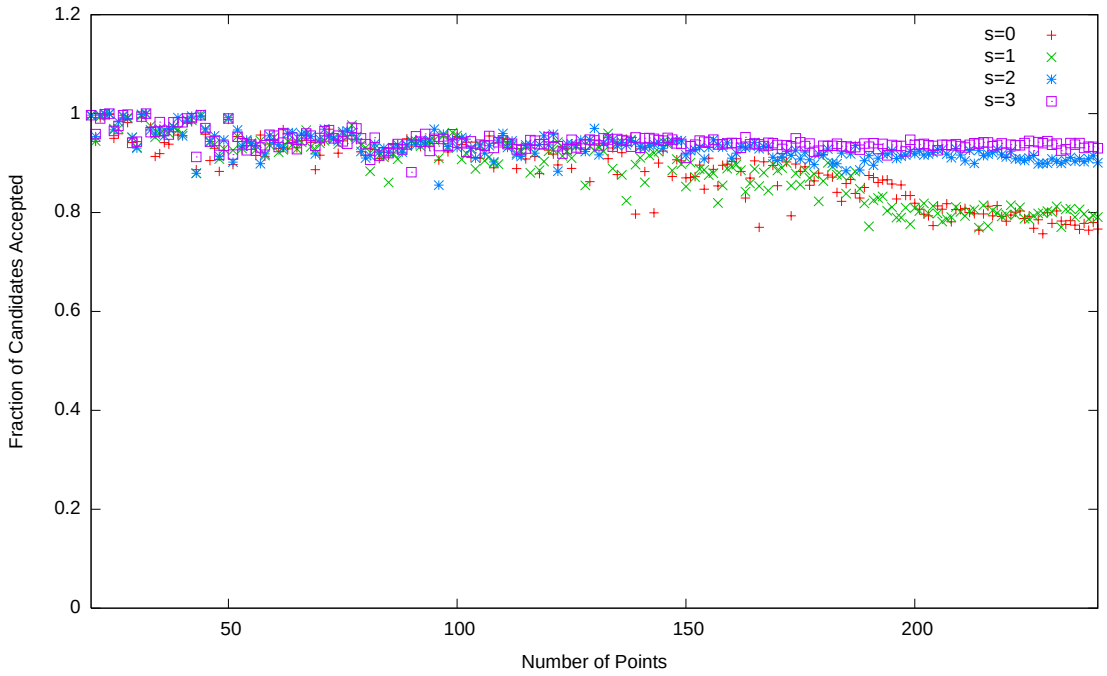

Figure 5.2: A plot of the fraction of the candidate configurations passing both tests for stability.

of the computations were performed at Vanderbilt's computing cluster on the Opteron and PowerPC processors. The second phase of the calculation that used the accurate summing techniques was run on servers at the Vanderbilt math department and at the author's home on the Core Duo processor.

The LAPACK library provides an interface to hardware accelerated matrix operations. This library is available for all the combinations of processor type and operating system listed and was used for the matrix operations described above. To test if the Hessian was positive-definite, we instruct LAPACK to perform a Cholesky decomposition. One of the error codes returned by this call reports that the matrix in question is not positive-definite. The eigenvalues of the Hessian were obtained by performing a singular-value decomposition.

For each value of $N = 20, \ldots, 500$ and $s = 0, 1, 3$ roughly one thousand candidate configurations were generated. For $s = 2$ and the same range of values of N, roughly 600 candidate configurations were generated.

5.6 **Computational Geometry**

Having generated configurations on $\mathbb{S}^2$ that pass our stability test, we would like to understand the relative positions of the points making up these configurations, and in particular we would like to establish a technique to compare two configurations rapidly and determine if there is an isometry mapping one configuration to another. A simple approach is to take the first configuration and place a point at $(0, 0, 1)$ and another point on the x-z plane, and then to search for a rotation and reflection of the second configuration that does the same and also causes the points to match up with each other. Because the rotations of the second configuration are indexed by pairs of points, there are $2N(N-1)$ possible rotations and reflections. Because the points in the configurations are ordered randomly, checking if a point in the first configuration corresponds to a point in the second configuration requires looking at every point in the second configuration. From this we see that this simple approach has a run time that is $O(N^4)$. We present a new method to compare configurations on $\mathbb{S}^2$ that is substantially faster.

One of the central tools we use is computational geometry. We begin with a review of some basic definitions. Given a collection of distinct points $\omega_N \subset \mathbb{R}^p$ the *Voronoi (alternatively Dirichlet) cells* for ω_N are convex subsets of $\mathbb{R}^p$ around each point in ω_N formed as follows: Pick $x \in \omega_N$. For every $y \in \omega_N$ let H_{xy} denote the closed half-space of $\mathbb{R}^p$ containing x that is bounded by the plane forming a perpendicular bisector of the line segment connecting x and y. The Voronoi cell V_x for the point x is given by

$$V_x := \bigcap_{y \in \omega_N \setminus \{x\}} H_{xy}.$$

The *convex hull* of ω_N is the intersection of all half-spaces that contain ω_N. The *Delaunay triangulation* of ω_N divides the convex hull of ω_N into simplices according to the following rule: A simplex K belongs to the Delaunay triangulation of $\omega_N \subset \mathbb{R}^p$ if, and only if, the

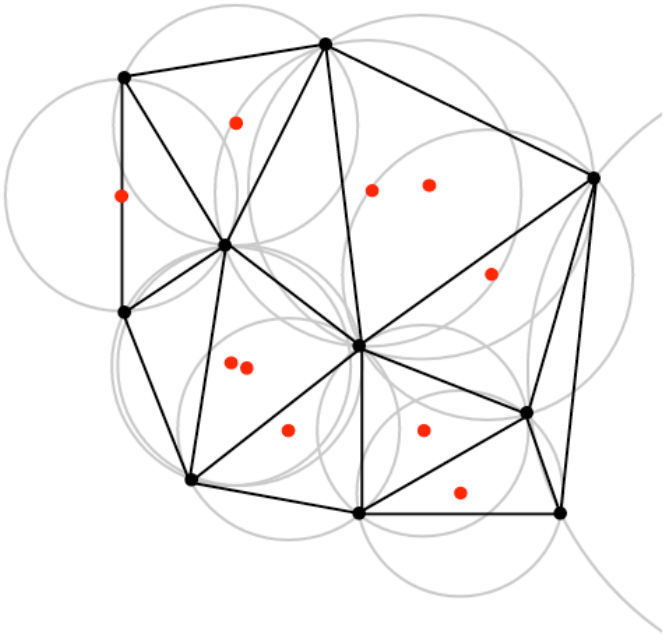

Figure 5.3: The circumcircles in gray associated with a Delaunay triangulation of the black points. (This image is courtesy of Wikipedia via the GNU free documentation license.)

$p + 1$ vertices of K are in ω_N and the interior of the sphere passing through these $p + 1$ points contains no point in ω_N.

It is a standard result that the Delaunay triangulation and Voronoi cells of a collection of points in $\mathbb{R}^p$ are geometric duals. More concretely, the Delaunay triangulation can be thought of as connecting nearest neighbors in $\mathbb{R}^p$. Figure 5.3 shows a collection of black points with their associated Delaunay triangulation and circumcircles. The centers of the circumcircles are the red points. Figure 5.4 shows the duality between the Voronoi cells and the Delaunay triangulation. Note that the centers of the circumcircles are the vertices of the Voronoi cells.

It is important to bear in mind that the Delaunay triangulation need not be unique. Given any finite collection P of $N > 2$ points distributed on $\mathbb{S}^1 \subset \mathbb{R}^2$ every triangulation of the convex hull of P consisting of triangles whose vertices are drawn from P is a Delaunay triangulation. This results from the simple fact that no point lies in the interior of the circle passing through any three elements of P. If we let $\tilde{x}$ denote the center of $\mathbb{S}^1$, and

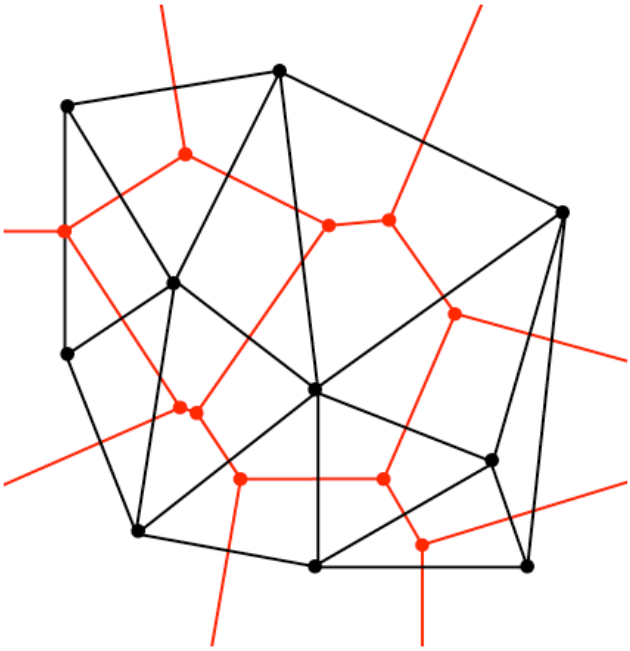

Figure 5.4: The Voronoi cells (bounded by the red lines) are the geometric dual of the Delaunay triangulation of the black points. (This image is courtesy of Wikipedia via the GNU free documentation license.)

let $\tilde{P} := P \cup \{\tilde{x}\}$, then the Delaunay triangulation of $\tilde{P}$ is unique. If we remove any edges containing $\tilde{x}$ as an endpoint, then we have a Delaunay triangulation of P that is in some sense restricted to $\mathbb{S}^1$. Note that the triangles in the Delaunay triangulation of $\omega_N \subset \mathbb{R}^2$ are replaced by line segments in the "circular Delaunay triangulation" of $\omega_N \subset \mathbb{S}^1$.

5.6.1 Spherical Delaunay Triangulations on $\mathbb{S}^2$

We shall extend the idea of circular Delaunay triangulations to $\mathbb{S}^2$. Given a configuration $\omega_N \subset \mathbb{S}^2$ we shall consider the Delaunay triangulation of $\omega_N \cup \{(0,0,0)\}$ and ignore any face that contain $(0,0,0)$ as a vertex. In the same manner that our circular triangulations are over lower dimension than the ambient space, here we replace tetrahedrons in $\mathbb{R}^3$ with triangles that are roughly speaking restricted to $\mathbb{S}^2$. When this algorithm succeeds we refer to the result as a *spherical Delaunay triangulation.* Figure 5.5 shows such an example.

There are two ways by which this method could fail to produce a usable spherical

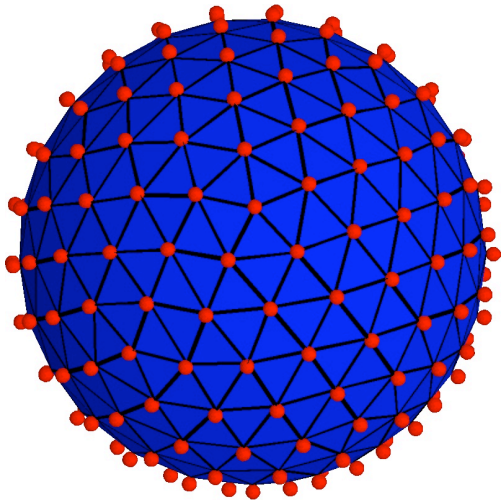

Figure 5.5: A sample spherical Delaunay triangulation from a configuration of 500 points on $\mathbb{S}^2$.

Delaunay triangulation. The first is if a configuration ω_N contains a subset of more than three points that is cospherical with $(0, 0, 0)$. This would occur if four points from ω_N lie on circle on the sphere – perhaps forming the vertices of a square – and no points in ω_N lie in the spherical cap bounded by the circle. The second is if more than three points in ω_N are nearly cospherical. This could occur if the actual stable configuration contains four points located at the vertices of a square, but the optimization software stops before the points reach those vertices. While this will give us a unique spherical Delaunay triangulation, another trial my produce a candidate configuration that is extremely close to the first candidate, but has a different spherical Delaunay triangulation. In Figures 5.6 and 5.7 two configurations are shown that, due minute changes in the location of the points, have different spherical Delaunay triangulations. Given that points in the configuration are nearly isometric, we do not want to treat these configurations as distinct. With this in mind we perform the following two tests to determine if we accept a spherical Delaunay triangulation of ω_N:

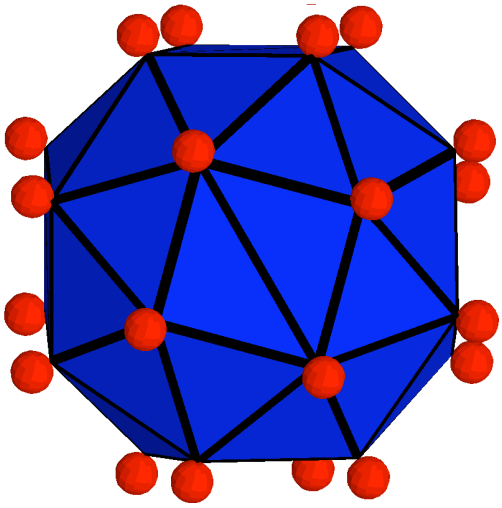

Figure 5.6: A Delaunay triangulation for a stable configuration of 24 points on $\mathbb{S}^2$.

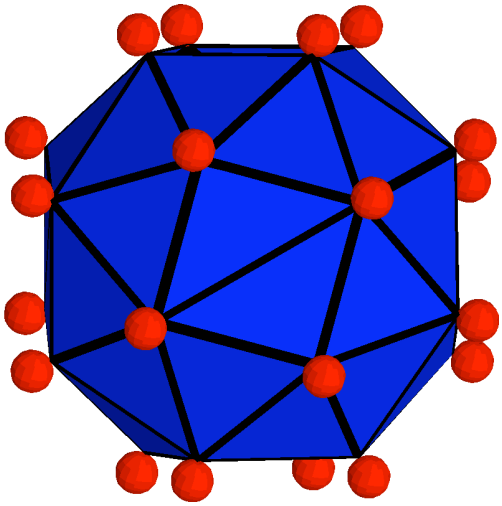

Figure 5.7: A Delaunay triangulation for a configuration that is very similar to the configuration in figure 5.6. Note that the orientation of the two triangles facing out of the page as compared to Figure 5.6.

First, if the convex hull of ω_N contains a face with more than three sides, the triangulation is marked as bad. If a triangulation passes the first test, we then examine the unit vectors normal to the faces in the triangulation. If the dot-product is too close to one, we conclude that we may be in the situation illustrated by Figures 5.6 and 5.7 and we mark the triangulation as bad. We appeal to the following approximation for determining how close is too close.

If we act under the assumption $\mathbb{S}^2$ can be triangulated with equilateral triangles – for most N it cannot, but Figure 5.5 suggests that the triangles are close to equilateral – then we may consider the distance between the center of one triangle and the center of the next and use this as a basis for estimating the minimum average dot-product between unit vectors normal to the faces in the spherical Delaunay triangulation on $\mathbb{S}^2$. Using a small angle approximation we obtain that the average minimum dot product should be roughly $1 - \dfrac{8\pi}{3\sqrt{3}F}$ where F is the number of faces. For a triangulation of ω_N we then compute the following:

$$d_{\min}(\omega_N) := \min\left\{ \frac{1 - a \cdot b}{8\pi/3\sqrt{3}F} \ : \ a \text{ and } b \text{ are normal to faces in the triangulation of } \omega_N \right\}.$$

The quantity $d_{\min}(\omega_N)$ has the benefit that it measures how close to parallel two faces are in a manner that is independent of F. If $d_{\min}(\omega_N) \leq 1/10,000$, we mark the spherical triangulation as bad.

5.6.2 **Spherical Voronoi Cells on $\mathbb{S}^2$**

Once we have an acceptable spherical Delaunay triangulation, we may generate Voronoi cells on $\mathbb{S}^2$ as follows: Given a point $x \in \omega_N$ consider the triangles in the triangulation of $\mathbb{S}^2$ for which x is a vertex. For each of those triangles find the intersection of the perpendicular bisectors of the edges of the triangle. Use those intersections as the vertices of a region that we shall call the Voronoi cell for x restricted to $\mathbb{S}^2$. Figure 5.8

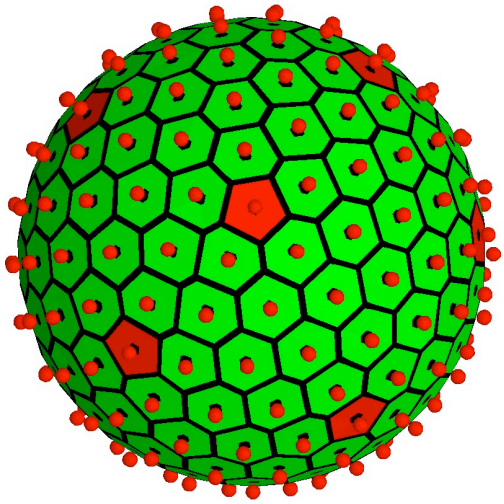

Figure 5.8: Sample Voronoi cells for the configuration of 500 points used in Figure 5.5.

provides an example of the Voronoi cells derived from the Delaunay triangulation shown in Figure 5.5. We have used the color of the Voronoi cell to indicate the number of nearest neighbors. In the stable minima for which we have generated and examined the Voronoi cells, the points on $\mathbb{S}^2$ appear to be arranged in a generally hexagonal pattern.

Following reasoning similar to that used to estimate the dot product for vectors that are normal to adjacent triangles in the triangulation of $\mathbb{S}^2$ we may estimate the distance between a point and its nearest neighbors by assuming that the sphere $\mathbb{S}^2$ is tiled with regular hexagons. In this case we approximate the distance between nearest neighbors in a configuration ω_N as $\sqrt{\frac{8\pi}{N\sqrt{3}}}$.

5.7 Implementation of Computational Geometry Tools

Generating the convex hull and the Delaunay triangulation of $\omega_N \subset \mathbb{R}^p$ was done using the QHull package[5]. The software to create and test the spherical Delaunay triangulations

[5]QHull was developed by the University of Minnesota's now defunct Geometry Center. This package was written by researchers specializing in computational geometry, was extremely fast and minimized the effects

and to create the Voronoi cells were written in the C and Java programming languages. They did not use any hardware specific features and could be run on any Posix compliant operating system for which there is a Java Virtual Machine (e.g. Linux and the Macintosh OS X operating systems.)

5.8 **Graph Theory**

If we have a collection of configurations on $\mathbb{S}^2$ and these configurations all have good spherical Delaunay triangulations, then we may speed the process of comparing the configurations by using an algorithm presented in [31] that is used for comparing planar graphs.[6] The essential idea is to identify a canonical representation for planar graphs so that two planar graphs are graph-isomorphic if, and only if, their canonical representations are the same. By excising a point that is separated from the vertices and edges of the spherical Delaunay triangulation of a configuration ω_N we may consider our spherical Delaunay triangulation as a planar graph.

The algorithm works as follows: For any edge (v_1, v_2) and any orientation (clockwise or counter clockwise) we number the vertices in the triangulation as follows:

step 1: Let v_1 be number 1 and let v_2 be number 2.

step 2: Find the already numbered vertex v_c with the lowest numbering that has an unnumbered neighbor. If no such vertex exists, we're done.

step 3: Start working around the neighbors of v_c in the chosen orientation, starting with the lowest numbered neighbor. Skipping the already numbered neighbors, assign the smallest unused number to any unnumbered neighbor.

step 4: If there is an unnumbered vertex go to step 2.

---

of roundoff error. Producing comparable software would not have generated results proportional to the time spent in development.

[6]The author is grateful to Mark Ellingham for describing the algorithm.

Once we have a numbering, we create a table whose rows and columns are indexed by the vertices as numbered by the preceding procedure. We place a 1 in the $i,\ j$-cell if there is an edge connecting vertex i and vertex j, otherwise place a 0 in that cell. We generate a row major encoding of the upper right triangle of this table. Because of size constraints, we then create an MD5 cryptographic digest of this encoding.

This process is repeated for every choice of edge and orientation. For every choice we record the ordering of vertices, the orientation and MD5 digest when the MD5 digest is lexically less than the current lowest digest. When this process completes we call the lexically lowest digest the *tag* for the graph and we rotate the configuration so that the first and second point in the corresponding numbering are at $(0, 0, 1)$ and in the x-z plane respectively. If the orientation associated with the tag is counter-clockwise, then we reflect the configuration across the x-z plane. We say a configuration that has been so rotated and reflected is in *canonical position*.

The algorithm for generating this tag runs in $O(EV)$ where E is the number of edges and V is the number of vertices in the spherical Delaunay triangulation. While this algorithm is somewhat expensive, it is expensive on a per configuration basis (i.e. $O(M)$ assuming we have M configurations to compare) as opposed to being expensive on a per comparison basis (i.e. $O(M^2)$.)

We use this algorithm to compare configurations in canonical position as follows: If two configurations of N points ω_N^1 and ω_N^2 have the same tag, then compute the following

$$d(\omega_N^1, \omega_N^2) := \max\{|x_i - y_i| \ :\ x_i \in \omega_N^1,\ y_i \in \omega_N^2,\ i \in 1, \ldots, N\}.$$

If $d(\omega_N^1, \omega_N^2) < 1/100,000$, then we say the configurations are the same. While this may seem like a fairly large threshold, our goal is to get a lower bound on the number of distinct stable configurations on $\mathbb{S}^2$ and errors resulting from this threshold being too large will undercount the number of distinct configurations. Note that the quantity $d(\omega_N^1, \omega_N^2)$ can be computed in $O(N)$ time.

While this graph theory based test is extremely valuable in identifying the isometry between two isometric configurations, we never use this test alone to conclude that two configurations are not isometric. There are two reasons for this. First, it is possible that there could be a configuration that has a good spherical Delaunay triangulation of $\mathbb{S}^2$, and that there is a graph-automorphism of this triangulation that does not correspond to an isometry. As an example consider a four sided polygon in the plane for which all the angles between sides are different. The group of graph-automorphism is the dihedral group D_4, but the group of isometries is trivial[7]. Second, the brute-force isometry test is a more concrete test and the corresponding software is easier to verify.

5.8.1 **Tagging Scars**

An important benefit of the graph theory algorithm is that it allows us to tag the portions of a configuration where the hexagonal structure breaks down. Any connected subgraph of the spherical Delaunay triangulation of $\mathbb{S}^2$ containing only vertices of degree other than six shall be called a *scar*. For each scar we generate a tag of the graph consisting of the scar, the vertices that are connected to the scar by a single edge and the edges connecting these neighboring vertices[8]. We include the neighbors of the scar when we form a tag because many scars have a chain like structure and the connections to the neighboring points provides information regarding how the chain bends within the larger triangulation.

5.9 **Counting Distinct Configurations**

We count the distinct configurations for a given value of N and s in two phases. In the first phase we generate the spherical Delaunay triangulation of every configuration and ignore the possibility that the spherical Delaunay triangulations are bad. We say that two configurations have energies which cannot be satisfactorily distinguished if the difference

[7] One could address this by storing every ordering of points corresponding to the lexicographically lowest tag

[8] Software to identify the scars was written with Whitney Goulart.

in energies is less than ten times maximum of the two summation errors as described in section 5.2.4. We sort the configurations by energy and bin them as follows: We start with the configuration with the lowest energy and create a bin for it. We go through the configurations by increasing energy until we find a configuration whose energy can be distinguished from the energy of the first configuration. We start a new bin for this configuration and continue the process. When we are done, all the configurations have been placed in bins. At this point we use the graph theory tags to search for isometric configurations. This subdivides bins into isometry classes. Within each class we keep the configuration with the lowest energy and drop the others. When the first phase completes we have reduced the number of configurations to a large degree. Even if the spherical Delaunay triangulation for two configurations do not pass our test for goodness, they may still happen to provide the correct ordering of points to show us that the configurations are isometric.

At this point we test the configurations for stability and test the validity of the spherical Delaunay triangulation. Any configuration that does not pass our stability test and doesn't have the lowest energy is discarded.

In the second phase we bin configurations by energy as we did in the first phase, but now we use a brute force isometry test to compare configurations. Because the number of configurations to test has been reduced as a result of the first phase, this process is computationally feasible. We end with a list of stable configurations.

5.10 **Implementation of Counting Algorithm**

All software implementing the graph theory algorithm and the counting method described in the previous sections was written in the Java programming language.

5.11 **Results**

This section describes some of the initial data analysis. One of the most important questions is: How does the minimal discrete energy for a given N and s depend on N and s? These questions have been addressed with theory, experiment and conjecture and we shall present our data in this context. More recent questions are: does the number of stable configurations increase exponentially with N? And what trends can be identified in the breakdown of the hexagonal structure?

The reader should bear in mind that numerical results can present upper bounds for the minimal discrete energy and lower bounds for the number of states. In regards to the number of states, we are really counting the number of states that pass our stability test and are not isometric to one another.

5.11.1 **Comparison with Prior Experiments**

Similar experiments with the goal of numerically approximating the minimal discrete energy have been performed in a variety of settings (cf. [11, 12, 36, 43].) We shall look closely at the results obtained in [36, 43] because the methodologies used in those experiments differ from ours and provide an interesting point of comparison.

In [43] Rakhmanov, Saff and Zhou perform related experiments. Those in common with ours are for $s = 0$, 1 ($\alpha = 0$, $\alpha = -1$ respectively in their paper) and $N = 2, \ldots, 200$, 212, 272 and 282. They parameterize the sphere using a stereographic projection and their parameter space is $(\mathbb{R}^2)^N$. For $s = 0$ they use a combination of steepest descent and a version of Newton's method that does not require solving the full linear system. For $s = 1$, they use conjugate gradient and a variable metric method. As with the experiments described here, they start with 1000 random initial configurations for a given value of N and s. For the descent-based methods, they do not use a line minimization but rather a step size computed from the state of the configuration. The absolute value of the differences between the results of Rakhmanov, Saff and Zhou and the results in this document for

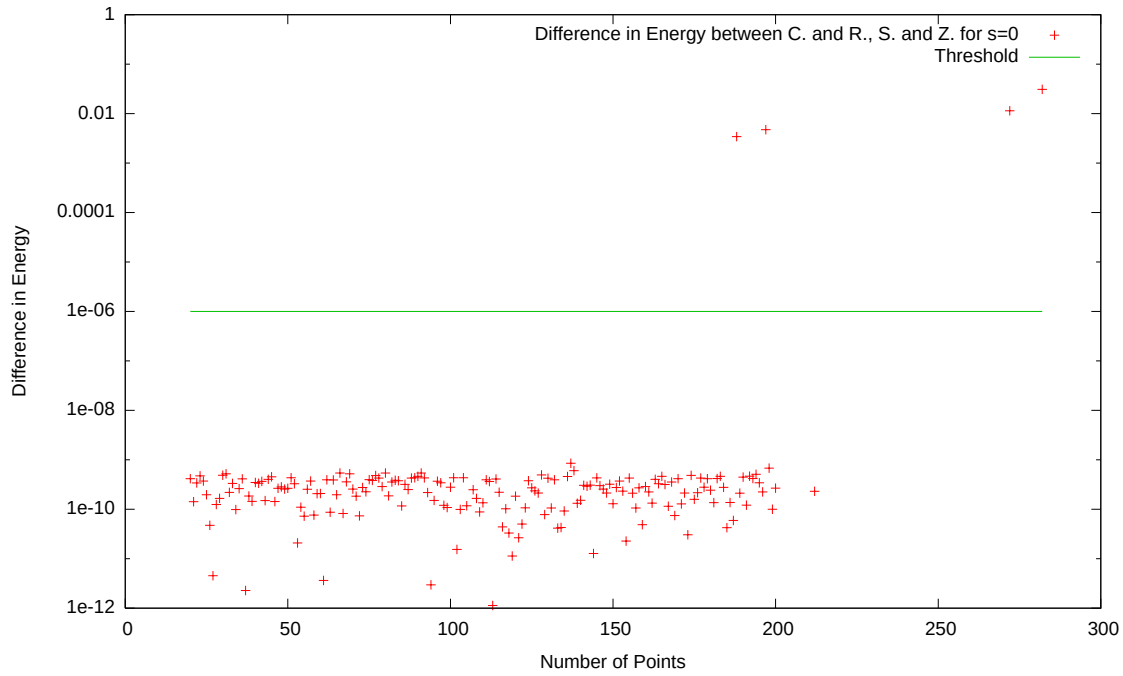

Figure 5.9: The absolute value of the difference of the minimal discrete $s = 0$ energies of the experiments described in this paper and the experiments of Rakhmanov, Saff and Zhou.

$s = 0$ and $s = 1$ are plotted in Figures 5.9 and 5.10 respectively. We examine the results that differ by more than 10^{-6}.

In [36] Morris, Deaven and Ho report results of similar experiments for $N = 112, \ldots, 200$ and $s = 1$. They indicate that for $10 \leq N \leq 132$ their results are in agreement with unpublished results of Erber. Morris, Deaven and Ho use a structured genetic algorithm combined with conjugate gradient. Each generation relaxes the candidate configurations using conjugate gradient and mimics "mating" by combining portions of configurations located on random hemispheres of the existing population of configurations. The absolute value of the differences between the results of Morris, Deaven and Ho and the results in this document are plotted in 5.11. We examine the results that differ by more than 10^{-6}.

Figures 5.9, 5.10 and 5.11 show that the mean difference in energies of our experiments and those of Morris, Deaven and Ho is higher than the mean difference in energies between our experiments and those of Rakhmanov, Saff and Zhou. One possible explanation for this

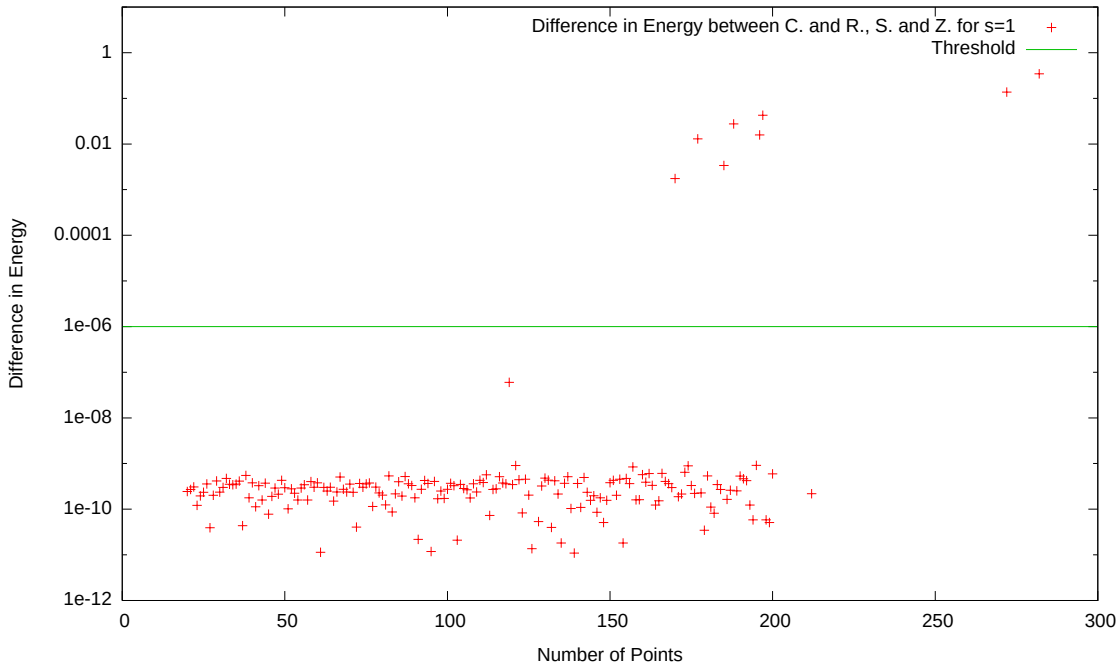

Figure 5.10: The absolute value of the difference of the minimal discrete $s = 1$ energies of the experiments described in this paper and the experiments of Rakhmanov, Saff and Zhou.

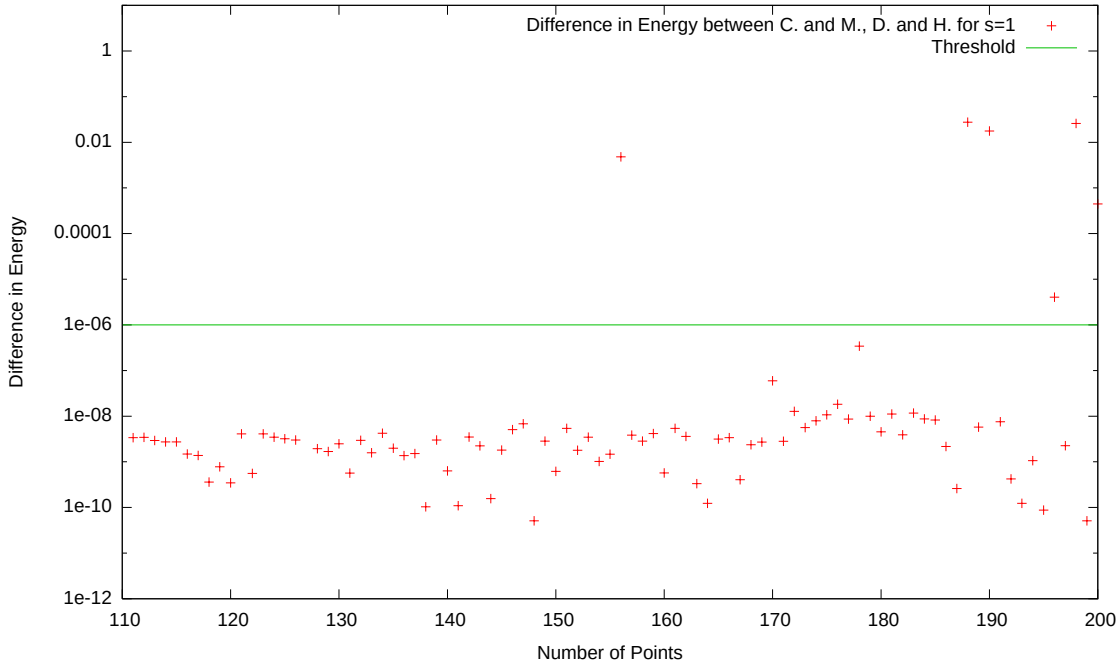

Figure 5.11: The absolute value of the difference of the minimal discrete $s = 1$ energies of the experiments described in this paper and the experiments of Morris, Deaven and Ho.

is that our experiments and the experiments of Rakhmanov, Saff and Zhou use a Newton-like method in conjunction with a descent based approach, whereas Morris, Deaven and Ho use conjugate gradient alone.

Table 5.1: Differences between current and prior results

N	s	C.	R., S. and Z.	M., D. and H.	Min.
188	0	(L) -3664.2434024129	-3664.239977217	N.A.	2^{nd}
197	0	-4013.1824623541	(L) -4013.187189799	N.A.	
272	0	-7533.1688007506	(L) -7533.180190868	N.A.	
282	0	-8084.9967902276	(L) -8085.027739960	N.A.	
156	1	(L) 11092.798311456	-	11092.80311478	2^{nd}
170	1	(L) 13226.681078541	13226.682823953	-	2^{nd}
177	1	14364.850519211	(L) 14364.837545298	-	
185	1	(L) 15723.720074072	15723.723463950	-	2^{nd}
188	1	(L) 16249.222678879	16249.250131462	16249.25013148	2^{nd}
190	1	(L) 16604.428338501	-	16604.44596500	2^{nd}
196	1	(L) 17693.460548082	17693.476356930	17693.46055212	2^{nd}
197	1	17878.382745772	(L) 17878.340162571	-	
198	1	(L) 18064.262177195	-	18064.28806296	5^{th}?
200	1	18438.842717530	-	(L) 18438.84227198	
272	1	34515.330488416	(L) 34515.193292687	N.A.	
282	1	37147.638541777	(L) 37147.294418462	N.A.	

Table 5.1 shows the experiments where the reported lowest energies differed by more than 10^{-6}. The columns N and s indicate the experiment performed. The columns "C", "R., S. and Z" and "M., D. and H" indicate the value of the energy as found by this author, by Rakhmanov, Saff and Zhou, and by Morris, Deaven and Ho respectively. A dash indicates that the energy is in agreement with the energy in column "C". When the column "C" contains the lowest energy, the column "Min." indicates the index of the stable configuration whose energy is in agreement with the other experimental values (the configuration with the lowest energy has index 1.) The lowest energy is marked by "(L)".

The case $N = 196$ and $s = 1$ indicates that the energies in this experiment differ from the energies in the experiment performed by Morris, Deaven and Ho by more than 10^{-6}. However, the second stable minimum we found was separated from our lowest minimum

by considerably more than the difference between the values reported by the experiments. We allow for the possibility that in this case Morris, Deaven and Ho had found the same minimum, but their conjugate gradient algorithm stopped prematurely.

The question mark next to the index of the minimum for $N = 198$ and $s = 1$ indicates that the energy reported by Morris Deavon and Ho lies between the energies of the fourth and fifth stable configurations we observed. This could indicate that their conjugate gradient algorithm stopped prematurely or that they found a stable configuration we did not.

The conclusion we draw is that for $20 \leq N \leq 200$ the experiments are largely in agreement. For $N > 200$ there are reasons to suspect that our experiments were unlikely to find the ground state configuration on the sphere. In [13] Erber and Hockney suggest that the number of stable configurations grows exponentially with N. If this is the case, then for N larger than 200 we expect that the number of stable configurations will greatly exceed the number of trials we ran. Consequently the chance of finding the global minimum decreases. For the cases $N = 272$ and 282; our lowest energy was so much higher than the lowest energy found by Rakhmanov, Saff and Zhou that it suggests that there are a number of states with energies laying between the energy they found and the energy we found. This indicates that we should not consider the lowest energies we have found for $N > 200$ as probably globally minimal.

Further confirmation is shown in Figure 5.12 where we plot the number of distinct configurations passing our stability tests divided by the number of trials that resulted in a stable configuration. As N grows much beyond 200, the number of distinct configurations found is approximately the total number of trials resulting in a good configuration. It is reasonable to assume that at this saturation point the next stable configuration resulting from running the optimization software would be a new one. For this reason it seems likely that the number of trials we performed is insufficient to find all the stable minima and in particular to find the ground state.

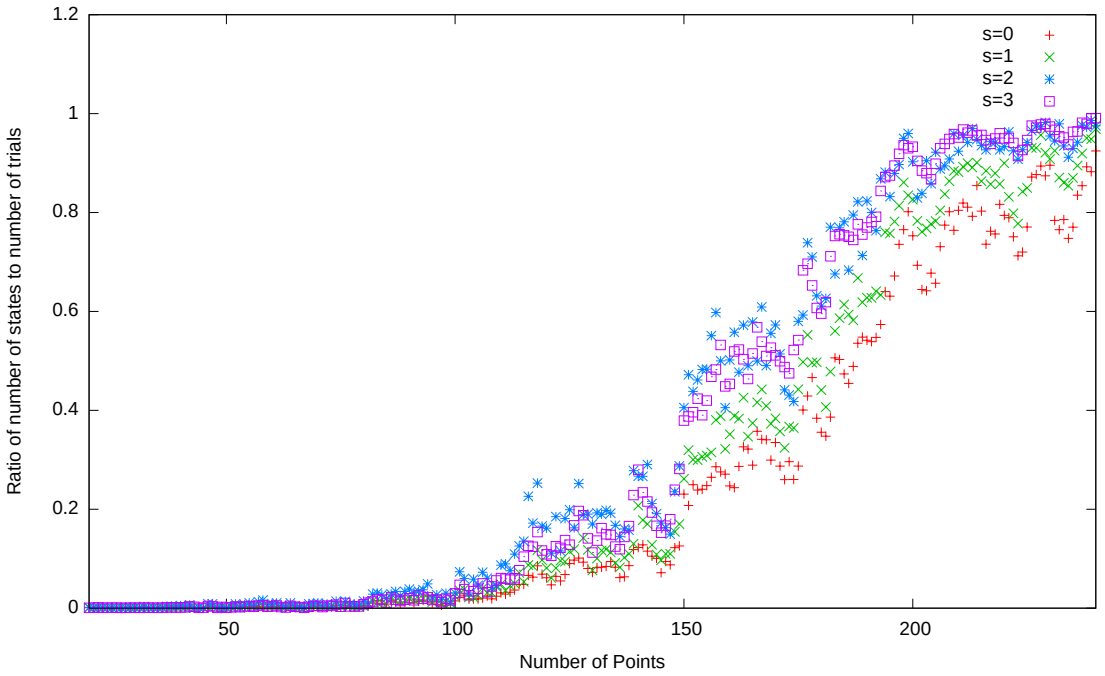

Figure 5.12: The ratio of the number of distinct states to the number of trials leading to good configurations as a function of the number of points N.

5.11.2 **Estimating Growth of the Number of Stable Minima**

Based on Figure 5.12 we shall try to estimate the values of N for which we can reasonably assume we have found most of the stable configurations. The growth of the graph with low N is most certainly due to the increase in the number of stable minima. The plateau at 1 starting at roughly $N = 200$ can be reasonably assumed to follow from the fact that there are more stable configurations than trials performed. Based on an admittedly subjective judgment, one could imagine that the former effect dominates for $N \leq 160$.

Figure 5.13 shows the growth of the number of distinct stable configurations as a function of N for the range of N where we have reason to believe we have seen the majority of stable configurations (i.e. $20 \leq N \leq 160$.) On the hypothesis of exponential growth as presented in [13], fitting these data to a function of the form $Ae^{\alpha N}$ gives parameters for growth. Table 5.2 shows the results.

Note that the results of this fit is highly dependent on the value of N chosen. If we fit data for $N = 20, \ldots, 180$ the value of A increases by an order of magnitude while the value

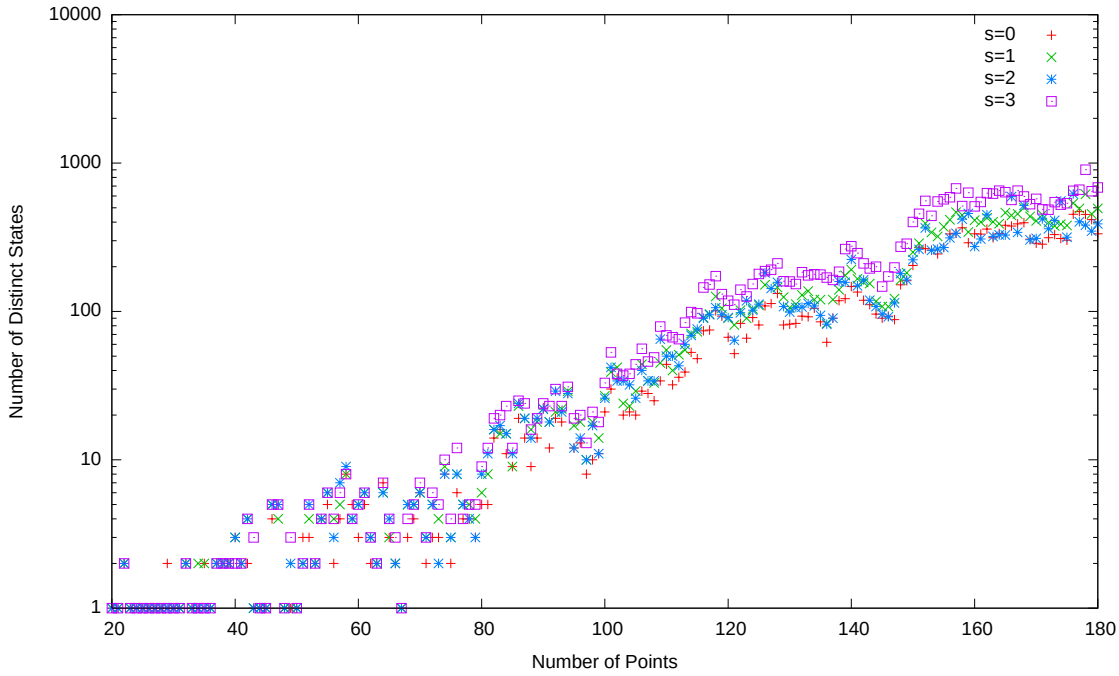

Figure 5.13: The number of distinct states as a function of the number of points N.

Table 5.2: Estimated growth of number of minima with N

s	A	α
0	0.173811 ± 0.04772	0.0472814 ± 0.00182
1	0.236733 ± 0.06899	0.046808 ± 0.001933
2	0.473013 ± 0.1389	0.0413641 ± 0.001966
3	0.355103 ± 0.09599	0.0466184 ± 0.001794

of α decreases. If these parameters reflect the actual growth of the number of stable minima with N, then for $N = 500$ we expect millions of distinct stable configurations and conclude that it is highly unlikely that we have observed the ground state configuration.

5.11.3 **Estimating the Growth of Energy**

In this section we compare our observed growth in minimal energy as a function of N with previous results, observations and conjectures.

The value in obtaining an accurate expansion of the minimal discrete energy in terms of N is that a given term in the expansion often provides a physical understanding of the

nature of the energy. Two examples are the N^2 term and the $N^{1+s/2}$ term. When $s < 2$, the leading term is of order N^2. This is proven in Proposition 2.5.2. The central idea in this proof is that the Riesz kernel is integrable, and that the minimal energy points provide a sampling set for the Riesz kernel that approximates the equilibrium measure – the term is N^2 because we are performing a double integral. More generally the N^2 term reflects an interaction over all pairs of points.

When $s > 2$, Hardin and Saff show in [24] that the leading term is order $N^{1+s/2}$. They prove this result first for the cube (or square as it applies to the case of $\mathbb{S}^2$) using a self-similarity argument. A result of their argument is that the $N^{1+s/2}$ term reflects the local structure of the configurations of minimal energy points. The conjectured value for this leading term is connected to the expectation that, for two-dimensional compact manifolds, the ground state will be largely hexagonal.[9]

Numerical results corroborate conjectures that for $0 < s < 2$ the second order term is order $N^{1+s/2}$ and for some range of $s > 2$ the second order term is N^2. A natural interpretation of these conjectures is that for $s < 2$ the discrete minimal energy reflects the global structure first and the local structure second, whereas, for some range of $s > 2$, the local structure dominates and the second term reflects the global structure.

The main tool in examining the expansion is the residual difference between the observed data and the expansion. The expansion may be qualitatively described as good if the residuals are small compared to the smallest term in the expansion for the range of N under consideration, and if the residuals do not have any obvious structure.

[9]While many accept that the hexagonal lattice is the ground state for particles on a two dimensional set interacting via a Riesz potential, there is no proof of this. If ones takes the appropriate limit as $s \uparrow \infty$, one obtains the problem of best packing. In this case it is proven in [19] (also cf. [20]) that the hexagonal lattice is optimal.

5.11.4 **Growth of Energy for $s = 0$**

In [42] the expansion for the minimal discrete $s = 0$ energy on the sphere is shown to be of the form

$$\mathcal{E}_0(\mathbb{S}^2, N) \approx -\frac{1}{4}\log\left(\frac{4}{e}\right)N^2 - \frac{1}{4}N\log N + BN + O(N)$$

for some B, and is conjectured to be of the form

$$\mathcal{E}_0(\mathbb{S}^2, N) \approx -\frac{1}{4}\log\left(\frac{4}{e}\right)N^2 - \frac{1}{4}N\log N + BN + C\log N + O(1). \tag{5.7}$$

The problem of minimizing the $s = 0$ energy is equivalent to the problem of maximizing the product of the pairwise distances between points on $\mathbb{S}^2$. Solutions to this problem are of considerable value and consequently the seventh of Smale's eighteen problems for the twenty-first century [46] is to find an algorithm whose run time grows as a polynomial in N that can create a configuration of points $\omega_N \subset \mathbb{S}^2$ so that

$$E_0(\omega_N) - \mathcal{E}_0(\mathbb{S}^2, N) < C\log N$$

for some value C. One of the difficulties of this problem is the lack of a theoretical description of growth accurate to within order $\log N$[10].

In [43] the authors use their results to suggest an expansion of the form

$$\mathcal{E}_0(\mathbb{S}^2, N) \approx -\frac{1}{4}\log\left(\frac{4}{e}\right)N^2 - \frac{1}{4}N\log N - 0.026422N + 0.13822. \tag{5.8}$$

Note that this expansion does not include a $\log N$ term.

Using the best available data for $N = 20, \ldots, 200$, 212, 272 and 282 from our

[10] Smale's eighteenth problem is to find the limits of human and artificial intelligence.

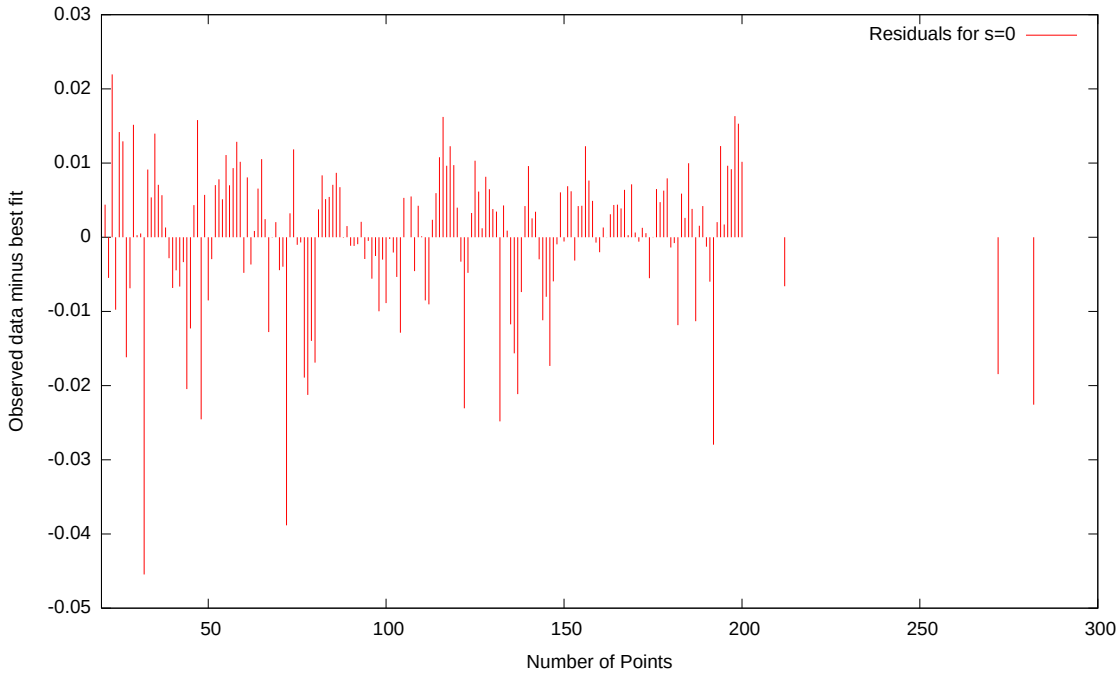

Figure 5.14: The difference between the best fit and the observed minimal discrete energy for $s = 0$.

experiments and from those found in [43] we vary α, β and γ to obtain a fit of the form

$$\mathcal{E}_0(\mathbb{S}^2, N) \approx -\frac{1}{4}\log\left(\frac{4}{e}\right)N^2 - \frac{1}{4}N\log N + \alpha N + \beta \log N + \gamma.$$

The results as computed by KaleidaGraph and confirmed with GNUPlot are: $\alpha = -.026669 \pm 4.5917 \times 10^{-5}$, $\beta = .023322 \pm .0042084$ and $\gamma = .056395 \pm .014392$, where the sum of the squares of the residuals is 0.0184548. One possible explanation for the difference between these values and those in (5.8) is the curve fitting algorithm. Both KaleidaGraph and GNUPlot require initial guesses for the free parameters and for both programs the results depend on the guesses. If the starting value of β is zero, then GNUPlot finds a solution very much like that in (5.8). However in that case the sum of the squares of the residuals is 0.0215498. We conclude that this curve fitting problem is a minimization problem with several local minima and that it is hard to know if a given minimum is the global minimum. More significantly we feel the data allow for a non-zero $\log N$ term.

5.11.5 **Growth of Energy for $s = 1$**

Proposition 2.5.2 implies that the first order term for the $s = 1$ minimal discrete energy is $\frac{1}{2}I_1(\mu^{1,\mathbb{S}^2})N^2$ (It is known that $I_1(\mu^{1,\mathbb{S}^2}) = 1$). In [29] the second order term is conjectured to be $C_s N^{1+s/2}$, where the constant C_s is given by

$$C_s := 3\left(\frac{\sqrt{3}}{8\pi}\right)^{s/2} \zeta(s/2)L_{-3}(s/2).$$

Here ζ is the classical Riemann zeta function – the analytic extension of

$$\tilde{\zeta}(\alpha) := \sum_{n=1}^{\infty} \frac{1}{n^\alpha}$$

and L_{-3} is the Dirichlet L-function given by

$$L_{-3}(\alpha) = 1 - \frac{1}{2^\alpha} + \frac{1}{4^\alpha} - \frac{1}{5^\alpha} + \frac{1}{7^\alpha} - \dots$$

In the case $s = 1$ numerical computations of C_s give a value of $-.553002$. In [42] the third order term is conjectured to be of the form $N^{s/2}$.

In [43] Rakhmanov, Saff and Zhou fit their data to obtain an expansion of the form

$$\mathcal{E}_1(\mathbb{S}^2, N) \approx \frac{N^2}{2} - 0.55230N^{3/2} + 0.0689N^{1/2}.$$

In [36] Morris Deaven and Ho perform a similar fit and obtain

$$\mathcal{E}_1(\mathbb{S}^2, N) \approx \frac{N^2}{2} - 0.55230N^{3/2} + 0.0685N^{1/2}.$$

Using the best available data from our experiments for $N = 20, \dots, 200$ and from [36,

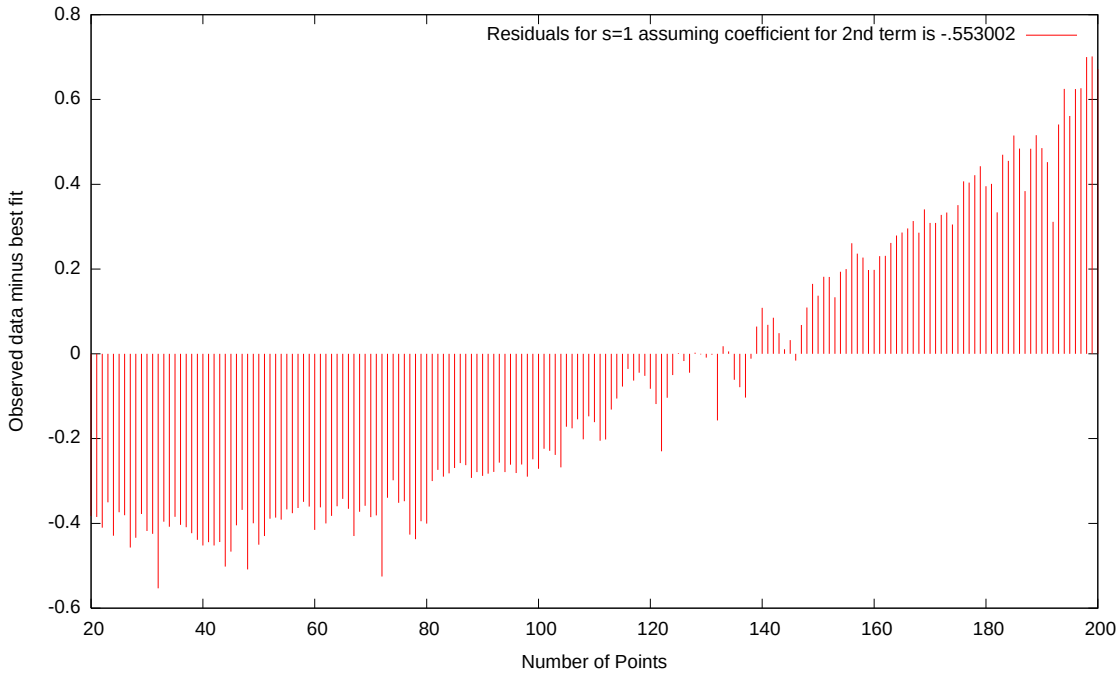

Figure 5.15: The difference between the best fit and the observed minimal discrete energy for $s = 1$ assuming the conjectured value for the coefficient of the second term.

43] we fit the following two expressions to the observed minimal discrete energy:

$$\mathcal{E}_1(\mathbb{S}^2, N) = \frac{N^2}{2} + \alpha N^{3/2} + \beta N^{1/2}, \tag{5.9}$$

$$\mathcal{E}_1(\mathbb{S}^2, N) = \frac{N^2}{2} - .553002 N^{3/2} + \gamma N^{1/2}. \tag{5.10}$$

The values of the parameters resulting from the fit are: $\alpha = -0.552311 \pm 7.707 \times 10^{-6}$, $\beta = 0.0691789 \pm 0.001098$ and $\gamma = 0.162383 \pm 0.002395$. The sum of the squares of the residuals for the fit involving α and β was 0.447483 and the sum of the square of the residuals for the fit for γ alone was 20.5643.

The structure in figure 5.15 immediately suggests that for the range of N considered, the expansion given in (5.10) isn't optimal. Reasonable hypotheses include: the data aren't the minimum values; the expansion isn't valid for the range of N considered, alternatively the higher order terms are significant for this range of N; finally the conjectured value of the coefficient for second order term isn't correct.

Given the similarity in the parameters we obtain in the fit of (5.9) to those obtained in [36, 43] we refer the interested reader to those papers for a plot of the residuals.

5.11.6 **Growth of Energy for** $s = 2$

In [29] and also in [24] the leading term in the growth of the minimal N point $s = 2$ energy is shown to be

$$\mathcal{E}_2(\mathbb{S}^2, N) = \frac{1}{4} N^2 \log N.$$

The next order term is conjectured to be of the form CN^2.

In the cases of $s = 2$ and $s = 3$ we do not have data from other experiments with which to compare our data. Given that we performed 600 trials and that approximately 90% (See Figure 5.2) of them lead to stable configurations, we assume that, at most, we could have identified 540 distinct stable states. The growth parameters from table 5.2 suggests that at $N = 173$ the number of stable configurations will exceed this. For this reason we examine the data for $N = 20, \ldots, 173$ when studying the expansion of the $s = 2$ energy as a function of N.

We fit the expression

$$\mathcal{E}_2(\mathbb{S}^2, N) = \alpha N^2 \log N + \beta N^2$$

to the data and obtain $\alpha = 0.124475 \pm 1.42 \times 10^{-5}$ and $\beta = -0.0392098 \pm 7.045 \times 10^{-5}$ and the sum of the square of the residuals is 38.4787

Figure 5.16 suggests that the residuals have some structure in that the observed data exceeds the expansion for low and high values of N examined.

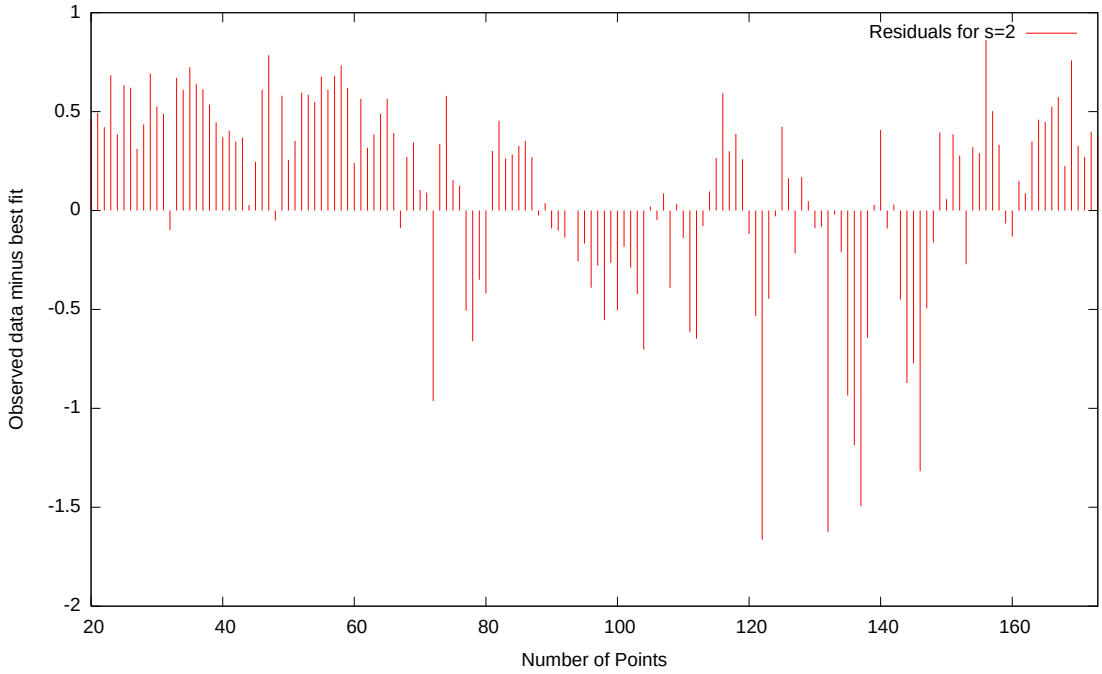

Figure 5.16: The difference between the best fit and the observed minimal discrete energy for $s = 2$.

5.11.7 **Growth of Energy for** $s = 3$

In [29] for the case $s > 2$ is shown that[11]

$$\limsup_{N\to\infty} \frac{\mathcal{E}_3(\mathbb{S}^2, N)}{N^{1+s/2}} \leq \frac{C_{s,2}}{\mathcal{H}^2(\mathbb{S}^2)^{s/2}} \tag{5.11}$$

The constant $C_{s,2}$ is given by

$$\frac{1}{2}\left(\frac{\sqrt{3}}{2}\right)^{s/2} \zeta_L(s),$$

where $\zeta_L(s)$ is the zeta function associated with the hexagonal lattice. That is if L consists of all points in the hexagonal lattice of edge length 1, then

$$\zeta_L(\alpha) = \sum_{r\in L\setminus\{0\}} \frac{1}{|r|^\alpha}.$$

In [29] it is conjectured, and in [24] it is shown, that the limit superior of the left hand

[11] In this result, the measure $\mathcal{H}^2$ has been normalized so that it agrees with $\mathcal{L}^2$ when restricted to $\mathbb{R}^2$.

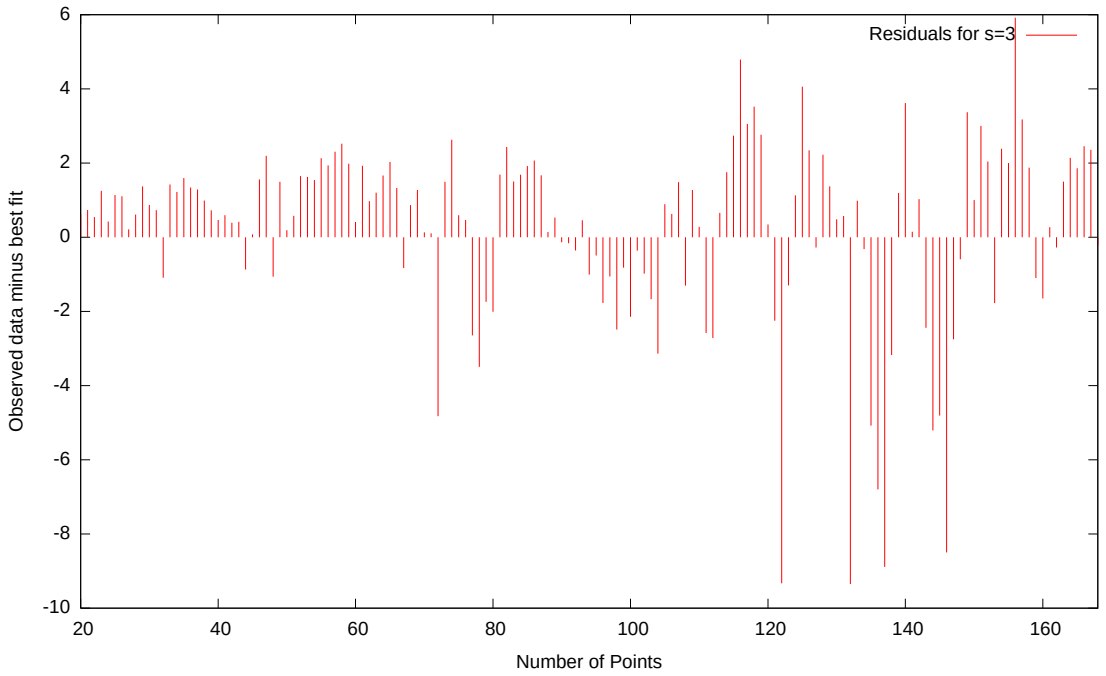

Figure 5.17: The difference between the best fit and the observed minimal discrete energy for $s = 3$.

side of (5.11) can be replaced by a limit. And in both papers it is conjectured that the value of the limit is the right hand side of (5.11). The results in [24] are broader in that $\mathbb{S}^2$ may be replaced by any compact d-rectifiable manifold.

For the range of s under consideration ($s > 2$) the function ζ_L has the following factorization(cf. [29])

$$\zeta_L(s) = 6\zeta(s/2)L_{-3}(s/2).$$

We compute the coefficient of the leading order term as 0.0998139 for the case $s = 3$. For this case the second order term is conjectured to be of the form CN^2.

Based on arguments similar to those in Section 5.11.6 we feel that for $N > 168$ we expect that there are more stable configurations than there are trials we have run that led to configurations passing our stability criteria. For this reason we examine data for $N = 20, \ldots, 168$.

Fitting a curve of the form

$$\mathcal{E}_3(\mathbb{S}^2, N) = \alpha N^{5/2} + \beta N^2$$

to the data gives $\alpha = 0.0999087 \pm 1.411 \times 10^{-5}$ and $\beta = -0.118845 \pm 0.0001673$ where the sum of the squares of the residuals is 962.77. The residuals are plotted in Figure 5.17 and suggest that the expansion is reasonable.

5.11.8 **Growth of Scars**

In the preceding analysis few assumptions have been made about the structure of the energy minimizing configurations. The conjectured values for the coefficient of the $N^{1+s/2}$ term were tangentially related to the assumption of a ground state dominated by a hexagonal lattice inasmuch as the terms are related to the zeta function for that lattice, however the bulk of the theory and questions have been agnostic about the local structure of the ground state.

In [5] Bowick, Cacciuto, Nelson and Travesset make the natural but unproven assumption that the ground state is roughly a hexagonal lattice. Because the Euler characteristic of $\mathbb{S}^2$ is two, $\mathbb{S}^2$ cannot be covered in hexagons. The Voronoi cells cannot all have six sides, consequently not all of the points can have six nearest neighbors. The points which do not have six nearest neighbors are referred to as *disclinations*. Further, numerical experiments suggest that disclinations group together. These groupings of disclinations are referred to as scars. However, unlike our definition of the term, these scars need not be connected. The approach in [5] is to view minimal configurations in terms of collections these groupings of disclinations. While the authors of [5] do not provide an exact definition of scars, they do refer to them as grain boundaries and in numerical experiments these scars often occur where the the orientation of the hexagonal lattice changes.

Figure 5.18 shows the Voronoi cells for a configuration with 1600 points resulting from

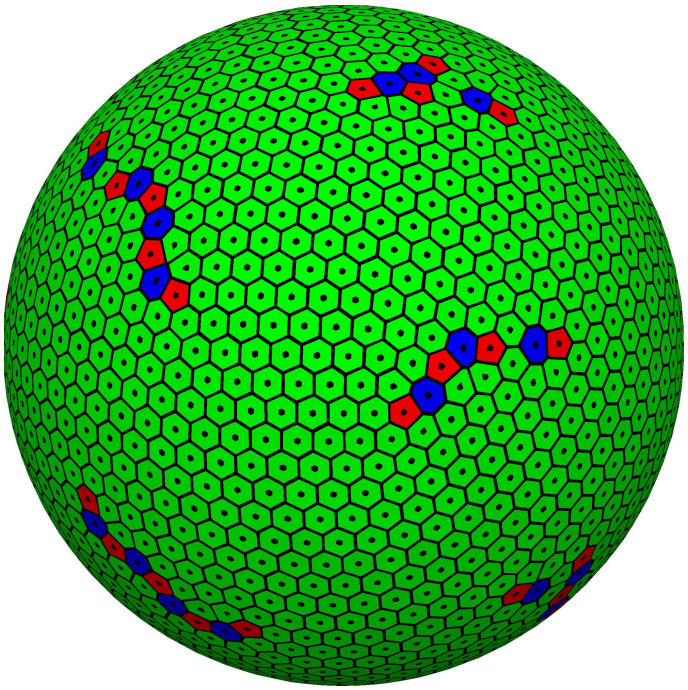

Figure 5.18: Examples of disconnected scars on a configuration resulting from optimizing $N = 1600$ points for $s = 4$.

numerically minimizing the $s = 4$ energy. The features of note are that the disclinations are gathered together into scars, that four of the five scars shown are disconnected, and lastly that the scars are located roughly at the vertices of an icosahedron circumscribed by the sphere. The idea presented in [5] is that the hexagonal lattice is flat and that the curvature of the sphere introduces strain in the lattice that increases with distance. The scars are the points where energy is lowered if the hexagonal structure is broken and the strain is relieved. The hypothesis is that the minimal configurations will have scars at the vertices of an inscribed icosahedron and that these scars will grow in size as N grows.

Our goal in this section is to examine this hypothesis. We use the scar tagging technique to count the number of connected components of scars in the observed minimal configurations. We also count the total number of disclinations. The results for this can be found in Figures 5.19, 5.20, 5.21 and 5.22. We note that the total number of scar components is fairly constant at 12. As N approaches 500 the number of scar components increases, although this is likely due to disconnected scars. The total number

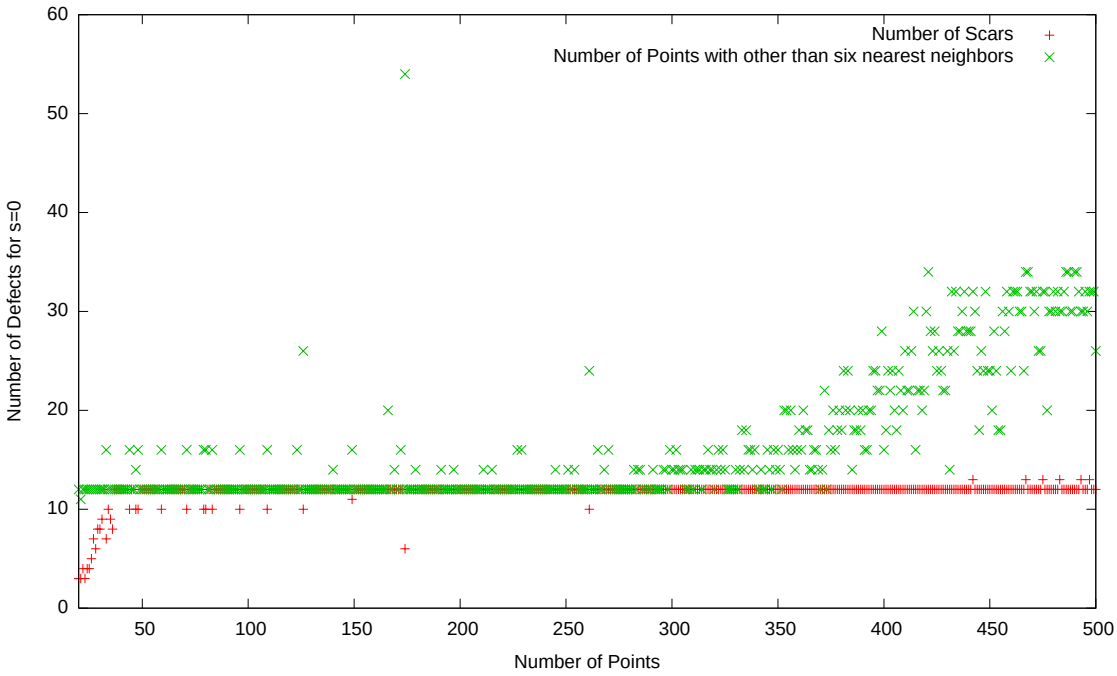

Figure 5.19: The growth of scars and disclinations for $s = 0$.

of disclinations grows and we conclude, based on these data, that scar size does grow with N. The small number of scars for small N is due to insufficiently many points to generate a hexagonal lattice of any extent.

One should bear in mind that in Figures 5.19, 5.20, 5.21 and 5.22, the consistent growth of the number of disclinations beyond 12 occurs for a range of N for which we do not expect that these experiments found the global minimal configuration.

Of particular interest is the point corresponding to $N = 174$, $s = 0$ in Figure 5.19. Here, in stark contrast to nearby values of N, there are only six scars and 54 disclinations. Figure 5.23 shows the Voronoi cells for the configuration. The scars are quite large compared to the size of scars for values of N near 174. Further, the scars appear to be located at the centers of faces of a cube enclosing the sphere, suggesting a symmetry that is not based on the icosahedron.

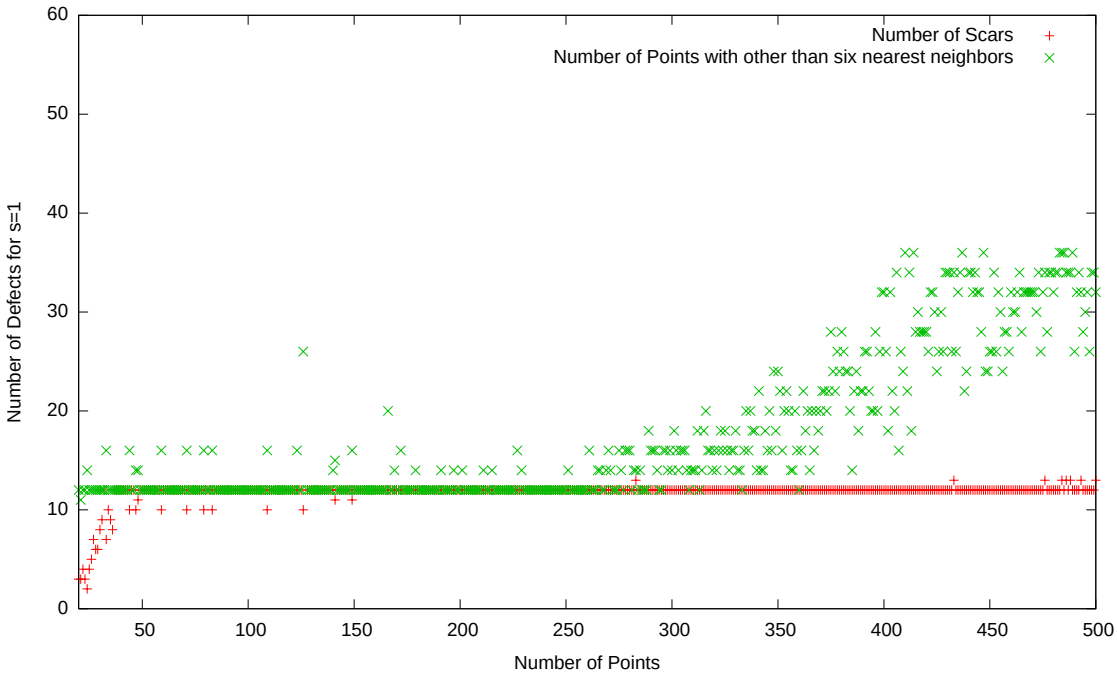

Figure 5.20: The growth of scars and disclinations for $s = 1$.

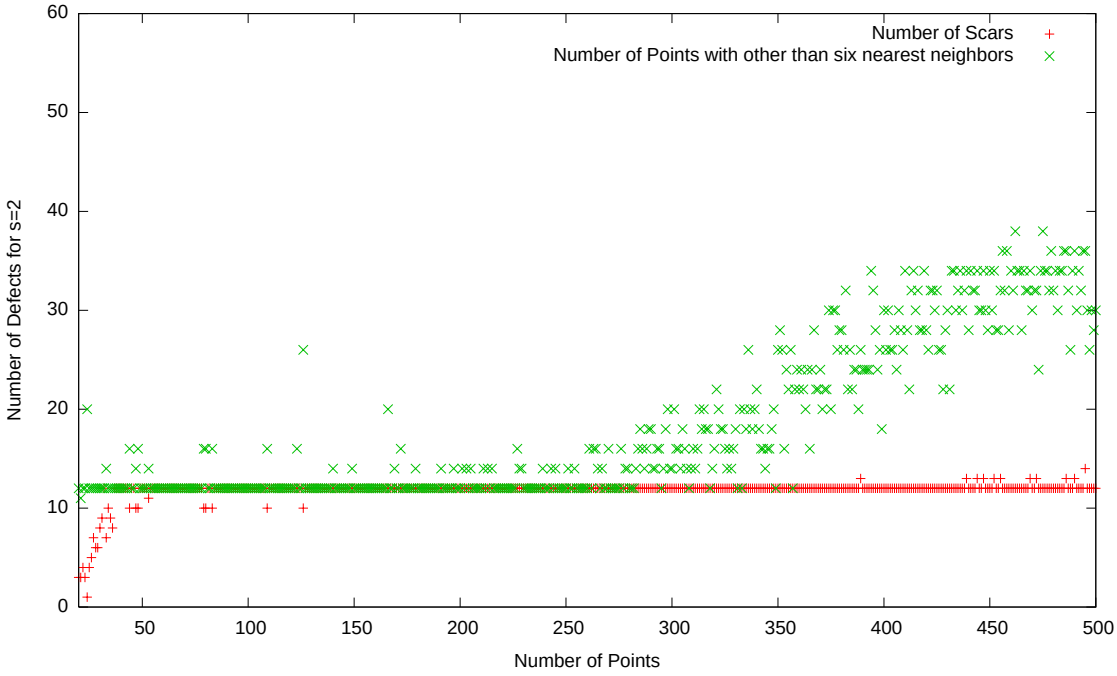

Figure 5.21: The growth of scars and disclinations for $s = 2$.

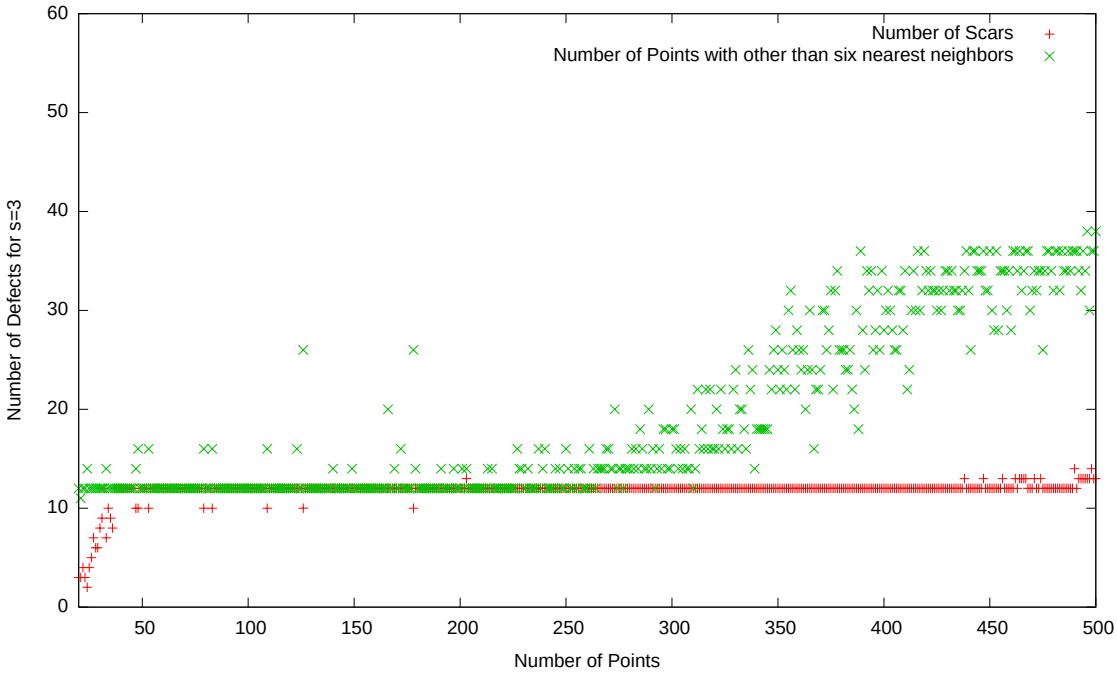

Figure 5.22: The growth of scars and disclinations for $s = 3$.

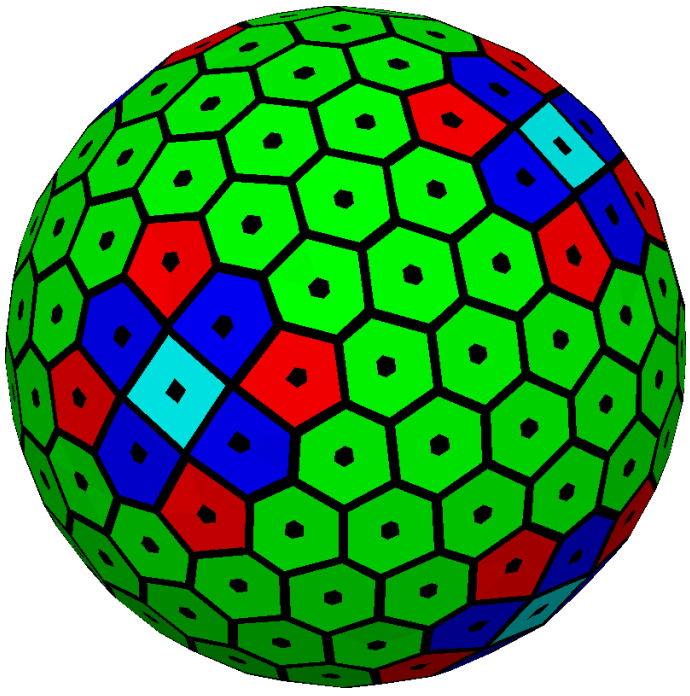

Figure 5.23: The Voronoi cells for an experimentally obtained ground state for $N = 174$ $s = 0$. Note the symmetry as compared to the configuration for $N = 24$ in Figure 5.6.

CHAPTER 6

OPEN QUESTIONS AND FUTURE WORK

The results presented so far suggest the following areas of inquiry:

(1) Can we show that the asymptotic distribution of minimal discrete d-energy configurations agrees with the minimizer of our normalized d-energy $\tilde{I}_d$? Such a result would likely be new for the case of strictly self-similar d-fractals. More generally, under what conditions can the asymptotic distribution of the minimal discrete s-energy configurations be related to a continuous problem? In [4] it is shown for a fractal set A and s sufficiently large, that $\mathcal{E}_s(A, N)$ oscillates, as $N \to \infty$, on a scale proportional to its highest order term. This suggests a set formed from the union of such a fractal and a d-rectifiable fractal of the same dimension might not have a single asymptotic distribution.

(2) Can one construct a weighted normalized d-energy whose unique minimizer agrees with a prescribed measure? In such a setting could similarly weighted s-energies produce s-equilibrium measures that converge to this prescribed measure?

(3) The two proofs that the s-equilibrium measures converged in the weak-star sense to the uniform measure both relied on different localization properties. Can this be generalized and applied to a broader class of sets?

(4) When is the equilibrium measure $\mu^{s,A}$ absolutely continuous with respect to $\mathcal{H}_A^d$? If $\mu^{s,A} \ll \mathcal{H}_A^d$ for some range of $s \in (s_0, d)$ does the convergence of $\mu^{s,A}$ to $\mathcal{H}_A^d/\mathcal{H}^d(A)$ occur within an $L^p(\mathcal{H}_A^d)$ space?

(5) For what measures μ is the function $f_\mu(s) := (d - s)I_s(\mu)$ analytic? What is the range of the analyticity? For example the analytic extension of $(1 - s)I_s(\mathcal{H}^1_{[-1,1]})$ has a pole at $s = 2$.

(6) Regarding the numerical experiments: why did the results of the least eigenvalue test for stability cluster as they did?

(7) Discrete N-point energy calculations are $O(N^2)$. Under what conditions can we use an approximate energy, such a multipole expansion, and still differentiate stable configurations? Relatedly, how deep are the energy wells separating the stable configurations?

(8) Can one develop and test models, such as that presented in [5], that describe interactions between scars.

(9) Are there good starting points that are in the basin of attraction for a stable minimum with energy close to that of the global minimum. This problem has been posed by others in earlier work, but its significance justifies its reiteration.

APPENDIX A

DATA

Data from the experiments described in Chapter 5 are presented in the following tables. Each tables presents data for a specific value of s and a range of values of N. The columns of the tables are as follows:

"N": The number of points.

"Minimum Energy": The lowest observed energy for the experiments for the given values of s and N.

"Stable States": The number of distinct stable states observed. The criteria for configurations to be considered stable and distinct is described in Chapter 5.

"$s = 0$", "$s = 1$", "$s = 2$", "$s = 3$": Graph information for other values of s. If the experiment in question had a bad graph-tag, then all of these columns are filled in with "B". If the experiment has a good graph-tag then a search is performed through the configurations for other values of s for the same values of N. The results of the search are then placed in the appropriate column. A number n indicates that the n^{th} stable minimum for the value of s associated to that column has the same graph-tag as the minimum configuration for the experiment performed. If the graph-tag occurs multiple times, the configuration with the lowest energy is chosen. The letter "N" indicates that the graph-tag for the minimal configuration did not occur in the list of tags for the stable minima for the value of s indicated. The letter "X" indicates that the graph-tag was found, but the configuration with the lowest energy bearing this graph-tag had a bad graph-tag. The presence of a number does not indicate that there is an isometry, only that the graph-tags are good and the same.

Table A.1: Data for $s = 0$, $N = 20, \ldots, 59$

N	Minimum Energy	Stable States	$s = 0$	$s = 1$	$s = 2$	$s = 3$
20	−54.01112997	1	-	1	1	1
21	−59.00091214	1	-	1	1	1
22	−64.20600776	2	-	1	1	1
23	−69.57838259	1	-	1	1	1
24	−75.21398479	1	B	B	B	B
25	−80.99750999	1	B	B	B	B
26	−87.00942306	1	-	1	1	1
27	−93.25198640	1	-	1	1	1
28	−99.65860938	1	-	1	1	1
29	−106.25457117	2	-	N	N	N
30	−113.08925550	1	-	1	1	1
31	−120.11034664	1	-	1	1	1
32	−127.37886761	2	-	1	1	1
33	−134.74782082	1	B	B	B	B
34	−142.37585227	1	-	1	1	1
35	−150.19205851	2	-	1	1	X
36	−158.22406843	1	-	1	1	1
37	−166.45069752	2	-	1	1	1
38	−174.88019715	2	-	1	1	1
39	−183.50922571	2	-	1	1	1
40	−192.33768992	3	-	1	1	1
41	−201.35920665	2	-	1	1	1
42	−210.58451156	2	-	1	1	1
43	−220.00347705	1	-	1	1	1
44	−229.64180149	1	B	B	B	B
45	−239.45369825	1	-	1	1	1
46	−249.45584790	4	-	1	1	3
47	−259.66175985	5	B	B	B	B
48	−270.11794996	1	B	B	B	B
49	−280.70190312	1	-	1	1	1
50	−291.52860066	1	-	1	1	1
51	−302.53367346	3	-	1	1	1
52	−313.73237194	3	-	1	1	1
53	−325.13823470	2	B	B	B	B
54	−336.74546440	4	-	1	1	1
55	−348.54179628	5	-	1	1	1
56	−360.54589924	2	-	2	2	2
57	−372.74120062	4	-	1	1	1
58	−385.13282979	8	-	1	1	1
59	−397.72814966	5	-	1	2	2

Table A.2: Data for $s = 0$, $N = 60, \ldots, 99$

N	Minimum Energy	Stable States	$s = 0$	$s = 1$	$s = 2$	$s = 3$
60	−410.53316279	3	-	1	1	1
61	−423.50763599	5	-	1	1	1
62	−436.70397924	2	-	1	1	1
63	−450.08123918	2	-	1	1	1
64	−463.65443299	7	-	1	1	1
65	−477.42642607	3	B	B	B	B
66	−491.40747003	2	-	2	2	2
67	−505.59261250	1	-	1	1	1
68	−519.94664229	3	-	1	1	1
69	−534.50818618	4	-	1	1	1
70	−549.27505585	6	B	B	B	B
71	−564.23169473	2	-	1	N	N
72	−579.42034577	3	-	1	1	1
73	−594.72869843	3	-	1	1	1
74	−610.26707141	8	-	2	N	N
75	−626.02346268	2	-	1	1	1
76	−641.96315052	6	-	1	1	1
77	−658.11780984	4	-	1	1	1
78	−674.45299419	4	-	2	2	2
79	−690.97490094	3	B	B	B	B
80	−707.70334618	5	B	B	B	B
81	−724.60446934	5	-	1	1	1
82	−741.71792246	14	-	1	1	3
83	−759.03535475	16	-	1	1	1
84	−776.54543156	11	-	1	1	1
85	−794.25031228	9	-	1	1	1
86	−812.15132187	19	-	2	2	2
87	−830.25191515	14	-	1	1	1
88	−848.55342692	9	-	1	1	1
89	−867.04251640	14	-	1	1	1
90	−885.73182177	22	-	1	1	1
91	−904.61441244	12	-	1	1	1
92	−923.69263633	19	-	1	1	1
93	−942.96395807	18	-	1	1	1
94	−962.43913215	28	-	1	1	1
95	−982.10267832	12	-	1	1	1
96	−1001.96953397	13	-	N	N	N
97	−1022.02397776	8	-	1	1	1
98	−1042.28469040	10	-	1	1	1
99	−1062.72666994	11	-	1	1	1

Table A.3: Data for $s = 0$, $N = 100, \ldots, 139$

N	Minimum Energy	Stable States	$s = 0$	$s = 1$	$s = 2$	$s = 3$
100	−1083.37714054	21	-	1	1	1
101	−1104.20875781	30	-	1	1	1
102	−1125.24648890	35	-	1	1	1
103	−1146.48126010	20	-	1	1	1
104	−1167.91583717	21	-	1	1	1
105	−1189.52030197	20	-	1	1	1
106	−1211.34105988	29	-	1	1	1
107	−1233.35192224	28	-	1	1	1
108	−1255.57113187	25	-	1	1	1
109	−1277.96692689	34	-	1	1	1
110	−1300.57108956	44	-	1	1	1
111	−1323.37521678	32	-	1	1	1
112	−1346.36661369	36	-	1	1	1
113	−1369.54147278	39	-	1	1	1
114	−1392.91949432	53	-	1	1	1
115	−1416.49160795	48	-	1	1	1
116	−1440.25846520	74	-	2	2	3
117	−1464.23264292	75	-	1	1	1
118	−1488.39287053	101	-	1	1	1
119	−1512.75357172	93	-	1	1	1
120	−1537.31267642	67	-	1	1	1
121	−1562.06859738	52	-	1	1	1
122	−1587.03219402	83	-	1	1	1
123	−1612.15297129	66	-	1	1	1
124	−1637.47911003	91	-	1	1	1
125	−1663.00144580	81	-	1	1	2
126	−1688.73013605	109	-	1	1	1
127	−1714.65474034	113	-	N	1	1
128	−1740.76259257	132	-	1	1	1
129	−1767.07413795	81	-	1	1	1
130	−1793.58178367	82	-	1	1	1
131	−1820.28217330	83	-	1	1	1
132	−1847.20554490	93	-	1	1	1
133	−1874.26656534	92	-	1	1	1
134	−1901.55512674	105	-	1	1	1
135	−1929.04793880	85	-	1	1	1
136	−1956.72704659	62	-	1	1	1
137	−1984.60269719	90	-	1	1	1
138	−2012.65407868	118	-	1	1	1
139	−2040.90259564	122	-	1	1	1

Table A.4: Data for $s = 0$, $N = 140, \ldots, 179$

N	Minimum Energy	Stable States	$s = 0$	$s = 1$	$s = 2$	$s = 3$
140	−2069.35226042	147	-	1	2	2
141	−2098.00927608	135	-	N	N	N
142	−2126.85329867	119	-	1	1	1
143	−2155.89952457	111	-	1	1	1
144	−2185.14244088	96	-	1	1	1
145	−2214.56887402	90	-	1	1	1
146	−2244.20265977	93	-	1	1	1
147	−2274.01059503	88	-	1	1	1
148	−2304.01977867	151	-	2	2	2
149	−2334.22178132	161	-	1	N	N
150	−2364.63224259	204	-	1	1	1
151	−2395.22345412	271	-	1	1	1
152	−2426.01759261	265	-	1	1	1
153	−2457.01518190	259	-	1	1	1
154	−2488.19087645	244	-	1	1	1
155	−2519.56863374	270	-	1	1	1
156	−2551.13317768	333	-	1	1	1
157	−2582.90510682	336	-	1	1	1
158	−2614.86990053	366	-	1	1	1
159	−2647.03231575	290	-	1	1	1
160	−2679.38513532	334	-	1	1	1
161	−2711.92800830	332	-	1	1	1
162	−2744.67023067	359	-	1	1	1
163	−2777.60275049	314	-	1	1	1
164	−2810.73179977	335	-	1	1	1
165	−2844.05672050	381	-	1	1	1
166	−2877.57686768	376	-	1	1	1
167	−2911.28864575	389	-	1	1	1
168	−2945.20367766	396	-	1	1	1
169	−2979.30037673	307	-	1	1	1
170	−3013.60507643	288	-	3	3	3
171	−3048.09911405	284	-	1	1	1
172	−3082.78465723	314	-	1	1	1
173	−3117.66740914	330	-	1	1	1
174	−3152.75008214	310	-	2	N	N
175	−3188.01572185	302	-	1	1	1
176	−3223.47504496	452	-	1	1	1
177	−3259.13716127	471	-	N	1	N
178	−3294.99049845	451	-	1	1	N
179	−3331.03831581	416	-	1	N	N

Table A.5: Data for $s = 0$, $N = 180, \ldots, 200$

N	Minimum Energy	Stable States	$s = 0$	$s = 1$	$s = 2$	$s = 3$
180	−3367.29162492	334	-	2	2	2
181	−3403.72956406	446	-	1	1	1
182	−3440.37370646	504	-	1	1	1
183	−3477.18355890	470	-	1	1	1
184	−3514.20892351	520	-	1	1	1
185	−3551.41816587	610	-	2	2	2
186	−3588.83543401	545	-	1	1	1
187	−3626.45617221	549	-	1	1	1
188	−3664.24340241	534	-	1	1	1
189	−3702.23529643	503	-	1	1	1
190	−3740.42981545	602	-	1	1	1
191	−3778.81801847	512	-	1	1	1
192	−3817.41795618	583	-	1	1	1
193	−3856.16036156	605	-	1	1	1
194	−3895.11694654	555	-	1	1	1
195	−3934.28880272	646	-	1	1	1
196	−3973.63658094	618	-	1	1	1
197	−4013.18246235	715	-	1	1	1
198	−4052.92459102	913	-	1	1	1
199	−4092.86457064	671	-	1	1	1
200	−4133.00307953	691	-	1	1	1

Table A.6: Data for $s = 1$, $N = 20, \ldots, 59$

N	Minimum Energy	Stable States	$s = 0$	$s = 1$	$s = 2$	$s = 3$
20	150.88156833	1	1	-	1	1
21	167.64162240	1	1	-	1	1
22	185.28753615	2	1	-	1	1
23	203.93019066	1	1	-	1	1
24	223.34707405	1	B	B	B	B
25	243.81276030	1	B	B	B	B
26	265.13332632	1	1	-	1	1
27	287.30261503	1	1	-	1	1
28	310.49154236	1	1	-	1	1
29	334.63443992	1	2	-	1	1
30	359.60394590	1	1	-	1	1
31	385.53083806	1	1	-	1	1
32	412.26127465	2	1	-	1	1
33	440.20405745	1	B	B	B	B
34	468.90485328	2	1	-	1	1
35	498.56987249	2	1	-	1	X
36	529.12240838	1	1	-	1	1
37	560.61888773	2	1	-	1	1
38	593.03850357	2	1	-	1	1
39	626.38900902	2	1	-	1	1
40	660.67527883	3	1	-	1	1
41	695.91674434	2	1	-	1	1
42	732.07810754	4	1	-	1	1
43	769.19084646	1	1	-	1	1
44	807.17426308	1	B	B	B	B
45	846.18840106	1	1	-	1	1
46	886.16711364	5	1	-	1	3
47	927.05927068	4	B	B	B	B
48	968.71345534	1	B	B	B	B
49	1011.55718265	1	1	-	1	1
50	1055.18231473	1	1	-	1	1
51	1099.81929032	2	1	-	1	1
52	1145.41896432	4	1	-	1	1
53	1191.92229042	2	B	B	B	B
54	1239.36147473	4	1	-	1	1
55	1287.77272078	6	1	-	1	1
56	1337.09494528	4	2	-	1	1
57	1387.38322925	5	1	-	1	1
58	1438.61825064	8	1	-	1	1
59	1490.77333528	4	1	-	2	2

Table A.7: Data for $s = 1$, $N = 60, \ldots, 99$

N	Minimum Energy	Stable States	$s = 0$	$s = 1$	$s = 2$	$s = 3$
60	1543.83040098	5	1	-	1	1
61	1597.94183020	6	1	-	1	1
62	1652.90940990	3	1	-	1	1
63	1708.87968150	2	1	-	1	1
64	1765.80257793	6	1	-	1	1
65	1823.66796026	3	X	-	1	1
66	1882.44152530	2	N	-	1	1
67	1942.12270041	1	1	-	1	1
68	2002.87470175	5	1	-	1	1
69	2064.53348323	5	1	-	1	1
70	2127.10090155	6	B	B	B	B
71	2190.64990643	3	1	-	N	N
72	2255.00119097	5	1	-	1	1
73	2320.63388375	4	1	-	1	1
74	2387.07298184	9	2	-	1	1
75	2454.36968904	3	1	-	1	1
76	2522.67487184	8	1	-	1	1
77	2591.85015235	5	1	-	1	1
78	2662.04647457	5	2	-	1	1
79	2733.24835748	4	B	B	B	B
80	2805.35587598	6	B	B	B	B
81	2878.52282966	8	1	-	1	1
82	2952.56967529	16	1	-	1	3
83	3027.52848892	15	1	-	1	1
84	3103.46512443	15	1	-	1	1
85	3180.36144294	9	1	-	1	1
86	3258.21160571	23	2	-	1	1
87	3337.00075001	19	1	-	1	1
88	3416.72019676	16	1	-	1	1
89	3497.43901862	18	1	-	1	1
90	3579.09122272	22	1	-	1	1
91	3661.71369932	18	1	-	1	1
92	3745.29163624	21	1	-	1	1
93	3829.84433842	22	1	-	1	1
94	3915.30926962	29	1	-	1	1
95	4001.77167557	17	1	-	1	1
96	4089.15401006	18	N	-	1	1
97	4177.53359962	10	1	-	1	1
98	4266.82246416	18	1	-	1	1
99	4357.13916313	14	1	-	1	1

Table A.8: Data for $s = 1$, $N = 100, \ldots, 139$

N	Minimum Energy	Stable States	$s = 0$	$s = 1$	$s = 2$	$s = 3$
100	4448.35063433	27	1	-	1	1
101	4540.59005169	39	1	-	1	1
102	4633.73656590	42	1	-	1	1
103	4727.83661683	24	1	-	1	1
104	4822.87652275	23	1	-	1	1
105	4919.00063762	29	1	-	1	1
106	5015.98459570	44	1	-	1	1
107	5113.95354771	34	1	-	1	1
108	5212.81350783	33	1	-	1	1
109	5312.73507992	45	1	-	1	1
110	5413.54929419	55	1	-	1	1
111	5515.29321459	40	1	-	1	1
112	5618.04488233	51	1	-	1	1
113	5721.82497803	55	1	-	1	1
114	5826.52157216	71	1	-	1	1
115	5932.18128578	73	1	-	1	1
116	6038.81559358	91	3	-	1	1
117	6146.34244658	96	1	-	1	1
118	6254.87702779	126	1	-	1	1
119	6364.34731748	105	1	-	1	1
120	6474.75632498	90	1	-	1	1
121	6586.12194958	81	1	-	1	1
122	6698.37449926	102	1	-	1	1
123	6811.82722817	90	1	-	1	1
124	6926.16997419	104	1	-	1	1
125	7041.47326402	110	1	-	1	2
126	7157.66922487	151	1	-	1	1
127						
128	7393.00744307	145	1	-	1	1
129	7512.10731927	125	1	-	1	1
130	7632.16737891	106	1	-	1	1
131	7753.20516694	112	1	-	1	1
132	7875.04534280	129	1	-	1	1
133	7998.17921290	137	1	-	1	1
134	8122.08972119	120	1	-	1	1
135	8246.90948699	120	1	-	1	1
136	8372.74330254	83	1	-	1	1
137	8499.53449478	120	1	-	1	1
138	8627.40638988	140	1	-	1	1
139	8756.22705695	175	1	-	1	1

Table A.9: Data for $s = 1$, $N = 140, \ldots, 179$

N	Minimum Energy	Stable States	$s = 0$	$s = 1$	$s = 2$	$s = 3$
140	8885.98060904	191	1	-	2	2
141	9016.61534919	166	B	B	B	B
142	9148.27157999	157	1	-	1	1
143	9280.83985119	154	1	-	1	1
144	9414.37179446	117	1	-	1	1
145	9548.92883723	108	1	-	1	1
146	9684.38182557	108	1	-	1	1
147	9820.93237837	122	1	-	1	1
148	9958.40600427	163	2	-	1	1
149	10096.85990740	182	1	-	N	N
150	10236.19643670	251	1	-	1	1
151	10376.57146927	288	1	-	1	1
152	10517.86759288	392	1	-	1	1
153	10660.08274824	341	1	-	1	1
154	10803.37242114	320	1	-	1	1
155	10947.57469228	372	1	-	1	1
156	11092.79831146	415	1	-	1	1
157	11238.90304116	466	1	-	1	1
158	11385.99018620	446	1	-	1	1
159	11534.02396096	343	1	-	1	1
160	11683.05480555	412	1	-	1	1
161	11833.08473946	400	1	-	1	1
162	11984.05033581	427	1	-	1	1
163	12136.01305322	402	1	-	1	1
164	12288.93010532	390	1	-	1	1
165	12442.80445137	463	1	-	1	1
166	12597.64907132	444	1	-	1	1
167	12753.46942975	454	1	-	1	1
168	12910.21267227	501	1	-	1	1
169	13068.00645113	437	1	-	1	1
170	13226.68107854	408	2	-	1	1
171	13386.35593072	449	1	-	1	1
172	13547.01810879	397	1	-	1	1
173	13708.63524303	377	1	-	1	1
174	13871.18709229	387	2	-	1	1
175	14034.78130693	380	1	-	1	1
176	14199.35477563	536	1	-	1	1
177	14364.85051921	495	N	-	2	2
178	14531.30955259	616	1	-	1	N
179	14698.75459422	454	1	-	N	N

Table A.10: Data for $s = 1$, $N = 180, \ldots, 200$

N	Minimum Energy	Stable States	$s = 0$	$s = 1$	$s = 2$	$s = 3$
180	14867.09992753	495	2	-	1	1
181	15036.46723977	531	1	-	1	1
182	15206.73061091	615	1	-	1	1
183	15378.16657103	624	1	-	1	1
184	15550.42145031	727	1	-	1	1
185	15723.72007407	713	2	-	1	1
186	15897.89743705	594	1	-	1	1
187	16072.97518632	584	1	-	1	1
188	16249.22267888	614	1	-	1	1
189	16426.37193886	572	1	-	1	1
190	16604.42833850	727	1	-	1	1
191	16783.45221936	603	1	-	1	1
192	16963.33838646	626	1	-	1	1
193	17144.56474088	702	1	-	1	1
194	17326.61613647	653	1	-	1	1
195	17509.48930393	656	1	-	1	1
196	17693.46054808	735	1	-	1	1
197	17878.38274577	712	1	-	1	1
198	18064.26217720	773	1	-	1	1
199	18251.08249564	797	1	-	1	1
200	18438.84271753	789	1	-	1	1

Table A.11: Data for $s = 2$, $N = 20, \ldots, 59$

N	Minimum Energy	Stable States	$s = 0$	$s = 1$	$s = 2$	$s = 3$
20	133.93697857	1	1	1	-	1
21	150.32512274	1	1	1	-	1
22	167.66578564	2	1	1	-	1
23	186.40371287	1	1	1	-	1
24	205.65843800	1	B	B	B	B
25	226.54507726	1	B	B	B	B
26	248.26713892	1	1	1	-	1
27	270.79840421	1	1	1	-	1
28	294.87847161	1	1	1	-	1
29	320.21603176	1	2	1	-	1
30	346.26363064	1	1	1	-	1
31	373.58086896	1	1	1	-	1
32	401.50000000	2	1	1	-	1
33	431.93183859	1	B	B	B	B
34	462.70123642	1	1	1	-	1
35	494.81643195	1	1	1	-	X
36	527.91425658	1	1	1	-	1
37	562.25563823	2	1	1	-	1
38	597.73945308	2	1	1	-	1
39	634.41533338	2	1	1	-	1
40	672.30935350	3	1	1	-	1
41	711.52615148	2	1	1	-	1
42	751.87519682	4	1	1	-	1
43	793.52188633	1	1	1	-	1
44	836.04183181	1	B	B	B	B
45	880.35796932	1	1	1	-	1
46	926.06234385	5	1	1	-	3
47	972.82374491	5	B	B	B	B
48	1019.82958059	1	B	B	B	B
49	1069.55973981	2	1	1	-	1
50	1119.59950653	1	1	1	-	1
51	1171.32838138	2	1	1	-	1
52	1224.47845607	5	1	1	-	1
53	1278.65220625	2	B	B	B	B
54	1334.08489536	4	1	1	-	1
55	1390.96919424	6	1	1	-	1
56	1448.95427411	3	2	1	-	1
57	1508.36883851	7	1	1	-	1
58	1569.06993853	9	1	1	-	1
59	1630.90965834	4	2	2	-	N

Table A.12: Data for $s = 2$, $N = 60, \ldots, 99$

N	Minimum Energy	Stable States	$s = 0$	$s = 1$	$s = 2$	$s = 3$
60	1693.79461177	5	1	1	-	1
61	1758.69713396	6	1	1	-	1
62	1824.34692636	3	1	1	-	1
63	1891.63233079	2	1	1	-	1
64	1960.28162697	6	1	1	-	1
65	2030.23367851	4	X	1	-	1
66	2101.27074682	2	N	1	-	1
67	2173.33824541	1	1	1	-	1
68	2247.58774197	5	1	1	-	1
69	2322.89604947	5	1	1	-	1
70	2399.23952414	6	B	B	B	B
71	2477.16344965	3	B	B	B	B
72	2555.40331495	5	1	1	-	1
73	2637.35501432	2	1	1	-	1
74	2719.61432209	8	2	1	-	1
75	2802.57081367	3	1	1	-	1
76	2887.29601466	8	1	1	-	1
77	2972.78857677	5	1	1	-	1
78	3060.13624953	4	2	1	-	1
79	3149.32797599	3	B	B	B	B
80	3239.52254745	8	B	B	B	B
81	3331.89217990	11	1	1	-	1
82	3425.08475447	16	1	1	-	3
83	3519.32494939	17	1	1	-	1
84	3615.17122267	15	1	1	-	1
85	3712.43793664	11	1	1	-	1
86	3811.08956067	24	2	1	-	1
87	3911.03614332	19	1	1	-	1
88	4012.17707431	14	1	1	-	1
89	4115.08458022	19	1	1	-	1
90	4219.21427750	22	1	1	-	1
91	4324.87611878	18	1	1	-	1
92	4431.93316704	29	1	1	-	1
93	4540.58291910	21	1	1	-	1
94	4650.25998102	28	1	1	-	1
95	4761.71053075	12	1	1	-	1
96	4874.27708664	14	N	1	-	1
97	4988.60996990	10	1	1	-	1
98	5103.98944253	17	1	1	-	1
99	5221.37043734	11	1	1	-	1

Table A.13: Data for $s = 2$, $N = 100, \ldots, 139$

N	Minimum Energy	Stable States	$s = 0$	$s = 1$	$s = 2$	$s = 3$
100	5339.66222912	26	1	1	-	1
101	5459.95420894	42	1	1	-	1
102	5581.26509648	34	1	1	-	1
103	5703.99384121	34	1	1	-	1
104	5828.02384908	32	1	1	-	1
105	5954.50986197	26	1	1	-	1
106	6081.65764494	40	1	1	-	1
107	6210.46346350	34	1	1	-	1
108	6340.11590277	34	1	1	-	1
109	6472.13078480	65	1	1	-	1
110	6605.01261375	50	1	1	-	1
111	6739.05470955	50	1	1	-	1
112	6875.00862394	43	1	1	-	1
113	7013.03290905	60	1	1	-	1
114	7152.13631359	69	1	1	-	1
115	7292.70695721	76	1	1	-	1
116	7434.91209894	90	3	1	-	1
117	7577.97606668	95	1	1	-	1
118	7722.90055012	106	1	1	-	1
119	7869.09201544	95	1	1	-	1
120	8016.51874402	91	1	1	-	1
121	8165.39574901	64	1	1	-	1
122	8315.04573336	98	1	1	-	1
123	8468.53352816	118	1	1	-	1
124	8622.71531086	102	1	1	-	1
125	8778.42640658	112	1	1	-	2
126	8934.92328855	182	1	1	-	1
127	9092.79887602	143	1	N	-	1
128	9252.94017309	157	1	1	-	1
129	9414.07791355	108	1	1	-	1
130	9576.70572069	99	1	1	-	1
131	9740.98241330	106	1	1	-	1
132	9905.21893494	107	1	1	-	1
133	10074.11435027	113	1	1	-	1
134	10242.72593933	109	1	1	-	1
135	10412.31895342	94	1	1	-	1
136	10583.90082868	82	1	1	-	1
137	10756.94326989	90	1	1	-	1
138	10932.66598141	159	1	1	-	1
139	11109.72897838	157	1	1	-	1

Table A.14: Data for $s = 2$, $N = 140, \ldots, 179$

N	Minimum Energy	Stable States	$s = 0$	$s = 1$	$s = 2$	$s = 3$
140	11288.02333318	224	N	2	-	1
141	11466.96666228	149	B	B	B	B
142	11648.05615753	163	1	1	-	1
143	11830.07319504	119	1	1	-	1
144	12013.67706409	108	1	1	-	1
145	12199.33607646	96	1	1	-	1
146	12385.88421282	92	1	1	-	1
147	12575.33713511	114	1	1	-	1
148	12765.83595181	180	2	1	-	1
149	12958.09798633	163	B	B	B	B
150	13151.00686986	223	1	1	-	1
151	13346.12314680	262	1	1	-	1
152	13542.34883108	365	1	1	-	1
153	13739.67763810	258	1	1	-	1
154	13939.69506964	263	1	1	-	1
155	14140.64034421	270	1	1	-	1
156	14343.73724426	313	1	1	-	1
157	14547.45445049	336	1	1	-	1
158	14752.91586068	419	1	1	-	1
159	14959.70362503	457	1	1	-	1
160	15168.38176793	274	1	1	-	1
161	15378.96405095	308	1	1	-	1
162	15590.76378090	449	1	1	-	1
163	15804.44924964	320	1	1	-	1
164	16019.54585555	328	1	1	-	1
165	16236.08499438	327	1	1	-	1
166	16454.27931547	594	1	1	-	1
167	16674.01270412	341	1	1	-	1
168	16894.91881228	518	1	1	-	1
169	17118.27720784	304	1	1	-	1
170	17342.24309237	311	2	1	-	1
171	17568.15613080	420	1	1	-	1
172	17795.82895023	361	1	1	-	1
173	18024.92946909	411	1	1	-	1
174	18255.26330399	555	2	1	-	1
175	18487.97845990	316	1	1	-	1
176	18722.42290446	620	1	1	-	1
177	18957.76297334	402	1	N	-	N
178	19194.87800291	382	1	1	-	N
179	19433.66536597	348	B	B	B	B

Table A.15: Data for $s = 2$, $N = 180, \ldots, 200$

N	Minimum Energy	Stable States	$s = 0$	$s = 1$	$s = 2$	$s = 3$
180	19673.30446923	389	2	1	-	1
181	19915.01560945	349	1	1	-	1
182	20157.55376950	208	1	1	-	1
183	20404.01522614	546	1	1	-	1
184	20650.30678755	636	1	1	-	1
185	20899.06525088	382	2	1	-	1
186	21148.41475532	671	1	1	-	1
187	21398.49429850	426	1	1	-	1
188	21652.51441151	281	1	1	-	1
189	21907.36432745	773	1	1	-	1
190	22163.05953397	452	1	1	-	1
191	22420.24950115	364	1	1	-	1
192	22677.94397770	832	1	1	-	1
193	22941.55632399	415	1	1	-	1
194	23205.00203699	454	1	1	-	1
195	23468.35335667	789	1	1	-	1
196	23734.77400254	414	1	1	-	1
197	24002.62215229	829	1	1	-	1
198	24271.92840886	436	1	1	-	1
199	24542.45458758	335	1	1	-	1
200	24814.22048170	777	1	1	-	1

Table A.16: Data for $s = 3$, $N = 20, \ldots, 59$

N	Minimum Energy	Stable States	$s = 0$	$s = 1$	$s = 2$	$s = 3$
20	131.81301439	1	1	1	1	-
21	150.23065116	1	1	1	1	-
22	169.83235594	2	1	1	1	-
23	191.85117003	1	1	1	1	-
24	213.89406549	1	B	B	B	B
25	239.07299697	1	B	B	B	B
26	265.14266151	1	1	1	1	-
27	292.02920993	1	1	1	1	-
28	321.90995073	1	1	1	1	-
29	353.90225089	1	2	1	1	-
30	386.40958628	1	1	1	1	-
31	421.09518013	1	1	1	1	-
32	455.94557013	2	1	1	1	-
33	497.01183920	1	B	B	B	B
34	537.28151396	1	1	1	1	-
35	580.06830338	1	B	B	B	B
36	624.20989776	1	1	1	1	-
37	670.55661428	2	1	1	1	-
38	718.70458293	2	1	1	1	-
39	768.95800949	2	1	1	1	-
40	821.32116611	2	1	1	1	-
41	876.19933407	2	1	1	1	-
42	932.90632010	4	1	1	1	-
43	992.03528464	3	1	1	1	-
44	1052.06978959	1	B	B	B	B
45	1116.58437324	1	1	1	1	-
46	1183.91364994	5	N	3	2	-
47	1252.69620404	5	B	B	B	B
48	1319.91872645	1	B	B	B	B
49	1395.30989274	3	1	1	1	-
50	1469.23151162	1	1	1	1	-
51	1547.25107892	2	1	1	1	-
52	1628.38979852	5	1	1	1	-
53	1710.90626912	2	B	B	B	B
54	1795.84509849	4	1	1	1	-
55	1883.97744449	6	1	1	1	-
56	1973.86312052	4	2	1	1	-
57	2066.87780942	6	1	1	1	-
58	2162.33366569	8	1	1	1	-
59	2259.64863823	4	N	N	N	-

Table A.17: Data for $s = 3$, $N = 60, \ldots, 99$

N	Minimum Energy	Stable States	$s = 0$	$s = 1$	$s = 2$	$s = 3$
60	2358.57143341	5	1	1	1	-
61	2463.24269494	6	1	1	1	-
62	2568.13434304	3	1	1	1	-
63	2676.92224484	2	1	1	1	-
64	2788.68063859	7	1	1	1	-
65	2903.10131931	4	X	1	1	-
66	3019.23782474	3	N	1	1	-
67	3136.71780064	1	1	1	1	-
68	3260.89141494	4	1	1	1	-
69	3386.62408637	5	1	1	1	-
70	3513.68078779	7	B	B	B	B
71	3644.74899401	3	N	N	X	-
72	3773.83567661	6	1	1	1	-
73	3917.10911520	5	1	1	1	-
74	4058.16286113	10	2	1	1	-
75	4199.03249875	4	1	1	1	-
76	4344.81548211	12	1	1	1	-
77	4490.64633677	4	1	1	1	-
78	4641.78690729	5	2	1	1	-
79	4798.59956213	5	B	B	B	B
80	4956.48522623	9	B	B	B	B
81	5121.45399891	12	1	1	1	-
82	5286.59507246	19	3	3	3	-
83	5453.22391000	20	1	1	1	-
84	5624.13726606	23	1	1	1	-
85	5798.30047654	12	1	1	1	-
86	5975.59375754	25	2	1	1	-
87	6155.57392106	24	1	1	1	-
88	6337.68178577	16	1	1	1	-
89	6524.98640466	19	1	1	1	-
90	6714.53306124	24	1	1	1	-
91	6908.03776675	23	1	1	1	-
92	7104.70386135	30	1	1	1	-
93	7305.74004347	23	1	1	1	-
94	7507.87251551	31	1	1	1	-
95	7715.37412160	19	1	1	1	-
96	7924.50387149	20	N	1	1	-
97	8139.05544943	13	1	1	1	-
98	8354.91348157	21	1	1	1	-
99	8577.34236268	18	1	1	1	-

Table A.18: Data for $s = 3$, $N = 100, \ldots, 139$

N	Minimum Energy	Stable States	$s = 0$	$s = 1$	$s = 2$	$s = 3$
100	8800.27062617	33	1	1	1	-
101	9029.81430383	53	1	1	1	-
102	9260.47829746	38	1	1	1	-
103	9494.62546179	37	1	1	1	-
104	9731.55503693	38	1	1	1	-
105	9977.56649366	44	1	1	1	-
106	10222.88571553	56	1	1	1	-
107	10472.94590658	46	1	1	1	-
108	10722.99946085	49	1	1	1	-
109	10982.07143555	79	1	1	1	-
110	11241.24646635	69	1	1	1	-
111	11502.24991054	67	1	1	1	-
112	11769.68324259	65	1	1	1	-
113	12044.35809148	84	1	1	1	-
114	12320.49652905	99	1	1	1	-
115	12600.28926845	97	1	1	1	-
116	12884.92473240	145	3	1	1	-
117	13169.57570430	152	1	1	1	-
118	13460.23998466	173	1	1	1	-
119	13753.51470550	131	1	1	1	-
120	14048.97507170	118	1	1	1	-
121	14348.12604524	111	1	1	1	-
122	14646.67735657	140	1	1	1	-
123	14964.23764922	126	1	1	1	-
124	15280.11291900	153	1	1	1	-
125	15600.42641944	179	3	3	2	-
126	15920.04505650	187	1	1	1	-
127	16242.72674082	191	1	N	1	-
128	16574.51202563	211	1	1	1	-
129	16906.94806653	160	1	1	1	-
130	17243.36460095	159	1	1	1	-
131	17584.79169861	153	1	1	1	-
132	17920.25855157	184	1	1	1	-
133	18280.04621605	175	1	1	1	-
134	18632.28363149	178	1	1	1	-
135	18985.16178856	177	1	1	1	-
136	19345.19696950	169	1	1	1	-
137	19708.99027019	163	1	1	1	-
138	20084.73495796	185	1	1	1	-
139	20463.30201191	263	1	1	1	-

Table A.19: Data for $s = 3$, $N = 140, \ldots, 179$

N	Minimum Energy	Stable States	$s = 0$	$s = 1$	$s = 2$	$s = 3$
140	20844.10151009	275	N	2	1	-
141	21223.20320818	247	B	B	B	B
142	21610.86206868	211	1	1	1	-
143	21998.40194030	195	1	1	1	-
144	22390.89068544	200	1	1	1	-
145	22790.79808379	147	1	1	1	-
146	23190.89318433	172	1	1	1	-
147	23604.71171383	198	1	1	1	-
148	24019.24696675	273	2	1	1	-
149	24439.90931002	286	B	B	B	B
150	24858.57224534	401	1	1	1	-
151	25285.95715233	455	1	1	1	-
152	25714.74918826	556	1	1	1	-
153	26145.06400851	441	1	1	1	-
154	26587.75130482	551	1	1	1	-
155	27030.30681227	570	1	1	1	-
156	27481.59284307	589	1	1	1	-
157	27930.65919754	674	1	1	1	-
158	28385.62145227	513	1	1	1	-
159	28843.38557028	631	1	1	1	-
160	29308.06167029	511	1	1	1	-
161	29779.70257156	547	1	1	1	-
162	30253.39892099	627	1	1	1	-
163	30733.94572101	622	1	1	1	-
164	31217.90462130	652	1	1	1	-
165	31705.50029489	636	1	1	1	-
166	32198.54688160	565	1	1	1	-
167	32695.49145497	652	1	1	1	-
168	33194.56119754	595	1	1	1	-
169	33704.59846337	529	1	1	1	-
170	34212.10797695	574	2	1	1	-
171	34727.20015355	488	1	1	1	-
172	35248.21400356	485	1	1	1	-
173	35772.70884894	546	1	1	1	-
174	36299.49376420	525	2	1	1	-
175	36836.86116351	536	1	1	1	-
176	37380.17760236	651	1	1	1	-
177	37924.00712566	661	N	N	3	-
178	38471.76330702	903	B	B	B	B
179	39026.19089549	646	N	N	X	-

Table A.20: Data for $s = 3$, $N = 180, \ldots, 200$

N	Minimum Energy	Stable States	$s = 0$	$s = 1$	$s = 2$	$s = 3$
180	39580.06329774	685	2	1	1	-
181	40141.77636064	742	1	1	1	-
182	40702.88513162	821	1	1	1	-
183	41286.59956422	870	1	1	1	-
184	41861.42945866	1020	1	1	1	-
185	42447.89792292	879	2	1	1	-
186	43031.80238055	700	1	1	1	-
187	43613.54103956	913	1	1	1	-
188	44218.36391431	968	1	1	1	-
189	44822.16926745	856	1	1	1	-
190	45424.98858514	1029	1	1	1	-
191	46031.18598693	799	1	1	1	-
192	46635.19914732	850	1	1	1	-
193	47277.48240312	945	1	1	1	-
194	47910.24695661	938	1	1	1	-
195	48535.10742495	1229	1	1	1	-
196	49176.23068582	1097	1	1	1	-
197	49821.11207943	986	1	1	1	-
198	50469.78078287	1075	1	1	1	-
199	51120.20797092	997	1	1	1	-
200	51772.69661064	1006	1	1	1	-

REFERENCES

[1] T. Bedford and A. M. Fisher. Analogues of the Lebesgue density theorem for fractal sets of reals and integers. *Proc. London Math. Soc. (3)*, 64(1):95–124, 1992.

[2] G. Björck. Distributions of positive mass, which maximize a certain generalized energy integral. *Ark. Mat.*, 3:255 – 269, 1956.

[3] S. Borodachov, D. Hardin, and E. Saff. Asymptotics for discrete weighted minimal energy problems on rectifiable sets. *Trans. Amer. Math. Soc.*, 360(3):1559–1580, March 2008.

[4] S. V. Borodachov, D. P. Hardin, and E. B. Saff. Asymptotics of best-packing on rectifiable sets. *Proc. Amer. Math. Soc.*, 135(8):2369–2380 (electronic), 2007.

[5] M. Bowick, A. Cacciuto, D. Nelson, and A. Travesset. Crystalline particle packings on a sphere with long range power law potentials. *Physical Review B*, 73(2), January 2006.

[6] M. Calef and D. Hardin. Riesz s-equilibrium measures on d-rectifiable sets as s approaches d. *Potential Analysis*, 30(4):385–401, May 2009.

[7] B. E. J. Dahlberg. On the distribution of Fekete points. *Duke Math. J.*, 45(3):537–542, 1978.

[8] E. DiBenedetto. *Partial differential equations*. Birkhäuser Boston Inc., Boston, MA, 1995.

[9] E. DiBenedetto. *Real Analysis*. Birkhäuser, Boston, MA, 2002.

[10] J. Duoandikoetxea. *Fourier Analysis*. American Mathematical Society, Providence, Rhode Island, 2001.

[11] T. Erber and G. Hockney. Equilibrium-configuratiosn of n equal charges on a sphere. *Journal of Physics A-Mathematical and General*, 24(23):L1369–L1377, December 1991.

[12] T. Erber and G. Hockney. Complex systems: Equilibrium configurations of n equal charges on a sphere ($2 \leq n \leq 112$). *Advances in Chemical Physics*, 98:495–594, 1997.

[13] T. Erber and G. M. Hockney. Comment on "method of constrained global optimization". *Phys. Rev. Lett.*, 74(8):1482, Feb 1995.

[14] L. Evans and R. Gariepy. *Measure Theory and Fine Properties of Functions*. CRC Press, Boca Raton, Florida, first edition, 1992.

[15] K. J. Falconer. *Fractal geometry*. John Wiley & Sons Ltd., Chichester, 1990. Mathematical foundations and applications.

[16] K. J. Falconer. Wavelet transforms and order-two densities of fractals. *J. Statist. Phys.*, 67(3-4):781–793, 1992.

[17] B. Farkas and B. Nagy. Transfinite diameter, Chebyshev constant and energy on locally compact spaces. *Potential Anal.*, 28(3):241–260, 2008.

[18] H. Federer. *Geometric Measure Theory*. Springer-Verlag, New York, first edition, 1969.

[19] L. Fejes Tóth. On the densest packing of circles in a convex domain. *Norske Vid. Selsk. Forh., Trondhjem*, 21(17):68–71, 1949.

[20] L. Fejes Tóth. *Regular figures*. A Pergamon Press Book. The Macmillan Co., New York, 1964.

[21] B. Fuglede. On the theory of potentials in locally compact spaces. *Acta Math.*, 103:139–215, 1960.

[22] M. Götz. On the Riesz energy of measures. *J. Approx. Theory*, 122(1):62–78, 2003.

[23] L. Grafakos. *Classical and modern Fourier analysis*. Pearson Education, Inc., Upper Saddle River, NJ, 2004.

[24] D. Hardin and E. Saff. Minimal riesz energy point configurations for rectifiable *d*-dimensional manifolds. *Adv. Math*, 193:174–204, 2005.

[25] D. P. Hardin and E. B. Saff. Discretizing manifolds via minimum energy points. *Notices Amer. Math. Soc.*, 51(10):1186–1194, 2004.

[26] M. Hinz. Average densities and limits of potentials. Master's thesis, Universität Jena, Jena, 2005.

[27] J. E. Hutchinson. Fractals and self-similarity. *Indiana Univ. Math. J.*, 30(5):713–747, 1981.

[28] L. V. Kantorovič. Functional analysis and applied mathematics. *Vestnik Leningrad. Univ.*, 3(6):3–18, 1948.

[29] A. Kuijlaars and E. Saff. Asymptotics for the minimal discrete energy on the sphere. *Transactions of the American Mathematical Society*, 350(2):523–538, February 1998.

[30] N. S. Landkof. *Foundations of Modern Potential Theory*. Springer-Verlag, New York, 1973.

[31] S. Lins. A sequence representation for maps. *Discrete Math.*, 30(3):249–263, 1980.

[32] J. M. Marstrand. The (φ, s) regular subsets of n-space. *Trans. Amer. Math. Soc.*, 113:369–392, 1964.

[33] A. Martínez-Finkelshtein, V. Maymeskul, E. Rakhmanov, and E. Saff. Asymptotics for minimal discrete riesz energy on curves in $\mathbb{R}^d$. *Canadian Journal of Mathematics*, 56:529–552, 2004.

[34] P. Mattila. *Geometry of Sets and Measures in Euclidian Spaces*. Cambridge University Press, Cambridge, UK, 1995.

[35] P. A. P. Moran. Additive functions of intervals and Hausdorff measure. *Proc. Cambridge Philos. Soc.*, 42:15–23, 1946.

[36] J. R. Morris, D. M. Deaven, and K. M. Ho. Genetic-algorithm energy minimization for point charges on a sphere. *Phys. Rev. B*, 53(4):R1740–R1743, Jan 1996.

[37] K. J. Nurmela. Minimum-energy point charge configurations on a circular disk. *Journal of Physics A: Mathematical and General*, 31(3), 1998.

[38] N. Patzschke and M. Zähle. Fractional differentiation in the self-affine case. IV. Random measures. *Stochastics Stochastics Rep.*, 49(1-2):87–98, 1994.

[39] D. Preiss. Geometry of measures in $\mathbf{R}^n$: distribution, rectifiability, and densities. *Ann. of Math. (2)*, 125(3):537–643, 1987.

[40] W. Press, S. A. Teukolsky, W. Vetterling, and B. Flannery. *Numerical Recipes in C: The Art of Scientific Computing*. Cambridge, Cambridge, England, second edition, 1992.

[41] M. Putinar. A renormalized Riesz potential and applications. In *Advances in constructive approximation: Vanderbilt 2003*, Mod. Methods Math., pages 433–465. Nashboro Press, Brentwood, TN, 2004.

[42] E. A. Rakhmanov, E. B. Saff, and Y. M. Zhou. Minimal discrete energy on the sphere. *Math. Res. Lett.*, 1(6):647–662, 1994.

[43] E. A. Rakhmanov, E. B. Saff, and Y. M. Zhou. Electrons on the sphere. In *Computational methods and function theory 1994 (Penang)*, volume 5 of *Ser. Approx. Decompos.*, pages 293–309. World Sci. Publ., River Edge, NJ, 1995.

[44] W. Rudin. *Real And Complex Analysis*. McGraw-Hill, New York, 3 edition, 1987.

[45] E. B. Saff and V. Totik. *Logarithmic potentials with external fields*. Springer-Verlag, Berlin, Germany, 1997.

[46] S. Smale. Mathematical problems for the next century. *Gac. R. Soc. Mat. Esp.*, 3(3):413–434, 2000. Translated from Math. Intelligencer **2**0 (1998), no. 2, 7–15 [MR1631413 (99h:01033)] by M. J. Alcón.

[47] P. Tammes. On the origin of number and arrangement of the places of exit on pollen grains. *Diss. Groningen*, 1930.

[48] J. J. Thomson. On the structure of the atom: an investigation of the stability and periods of oscillation of a number of corpuscles arranged at equal intervals around the circumference of a circle; with application of the results to the theory of atomic structure. *Philosophical Magazine Series 6*, 7(39):237–265, March 1904.

[49] R. Wheeden and A. Zygmund. *Measure and Integral*. Marcel Dekker, Inc., New York, NY, first edition, 1977.

[50] T. H. Wolff. *Lectures on harmonic analysis*, volume 29 of *University Lecture Series*. American Mathematical Society, Providence, RI, 2003.

[51] M. Zähle. The average density of self-conformal measures. *J. London Math. Soc. (2)*, 63(3):721–734, 2001.

[52] M. Zähle. Forward integrals and stochastic differential equations. In *Seminar on Stochastic Analysis, Random Fields and Applications, III (Ascona, 1999)*, volume 52 of *Progr. Probab.*, pages 293–302. Birkhäuser, Basel, 2002.